ARIZONA DEPARTMENT OF TRANSPORTATION

REPORT NUMBER: FHWA-AZ88-202-II

SMALL SIGN SUPPORT ANALYSIS

Phase II
Static, Pendulum and Full-Scale Crash Test Programs
Volume I (Report)

Prepared by:
James R. Morgan
Hayes E. Ross, Jr.
Richard E. Schuler
Wanda L. Campise

Texas Transportation Institute
Texas A&M University
College Station, Texas 77843

August 1988

Prepared for:
Arizona Department of Transportation
206 South 17th Avenue
Phoenix, Arizona 85007
in cooperation with
U.S. Department of Transportation
Federal Highway Administration

TECHNICAL REPORT STANDARD TITLE PAGE

1. Report No.	2. Government Accession No.	3. Recipient's Catalog No.
FHWA-AZ88-202-2		

4. Title and Subtitle	5. Report Date
SMALL SIGN SUPPORT ANALYSIS PHASE II - STATIC, PENDULUM AND FULL-SCALE CRASH TEST PROGRAMS, VOLUME I (REPORT)	August 1988 6. Performing Organization Code

7. Author(s)	8. Performing Organization Report No.
James R. Morgan, Hayes E. Ross, Jr., Richard E. Schuler, and Wanda L. Campise	Research Report 7024-2

9. Performing Organization Name and Address	10. Work Unit No.
Texas Transportation Institute Texas A&M University College Station, Texas 77843	11. Contract or Grant No. HPR-PL-1(31) Item 202

12. Sponsoring Agency Name and Address	13. Type of Report and Period Covered
Arizona Department of Transportation Highway Division 206 South Seventeenth Avenue Phoenix, Arizona 85007	Final Report Phase II - Volume I 14. Sponsoring Agency Code

15. Supplementary Notes

ADOT Contacts: Rudy Kolaja
Larry Scofield
Mumtaz Sarsam

16. Abstract

This report, in two volumes, compiles the static, pendulum and full-scale crash test results of alternative small sign support systems for Arizona Department of Transportation (ADOT). The tests were conducted and evaluated in accordance with the recommendations of NCHRP Report 230 and the 1985 AASHTO "Standard Specifications for Structural Supports for Highway Signs, Luminaires and Traffic Signals."

Results of this research indicate that three-3 lb/ft or (based on energy based analysis) two-4 lb/ft 80 ksi Marion steel u-post supports and stubs assembled using a 4 in. nested splice (support assembled behind the stub) with 1/2 in. spacers and grade 9 bolts, nuts and washers will meet the evaluation criteria. It also is apparent from the results of this study that a slip-base retrofit for a sign support system with up to three P2 Uni-Strut posts will meet the evaluation criteria.

In all cases, tests were conducted in NCHRP Report 230 (2) Classification S1 (STRONG) soil. In cases where installation in a "weak" soil is anticipated, further evaluation is required.

This report is one of three reports prepared in the subject project. The other two are:
Small Sign Support Analysis:
Phase I - Crash Test Program
Phase III - Benefit/Cost Analysis

17. Key Words	18. Distribution Statement
Sign, Support, Safety, Test, Crash, Small, Impact, Upgrade, Retrofit, Cost Effectiveness	

19. Security Classif. (of this report)	20. Security Classif. (of this page)	21. No. of Pages	22. Price
		121	

Form DOT F 1700.7 (8-69)

ACKNOWELEDGMENTS

The authors express their sincere appreciation for the cooperation and guidance of Mumtaz Sarsam, Donald Cornelison, Larry Scofield, Rudy Kolaja, and Frank McCullagh of ADOT. Other ADOT personnel on the Project Advisory Committee who provided valuable input included John Hauskins, James Pyne, Roger Hatton, Roger Cromley, and Richard Powers. The suggestions of Nate Banks of FHWA were also appreciated.

Special thanks also goes to Don Cangelose and his associates for their excellent job in setting up and conducting the crash tests.

PREFACE

Arizona Department of Transportation (ADOT) Project HPR-PL-1(31), Item 202, "Small Sign Support Analysis," was initiated by the Texas Transportation Institute (TTI) October 1, 1984. Originally, the project consisted of 18 full-scale vehicular crash tests to evaluate ADOT small sign supports. Upon completion of one-half of the tests it became evident that additional tests would be needed. The project was modified May 31, 1985 to increase the number of tests to 23. Also, the modification included a benefit/cost (B/C) study to develop guidelines for upgrading existing ADOT small sign supports and for selection of new small sign supports. The project was again modified in August, 1986 to develop an improved small sign support system. The B/C study was also modified to include results of the improved support system.

A description of the 23 crash tests and results therefrom are presented in a report entitled "Small Sign Support Analysis: Phase I - Crash Test Program."

A description of the study in which improved sign support systems were developed is reported in two volumes. Volume I of this report contains results and recommendations for ADOT regarding new small sign support standards and are presented herein. Volume II - Appendices contains the results of static tests, physical and chemical tests of the steel signposts, and pullout tests.

A description of the B/C study and results therefrom are presented in a report entitled "Small Sign Support Analysis: Phase III - Benefit/Cost Analysis.

TABLE OF CONTENTS
PHASE I

TABLE OF CONTENTS
PHASE I (continued)

TABLE OF CONTENTS
PHASE II

Volume I (Report)

TABLE OF CONTENTS
PHASE II (continued)

TABLE OF CONTENTS
PHASE II (continued)

TABLE OF CONTENTS
PHASE II (continued)

TABLE OF CONTENTS
PHASE II (continued)

LIST OF FIGURES
PHASE II

LIST OF FIGURES
PHASE II (continued)

LIST OF FIGURES
PHASE II (continued)

LIST OF FIGURES
PHASE II (continued)

LIST OF FIGURES
PHASE II (continued)

LIST OF TABLES
PHASE II

TABLE OF CONTENTS
PHASE III

METRIC CONVERSION FACTORS

Approximate Conversions to Metric Measures

Symbol	When You Know	Multiply by	To Find	Symbol
		LENGTH		
in	inches	*2.5	centimeters	cm
ft	feet	30	centimeters	cm
yd	yards	0.9	meters	m
mi	miles	1.6	kilometers	km
		AREA		
in^2	square inches	6.5	square centimeters	cm^2
ft^2	square feet	0.09	square meters	m^2
yd^2	square yards	0.8	square meters	m^2
mi^2	square miles	2.6	square kilometers	km^2
	acres	0.4	hectares	ha
		MASS (weight)		
oz	ounces	28	grams	g
lb	pounds	0.45	kilograms	kg
	short tons (2000 lb)	0.9	tonnes	t
		VOLUME		
tsp	teaspoons	5	milliliters	ml
Tbsp	tablespoons	15	milliliters	ml
fl oz	fluid ounces	30	milliliters	ml
c	cups	0.24	liters	l
pt	pints	0.47	liters	l
qt	quarts	0.95	liters	l
gal	gallons	3.8	liters	l
ft^3	cubic feet	0.03	cubic meters	m^3
yd^3	cubic yards	0.76	cubic meters	m^3
		TEMPERATURE (exact)		
°F	Fahrenheit temperature	5/9 (after subtracting 32)	Celsius temperature	°C

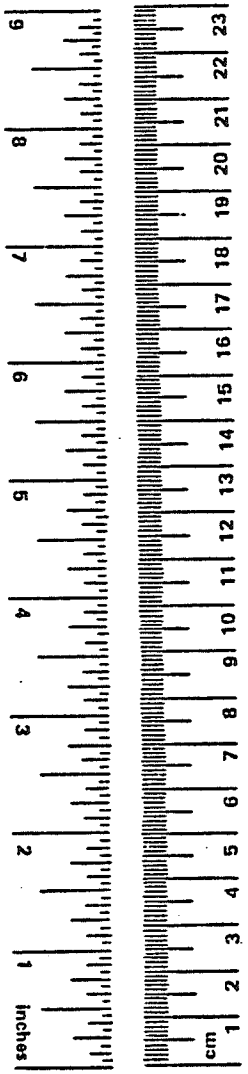

Approximate Conversions from Metric Measures

Symbol	When You Know	Multiply by	To Find	Symbol
		LENGTH		
mm	millimeters	0.04	inches	in
cm	centimeters	0.4	inches	in
m	meters	3.3	feet	ft
m	meters	1.1	yards	yd
km	kilometers	0.6	miles	mi
		AREA		
cm^2	square centimeters	0.16	square inches	in^2
m^2	square meters	1.2	square yards	yd^2
km^2	square kilometers	0.4	square miles	mi^2
ha	hectares (10,000 m^2)	2.5	acres	
		MASS (weight)		
g	grams	0.035	ounces	oz
kg	kilograms	2.2	pounds	lb
t	tonnes (1000 kg)	1.1	short tons	
		VOLUME		
ml	milliliters	0.03	fluid ounces	fl oz
l	liters	2.1	pints	pt
l	liters	1.06	quarts	qt
l	liters	0.26	gallons	gal
m^3	cubic meters	35	cubic feet	ft^3
m^3	cubic meters	1.3	cubic yards	yd^3
		TEMPERATURE (exact)		
°C	Celsius temperature	9/5 (then add 32)	Fahrenheit temperature	°F

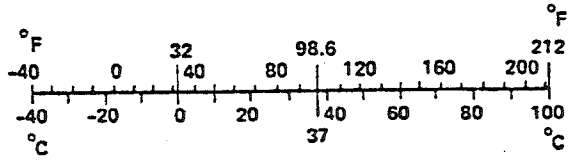

*1 in = 2.54 (exactly). For other exact conversions and more detailed tables, see NBS Misc. Publ. 286, Units of Weights and Measures, Price $2.25, SD Catalog No. C13.10:286.

1 INTRODUCTION

The primary objectives of this project were to develop and test a generic u-post lap splice for small highway signs and to provide a retrofit design for existing small sign systems. Franklin Steel Company (Franklin, PA.) and Marion Steel Company (Marion, OH.) 3 and 4 lb/ft u-posts were used for the u-post phase of the study. The nominal yield stress of the Franklin and Marion posts was 60 and 80 ksi respectively. A slip-base retrofit for a system utilizing Unistrut square perforated tubing also was tested.

Criteria for an acceptable design include:

1. Transfer design wind loads without splice failure
2. Develop nominal yield stress of the signpost
3. Meet federal criteria for roadside appurtenances (NCHRP Report 230 (2) and ASSHTO (5))
4. Use standard "off the shelf" materials for splice assembly (ie: no special machining, ordering, etc.)
5. Assembly simple enough to be handled by one field worker

The first three criteria address essential requirements in design and safety. Criteria 4 and 5 are important in minimizing inventory and maintenance expenses.

Testing of the u-post was divided into static and dynamic phases. The objective of the static test phase was to develop a splice which satisfied criteria 1 and 2. Four types of splices were included for testing: 1) back to back, 2) nested 3) face to face and 4) box (Fig. 2.3-6). The dynamic test phase addressed criteria 3. All tests were run with standard materials in accordance with criteria 4. For example, the bolted splices used commercially available 5/16 inch grade 5 and 9 bolts and washers. Box sections and pipe for spacers used standard 36 ksi steel sections. Attempts were made to keep connections and erection procedures as simple as possible; however, meeting criteria 5 may not be possible for large signs.

Slip-bases have been the subject of extensive use and testing prior to this project, therefore, there is no doubt that a slip-base retrofit can satisfy criteria 1 and 2. Testing of the slip-base retrofit consisted of full-scale crash tests to assure satisfactory performance under criteria 3. Even though it is unlikely that either criteria 4 or 5 can be met with a slip-base retrofit, there may be cases where this system is the most cost effective solution. In those cases where a tubular sign support system already is in place, a retrofit of this type

may be the only reasonable alternative.

The remainder of this report consists of a discussion of the analysis and preliminary testing of the u-post lap splice design (Chapters 2 through 6), the results of full-scale crash tests on both u-post and slip-base systems (Chapter 8) and conclusions (Chapter 9). A companion volume (Volume II, the appendix) contains a collection of data from the static tests, the physical and chemical properties of the u-posts, and the results of sign blank fastner pull-out tests.

2 SPLICE CONFIGURATIONS

Four splice designs were evaluated in static testing:

1. Back to Back
2. Nested
3. Face to Face
4. Box

All four designs met criteria 4 and 5, in that assembly was simple and could be accomplished with commonly available materials. Back to back, nested and face to face splices were assembled in the same manner for both Franklin and Marion posts. Box section splices used in testing were limited to Franklin 4 lb/ft posts due to geometric constraints of commercially available rectangular tubing, i.e., the Marion posts did not fit standard tubing sizes.

2.1 SELECTION OF MOMENT ARM LENGTHS

A splice must be acceptable from both static and dynamic standpoints, therefore bending tests were conducted such that both cases were modeled. A 17 inch moment arm was selected to simulate a bumper level impact for a low speed (<20 mph) test. This length corresponds to the bumper height of a Honda Civic, the test vehicle specified by the National Cooperative Highway Research Program (NCHRP (2)). A 20 kip Material Testing Service (MTS) hydraulic actuator was used for the 17 inch tests to apply load required to develop the nominal yield strength of the signposts in bending. The actuator was bolted to a steel frame and secured to the signpost which was bolted to a fixed base.

A 71 inch moment arm length was chosen to simulate the wind load because it was the maximum cantilever length that could be erected in the frame. Tests using both 17 and 71 inch moment arm lengths were run without moving the fixed base in order to evaluate the load transfer mechanics for wind and low speed impact.

The 17 inch tests do not exactly model the actual impact loading on a signpost. Since the bending loads were applied statically, a correlation of bolt failure is not assured between test and impact loadings (see Fig. 2.1). In a 20 mph test, the inertia of the sign and wind resistance on the panel as it rotates toward the ground, as well as the failure characteristics of the soil increase the load required to fail a bolt in the splice. These effects however, are small in comparison to the load required to fail a field bolt in a static test. The inertial effects are greatly increased in a 60 mph test. At this

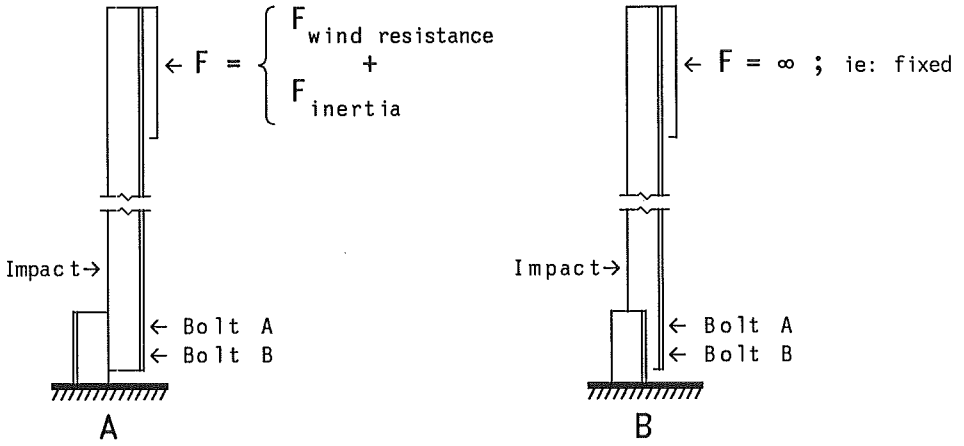

FIGURE 2.1. *ILLUSTRATION OF SIGN PANEL RESISTANCES FOR A) 20 MPH AND B) 60 MPH IMPACT VELOCITIES FOR 17 INCH TESTS.INCH TESTS.*

speed, the force required to accelerate the sign blank is large enough to consider the sign panel as fixed. As a result, the 17 inch tests were used to approximate the load-resistance characteristics of a 20 mph test.

2.2 ASSUMPTIONS AND CALCULATIONS

All stress calculations were made assuming small angle beam theory ($\sin\alpha = \tan\alpha = \alpha$). Since the maximum tip deflection measured in any dead load test was 8.7 inches, the slope at the post tip (α) was such that values for $\sin\alpha$, $\tan\alpha$ and α (radians) were within one percent. This degree of accuracy exceeds that of the systematic error in the test procedures, so the flexure formula given in Equation 2.1 is valid.

$$\sigma_{xx} = \frac{M_x y}{I_x} \tag{2.1}$$

where σ_{xx} is the bending stress, M_x is the applied moment, y is the distance between the neutral axis and the extreme outer fiber, and I_x is the moment of inertia about the axis of bending. Since deflections for the u-post section met the criteria for small angle beam theory, the axial component of deflection was negligible (Appendix I), so the axial stresses (P/A) were omitted for simplicity of calculation.

Deflection due to shear could be a substantial percentage of the measured deflection for the 17 inch tests. Castigliano's theorem for shear and moment deflection can be written as

$$\delta_M = \int \frac{M}{EI}\left(\frac{\partial M}{\partial P}\right) dz \qquad \delta_V = \int \frac{k V}{GA}\left(\frac{\partial V}{\partial P}\right) dz \tag{2.2}$$

where E is the modulus of elasticity, δ_M and δ_V are the deflections due to bending and shear, respectively, and k is the correction coefficient for strain energy due to shear and was assumed to be 1.0 for channel sections (1,3). As a worst case, consider a 17 inch cantilever test. The load required to develop the normal yield stress is 4.2 times a 71 inch test, so the shear deflection is maximized. If a 4 lb/ft Marion post is used (maximum I/A ratio of the four sections), the ratio of bending to shear deflection (Eq 1.2) is minimized and

$$\frac{\delta_M}{\delta_V} = 235 \tag{2.3}$$

This relationship illustrates that shear deflection for a 17 inch cantilever was an insignificant part of the total deflection for the u-post sections tested.

The magnitude of shear stress due to bending was also evaluated to see if it could be neglected for base stress calculations. Shear stress is defined as

$$\tau = \frac{VQ}{I_x t} \tag{2.4}$$

where V is the applied load, Q is first moment of the area about its neutral axis, and t is the thickness of the section along its width. Since the shear stress (VQ/It) due to bending for the 17 and 71 inch tests were 2.1 and 0.5 per cent respectively of the normal bending stress, its effect on the principal stress was negligible.

Base stress calculations for combined bending and torsion tests required the principal combination of the normal bending stress, and normal and shear stresses due to warping. Stress due to bending was calculated using the flexure formula. Shear stress was calculated as the pure torsion component of the applied load. Since the stub was bolted to the fixed base by means of a plate above the section, the section was found to be partially confined, therefore out of plane warping was assumed. Because the the u-post sections were made up of long narrow rectangles and the section experienced warping, the shear stress due to torsion reduced to

$$\tau_{max} = \frac{Th}{J} \tag{2.5}$$

where T is the applied torque, h is the maximum thickness of any leg in the section and J is the torsional rigidity factor. Due to the complexity of the cross sectional shapes (especially the Marion posts), J was obtained experimentally from the torsion tests using the following relationship

$$\theta = \frac{TL}{JG} \tag{2.6}$$

In this equation, θ is the total post rotation in radians, T is the applied torque, L is the length of the post and G is the shear modulus of the post material (assumed at 11,200 psi for steel). Axial stress was omitted and calculation of maximum (principal) base stress became

$$\sigma_{xx} = \frac{M_x y}{2I_x} + \sqrt{\left(\frac{M_x y}{2I_x}\right) + \frac{Th}{J}} \tag{2.7}$$

2.3 CALIBRATED BOLTS

For scheduling and economic reasons, the calibrated bolts were fabricated in house rather than obtained commercially. This eliminated the need to keep an inventory of the two bolt lengths required, or delay testing while a commercial bolt was shipped. Since 78 tests were run with calibrated bolts, failure and inaccurate strain measurements due to metal fatigue were expected. When a bolt failed, another set was calibrated and testing proceeded within one day.

The calibrated bolts were assembled by boring a 2.5mm hole through the shank of the bolt. A TML bolt strain gauge (Tokyo Sokki Kenkyujo Co. Ltd, Tokyo, Japan) was inserted and the hole filled with epoxy (Fig. 2.2). The initial tests of calibrated bolts using TML epoxy were not acceptable due to difficulties in curing and creep measured during calibration. As a result Micro-Measurements Division (MM); (Measurements Group Inc., Raleigh N.C.) AE-10 epoxy was substituted. Once the epoxy had cured, the bolt was calibrated in an MTS tension testing machine. The millivolt values read at each load step (2 kips) were plotted to develop the calibration curves (Appendix W).

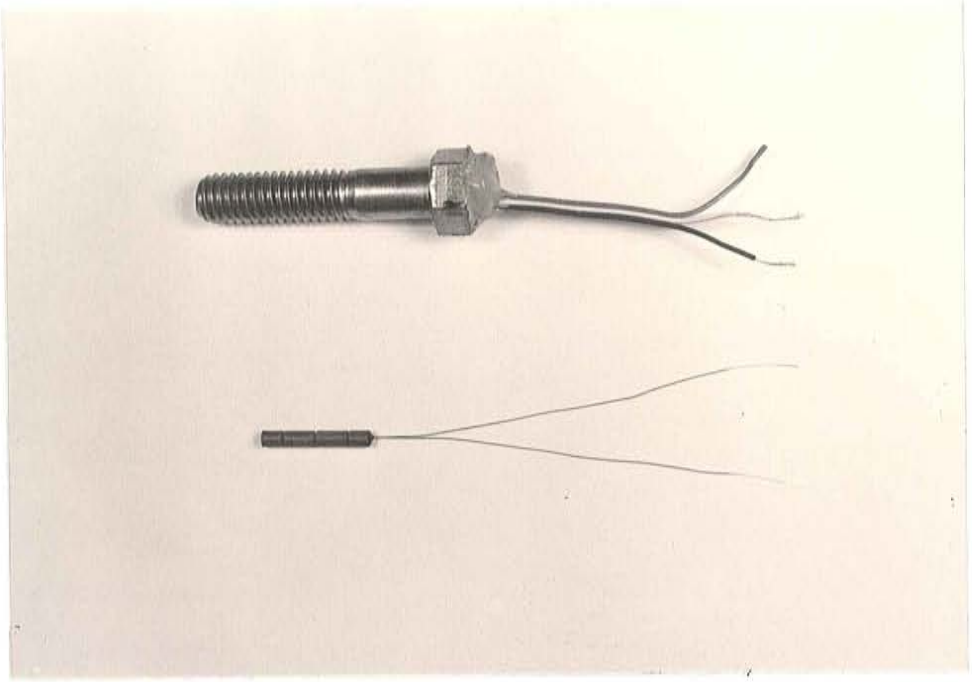

FIGURE 2.2. *PHOTOGRAPH OF MTS STRAIN GAUGE AND ASSEMBLED STRAIN GAUGED BOLT.*

2.4 BACK TO BACK SPLICES

Back to back splices were assembled by bolting the backs of the post and stub together (Fig. 2.3). Bolts and washers were inserted at the proper spacing for a given signpost (Table 2.1) and tightened to the specified rotation.

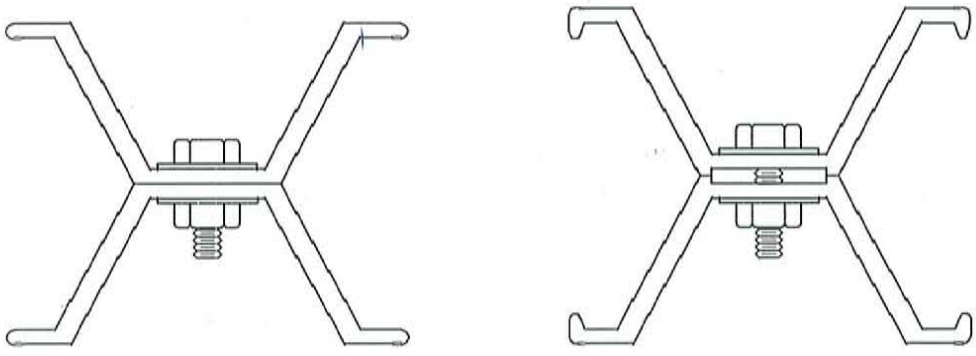

FIGURE 2.3. *ILLUSTRATION OF (A) FRANKLIN AND (B) MARION BACK TO BACK SPLICES.*

TABLE 2.1. *BOLT SPACING AND GRADES USED IN BACK TO BACK, NESTED AND FACE TO FACE SPLICES.*

Manufacturer	3 lb/ft Post		4 lb/ft Post	
	Grade	Spacing	Grade	Spacing
Franklin (60 ksi)	5	3 in	5	4 in
Marion (80 ksi)	9	3 in	9	4 in

2.5 NESTED SPLICES

Nested splices were assembled by bolting the post and stub sections together as shown in Fig. 2.4. A spacer was inserted between the sections to prevent the post and stub from distorting each other as the splice bolts were tightened. It was determined that a spacer length of 1/16 inch less than the distance between the posts when laid in the nested configuraton (without bolt tension) performed satisfactorly. This spacer length assured contact between the legs of the section once the bolts were tightened (for the rolling tolerances of the u-post sections).

Recommended spacer lengths are given in Table 2.2.

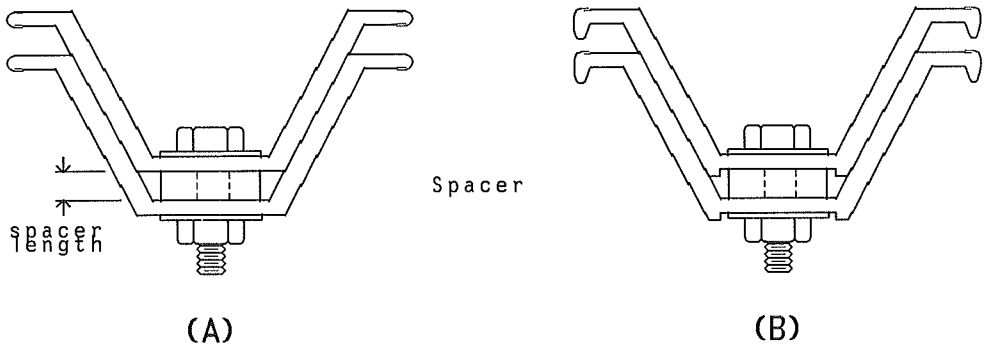

FIGURE 2.4. *ILLUSTRATION OF (A) FRANKLIN AND (B) MARION NESTED SPLICES.*

TABLE 2.2. *SPACER LENGTHS USED FOR NESTED AND FACE TO FACE SPLICES.*

Manufacturer	3 lb/ft Post		4 lb/ft Post	
	Nested	Face to Face	Nested	Face to Face
Franklin (60 ksi)	5/8 in	3-3/16in	9/16in	3-1/16in
Marion (80 ksi)	5/8 in	3-3/8 in	1/2 in	3-5/16in

2.6 FACE TO FACE SPLICES

Face to face splices were assembled by bolting the signpost and stub sections together at the faces (Fig. 2.5). Washers were placed between the nut and bolt and the back of each section. The bolt was inserted through the post section and a 1/2 inch standard steel pipe. The pipe acted as a spacer and was assembled with washers at either end. The spacer length used was 1/32 inch less than the distance between the section backs (Table 2.1), as described for nested splices. The function of the spacer was to limit the stresses in the post and stub during installation by keeping the sections from being drawn together as the bolts were tightened.

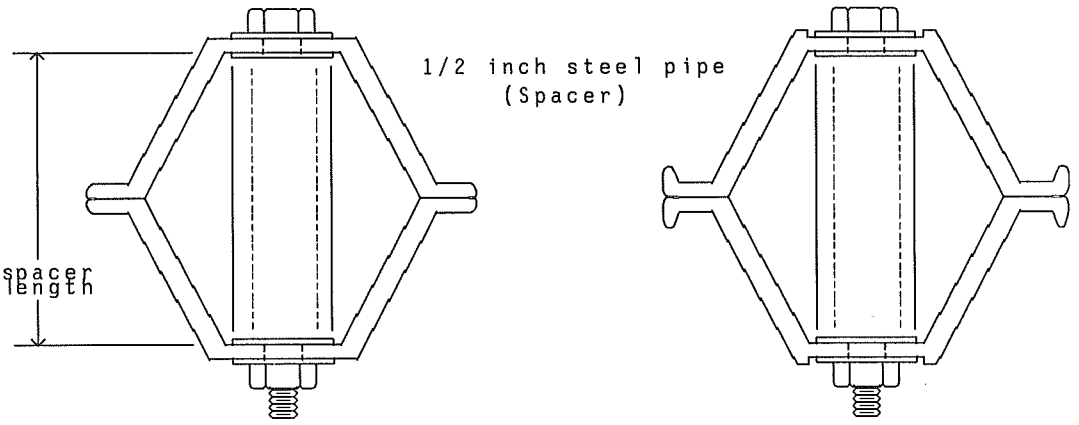

FIGURE 2.5. *ILLUSTRATION OF (A) FRANKLIN AND (B) MARION FACE TO FACE SPLICES.*

2.7 BOX SPLICES

Box splices were assembled by inserting the post and stub into a 36 ksi steel box section. Constraints imposed by the inside box dimensions limited convenient and economical testing of the prototype to Franklin 4 lb/ft posts. Commercial box sections were readily available for 3 and 4 lb/ft Franklin posts. If the design proved successful, sections easily could be fabricated with appropriate dimensions for other posts.

The splice was secured with a bolt through the box, post and stub (Fig. 2.6) tested in both back to back and face to face configurations. Because the box section transferred the load across the splice, the bolt was a non-structural element.

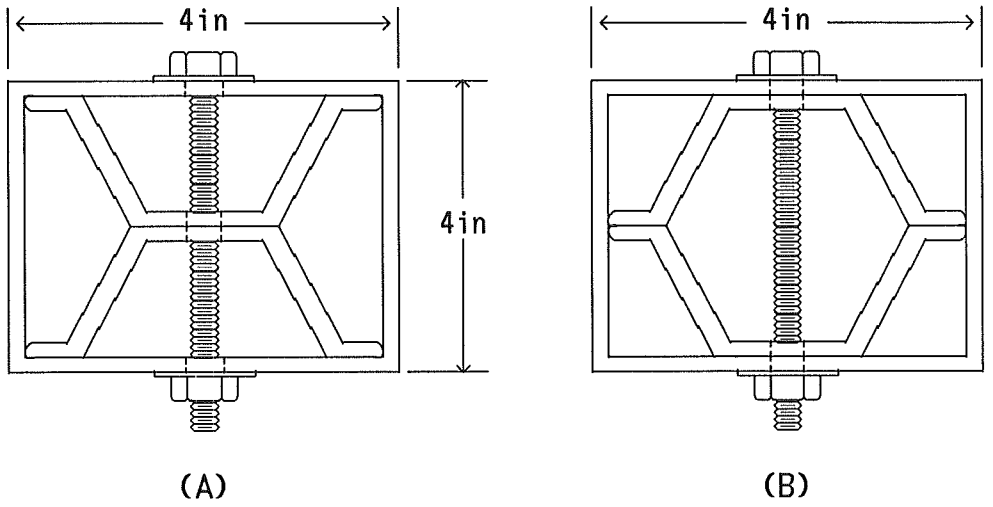

FIGURE 2.6. *ILLUSTRATION OF (A) BACK TO BACK AND(B) FACE TO FACE BOXED IN SPLICES.*

3 Test Procedures

Three types of static tests were run for each splice configuration:

1. Bending
2. Torsion
3. Combined bending and torsion

Splices which developed the yield strength of the signpost without undesireable behavior (ie: large deflections or instability) were used in the dynamic testing phase. Preliminary bending tests were run with Marion 3 lb/ft (80 ksi) posts only (Appendices A,F,J,O). These initial tests determined the bolt grades and spacing to be used for all bolted splices (Table 2.1).

Tests using the calibrated bolts were run initially. Bolt and post strains were recorded to calibrate the strain readings. The bolts were spaced as shown in Table 2.1 and tightened 3/4 revolutions beyond finger tight. Strains were recorded again to calculate the initial bolt tension. The assembly was fixed to the frame and the dead load strains were recorded. Applied load, tip deflection and strain readings were taken at each load step (16-32 lbs) until the calculated stress at the base reached yield (Mc/I), or the tension in one of the calibrated bolts reached 6 kips. The load was then removed and the calibrated bolts were replaced with field bolts. The test proceeded as described above. The load and tip deflection were recorded at each load step and the test was concluded when one of the bolts failed.

3.1 PURE BENDING

Splice capacity in bending was evaluated by applying a load at 71 and 17 inches from the fixed base of a cantilevered post. Load applied at 71 (Fig. 3.1) inches modeled the wind force on multi-post signs. Application of the load at 17 inches (Fig. 3.2) from the base corresponds to the bumper height of the Honda Civic. Data derived from these tests was used to determine the static load transfer mechanics for wind and vehicular impact velocities below 20 mph.

Strain gauges were fixed to one side of the section face at a distance two times the depth of the section. At this distance, effects of local stiffening from the splice were assumed to be negligible, therefore strain measurements could be used to confirm calculations.

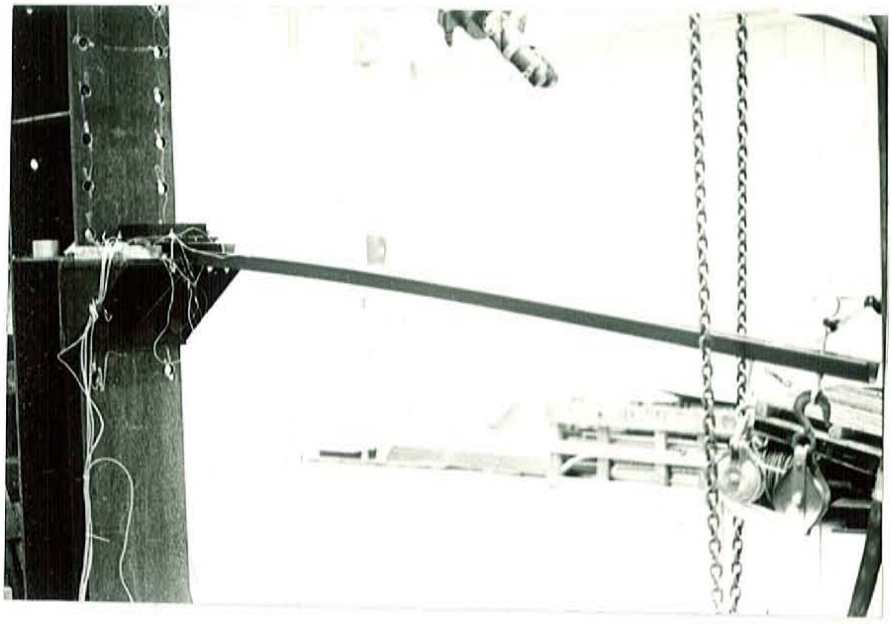

FIGURE 3.1. *PHOTOGRAPH OF 71 INCH MOMENT ARM TEST SETUP.*

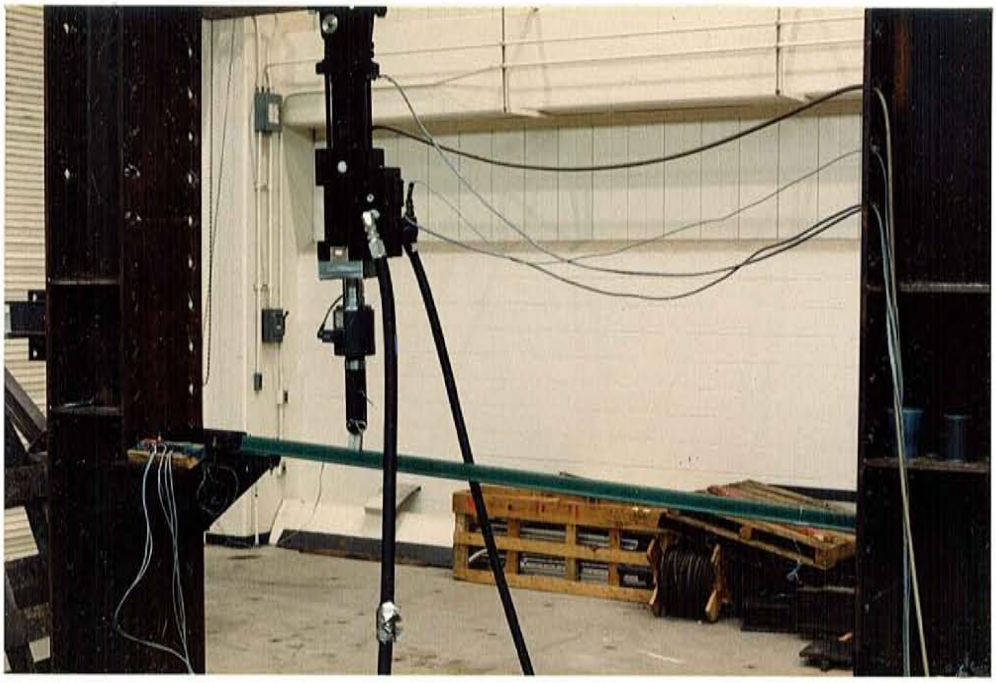

FIGURE 3.2. *PHOTOGRAPH OF 17 INCH MOMENT ARM TEST SETUP.*

Load was applied to the post at 71 inches from the base by pouring a known weight of lead into a bucket. The bucket was suspended from the post by a pulley system which was used to double the weight applied to the sign post. The 17 inch load was applied using an MTS 20 kip actuator bolted to the post with an adapter (Fig. 3.2).

The signpost could be loaded from either side, resulting in two different configurations. Because the load transfer mechanics differ for each configuration, both were tested. The post and stub were spliced (Section 2.1-4) and the stub was secured to a fixed base. Upon conclusion of calibrated and field bolt tests (described above), the signpost was removed and a second splice was assembled and fixed to the frame so that it was loaded in the opposite direction.

3.2 TORSION TESTS

The objective of the pure torsion tests was to evaluate the ability of the splice to transfer torque thereby simulating torsion induced by wind loads. Sign posts were tested with and without splices and the behavior of each configuration was compared.

The pure torsion test apparatus is shown in Figure 3.3. Splice assembly proceeded as described above (Section 3.1). One end of the signpost was bolted to a fixed base and the other secured to an eight inch diameter pulley. Tension was applied to a cable which was wrapped around the pulley. A calibrated load cell determined the tension and the applied torsion can be defined as

$$T = R_P P \tag{3.1}$$

where R_p was the radius of the pulley and P was the tension in the cable. Readings taken at each load step (100-200 lbs) included: tension in the load cell, angle of post rotation, and strain in the calibrated bolts. Strain gauges were omitted for the torsion tests since rotational capacity was the test criteria, not the stress developed at the fixed base.

Since the fixed base and center of the pulley were constructed without an offset, splices were assembled at both ends of the signpost. In this manner, the centerline of the stubs and post remained parallel to the center of the test apparatus prior to running a test (Fig. 3.4). In addition to maintaining alignment, this test configuration enabled the calibrated and field bolts to be tested simultaneously.

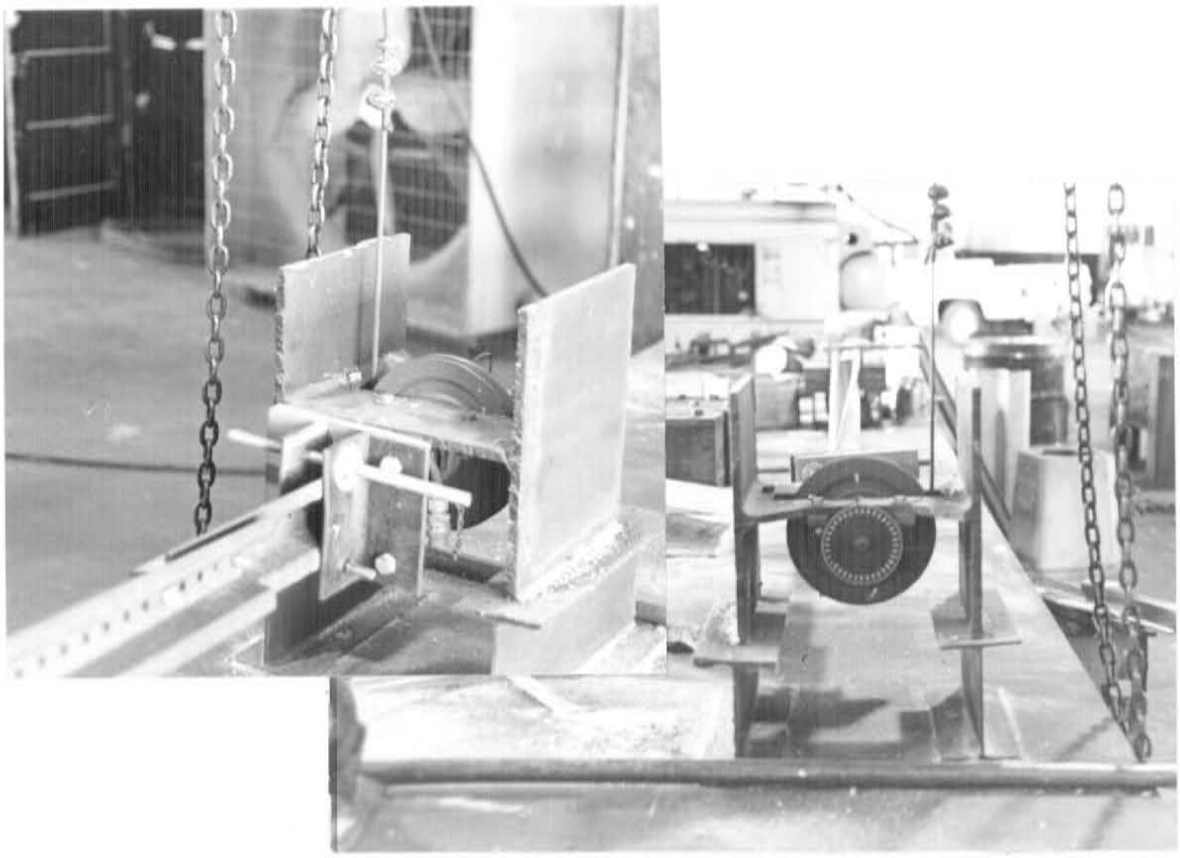

FIGURE 3.3. *PHOTOGRAPHS OF PURE TORSION TEST APPARATUS.*

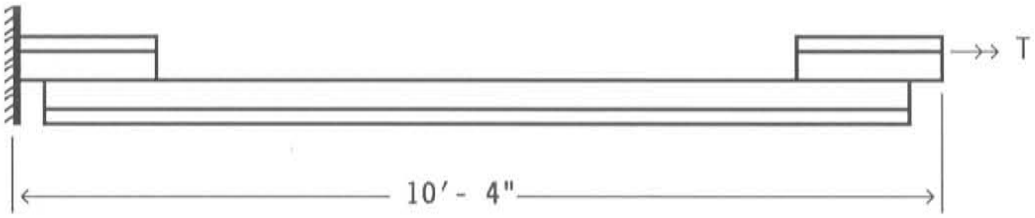

FIGURE 3.4. *ILLUSTRATION OF SPLICE ARRANGEMENT FOR TORSION TEST.*

Sign rotation due to wind loading for a single post installation normally cannot exceed ninety degrees. At this point the sign would be parallel to the windflow and no additional torque would be applied to the post. However, in order to verify the load transfer mechanics of the splices, all signpost assemblies were rotated at least 250 degrees.

3.3 COMBINED BENDING AND TORSION

The objective of the combined bending and torsion tests was to examine the capability of the splice to develop the yield stress of the signpost through the combination of bending and shear. This test simulates the bending moment and sign flutter torque which occur simultaneously in single post signs as a result of wind loads. All tests were run with a moment arm of 75 inches (Fig. 3.5). The load was applied at an eccentricity of 6.2 inches using a steel bracket bolted to the u-post section. This eccentricity corresponds to the American Association of State Highway Transportation Engineers (AASHTO) recommendations (5) for the largest sign expected for use with a single post (Fig. 3.6).

Test procedures were similar to those described above (Section 3.2). Seventeen inch tests were not run because sign flutter is a wind rather than an impact load phenomenon. Calibrated bolts were loaded until a tension of 6 kips was measured. The data recorded included bolt and post strain. Data recorded for the field bolt test included the lateral

FIGURE 3.5. *PHOTOGRAPH SHOWING COMBINED BENDING AND TORSION TEST APPARATUS.*

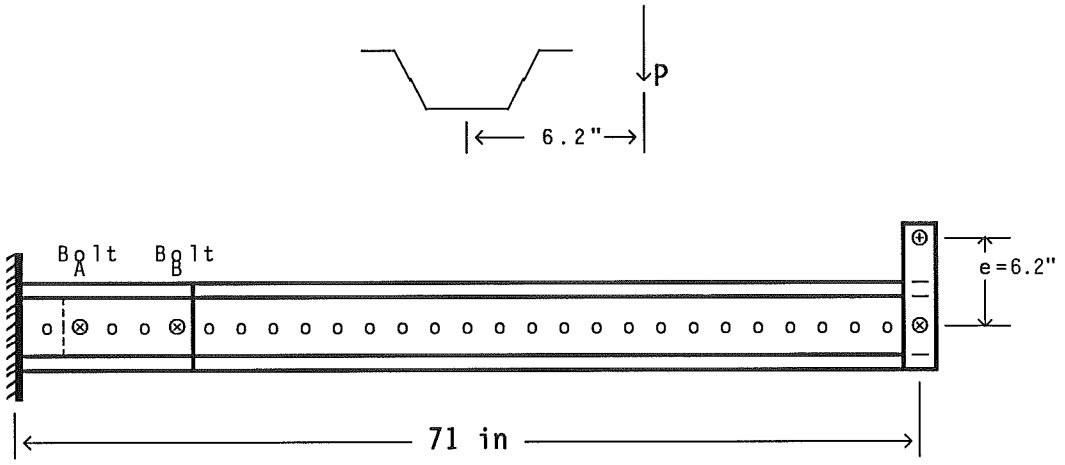

FIGURE 3.6. *END AND PLAN VIEW ILLUSTRATIONS OF COMBINED BENDING AND TORSION TEST SETUP DEMONSTRATING THE ECCENTRICITY IN THE APPLIED LOAD.*

deflection at the point of load and post centerline and longitudinal displacement of the centerline of the section. Since a gravity load was applied to the bracket, the effective eccentricity decreased as the post tip rotated. The applied torque was therefore expressed as

$$T = P(6.2\cos\alpha) \tag{3.2}$$

where T, P and α were the torque, applied load and the rotation measured at the post tip.

4 RESULTS

4.1 BENDING TESTS (Appendices A,B,C,F,G,H,J,K,L,O,P,Q,S,U)

Tables and graphs of bending test data presented in this and subsequent sections contain the following items:

Moment arm: Distance from fixed base to point of load (in).

Load: Applied at the specified moment arm (lbs).

Deflection: Deflection of signpost at point of load (in).

Base stress: Absolute value of stress calculated at base of section for bending or bending combined with torsion (ksi).

Relative load: Bolt load measured after deducting tension at deadload (kips).

Absolute load: Actual measured tension in bolt (kips).

In all bending test cases, *the field bolts failed prior to failure of the u-post.* In addition, permanent set was not observed along the posts length after any test, indicating that the *actual* yield stress (as opposed to the specified nominal yield stress; Franklin - 60 ksi and Marion - 80 ksi) was not reached. Local yielding however was observed around the bolt holes in the 3 lb/ft post tests. This behavior resulted in high base stresses and deflections at critical bolt failure.

The base stress calculated at field bolt failure varied with the configuration of the splice being tested (ie: the direction load was applied relative to the splice). The minimum calculated base stress at bolt failure is critical for wind load design in all but the box splice design (Table 4.1).

Minimum base stress at field bolt failure for back to back splices was 5% lower than nested splices. As a result, back to back splices (Fig. 2.1) were only able to develop the nominal yield stress of the 3 lb/ft posts. Nested splices (Fig. 2.2) were found to develop the nominal yield stress for all post weights and manufacturers.

Measured tip deflection was found to be independent of splice type (Fig. 4.1) and bolt grade (Fig. 4.2) for back to back and nested splices. Marion posts (80 ksi) had less deflection at a given base stress than the Franklin posts (60 ksi). Relative bolt tension was greater for Marion (80 ksi) than Franklin (60 ksi) signposts (Fig. 4.3). Higher relative bolt tension was also recorded for nested splices.

TABLE 4.1. *SUMMARY OF MINIMUM BASE STRESS CALCULATED AT FIELD BOLT FAILURE FOR BACK TO BACK, NESTED AND FACE TO FACE SPLICES*

BENDING TEST RESULTS MINIMUM BASE STRESS AT BOLT FAILURE (ksi) Franklin and Marion Posts											
Mom Arm (in)	No Run	FRANKLIN - 60 ksi					MARION - 80 ksi				
		Gr Bolt	3 lb/ft Back	3 lb/ft Nest	4 lb/ft Back	4 lb/ft Nest	Gr Bolt	3 lb/ft Back	3 lb/ft Nest	4 lb/ft Back	4 lb/ft Nest
17	1	5	64.9	78.7	56.6	61.3	5 9	78.0 --	92.6 --	63.3 84.9	-- 87.0
51	5	5	--	--	54.1 (0.83)	59.8 (0.42)	9	--	--	75.3 (1.06)	78.2 (1.47)
71	1	5	77.3	69.1	56.0	60.0	5 9	66.0 87.4	65.7 87.4	57.8 78.8	64.6 83.5
145*	3	5	--	--	--	44.4 (1.50)	-	--	--	--	--
		8	--	--	--	57.3 (1.50)	-	--	--	--	--

** Nominal yield stress

-- Test not run

() Standard deviation from the mean

* Results from TTI Project RF 4277 (4)

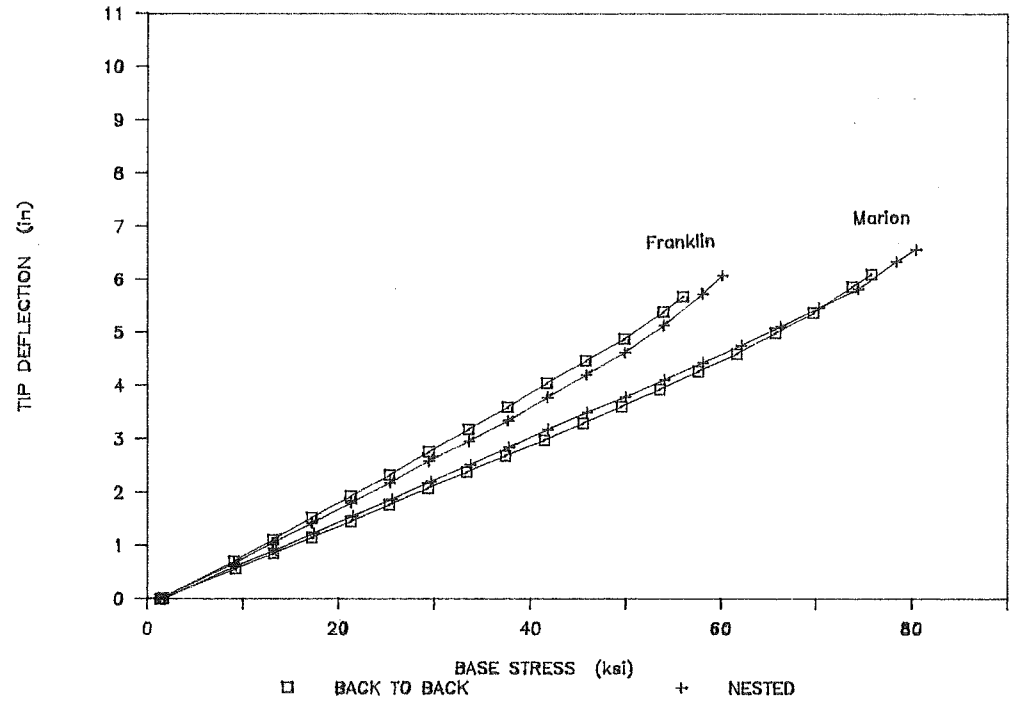

FIGURE 4.1. *BASE STRESS VS TIP DEFLECTION FOR FRANKLIN AND MARION 4 LB/FT POSTS.*

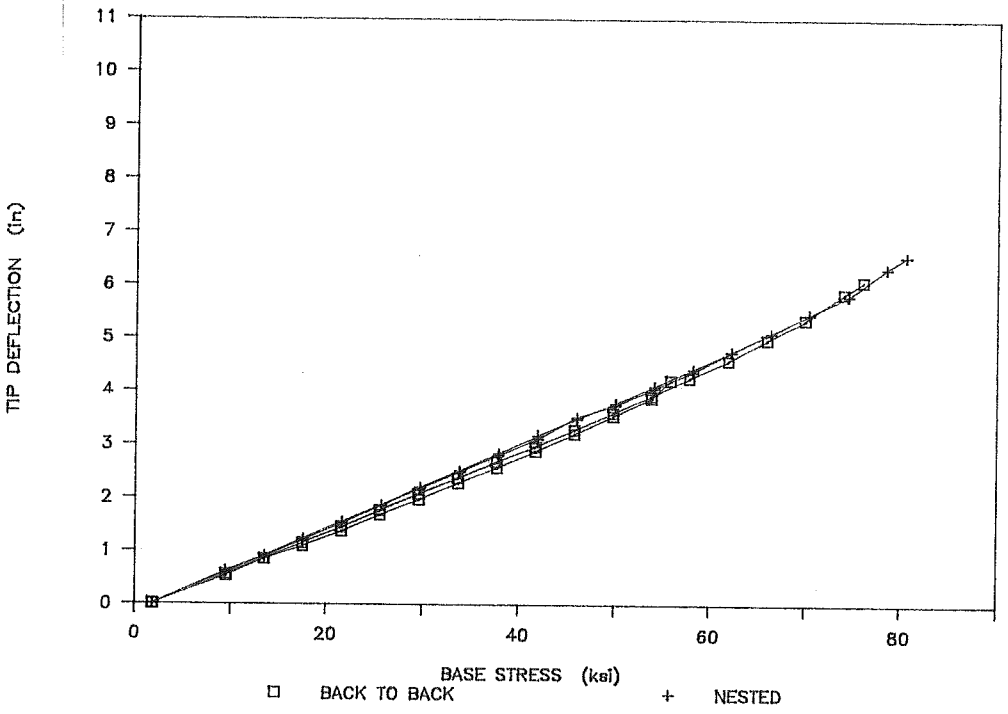

FIGURE 4.2. *BASE STRESS VS TIP DEFLECTION FOR MARION 4 LB/FT POSTS FOR GRADES 5 AND 9 BOLTS.*

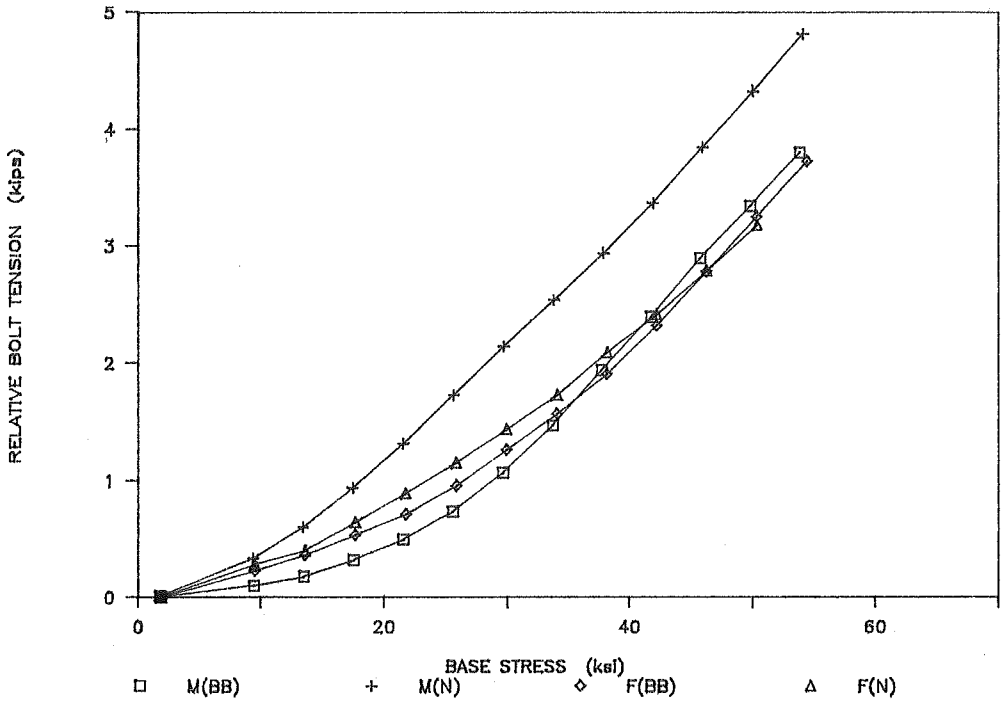

FIGURE 4.3. *BASE STRESS VS RELATIVE BOLT LOAD FOR FRANKLIN AND MARION 4 LB/FT POSTS*

Face to face splices (Fig. 2.3) were eliminated as a result of instability. In two 17 inch tests (Franklin 3 lb/ft and Marion 4 lb/ft), rotation occurred within the splice which resulted in 18 inches of lateral tip deflection and conclusion of the test prior to failing a field bolt (Fig. 4.4). This instability was not acceptable and no further testing was done using face to face splices.

The steel box splice (Fig. 2.4) was eliminated due to excessive post deflection. Local yielding of the box resulted in measured deflections nearly three times that of the bolted back to back or nested splices (Fig. 4.5). In addition, the splice, while snug before a test, became loose following one load sequence. As a result of excessive post deflection, no further testing was done using box splices.

Minimum effective splice lengths (see section 5.6) were 15% greater for the 17 inch than the 71 inch tests (Table 4.2). In addition, effective splice lengths for the 71 inch tests using back to back splices were typically 5% higher than nested.

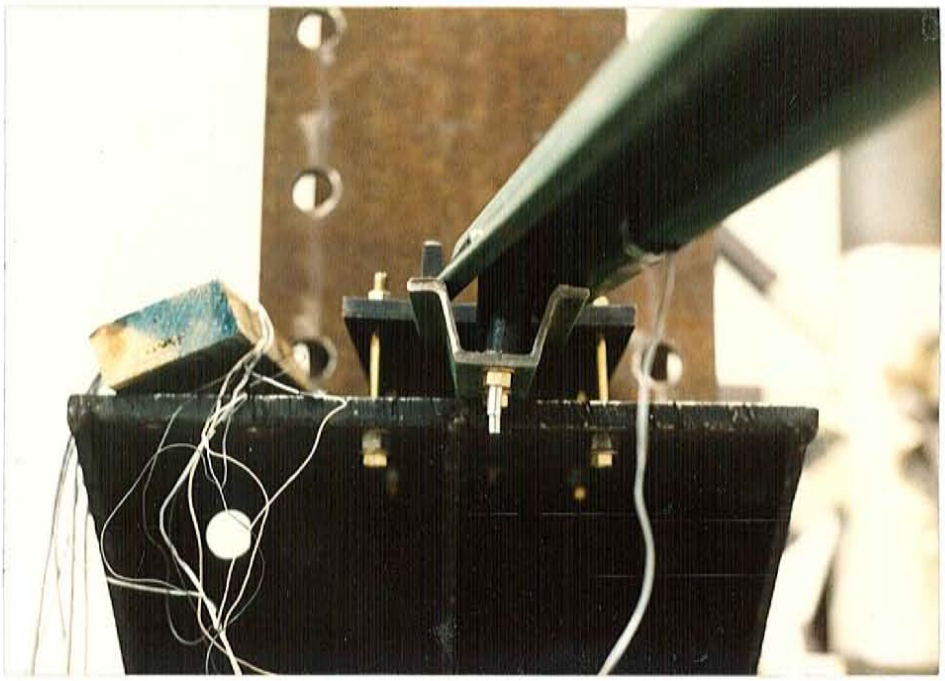

FIGURE 4.4. *PHOTOGRAPH ILLUSTRATING LATERAL TRANSLATION OF MARION FACE TO FACE SPLICE.*

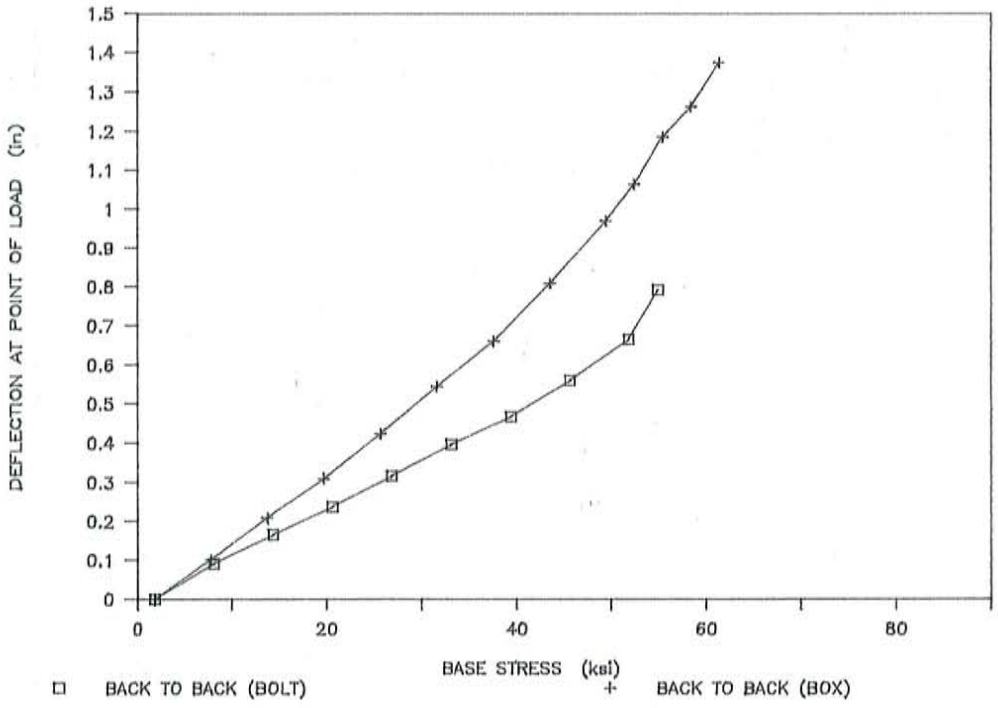

FIGURE 4.5. *BASE STRESS VS TIP DEFLECTION FOR FRANKLIN 4 LB/FT BACK TO BACK BOLTED AND BOX SPLICES.*

TABLE 4.2. *SUMMARY OF MINIMUM EFFECTIVE SPLICE LENGTHS FOR FRANKLIN AND MARION POSTS.*

BENDING TEST RESULTS MINIMUM EFFECTIVE SPLICE LENGTH Franklin and Marion Posts								
Mom Arm (in)	3 lb/ft				4 lb/ft			
	Splice (in)	Back	Nest	Face	Splice (in)	Back	Nest	Face
	Franklin Posts - 60 ksi *							
17	3	3.3	3.4	3.4	4	4.4	4.7	4.4
71	3	3.8	3.2	--	4	4.0	3.8	--
	Marion Posts - 80 ksi *							
17	3	6.2	5.1	4.1	4	4.9	4.7	4.6
71	3	3.4	3.1	--	4	4.0	4.0	--
72	3	5.0	3.8	3.1		--	--	--
	4	4.3	3.8	4.2		--	--	--

* Nominal yield stress

-- Test not run

4.2 TORSION TESTS (Appendices D,M,T)

Tables and graphs of torsion test data presented in this and subsequent sections contain the following items:

Applied moment: Pure torque applied at end of signpost (kip-in).

Theta: Measured rotation of signpost (degrees).

The maximum wind induced rotation a sign could undergo is ninety degrees, however in order to verify load transfer mechanics, all posts were twisted at least 250 degrees. Torsional stiffness was found to be unaffected by the addition of a splice (Fig. 4.6). Both back to back and nested splices performed as well as a spliceless post and no field or calibrated bolt failures were observed in any test. No tests were run using either face-to-face or box section splices due to the bending test results (Section 4.1).

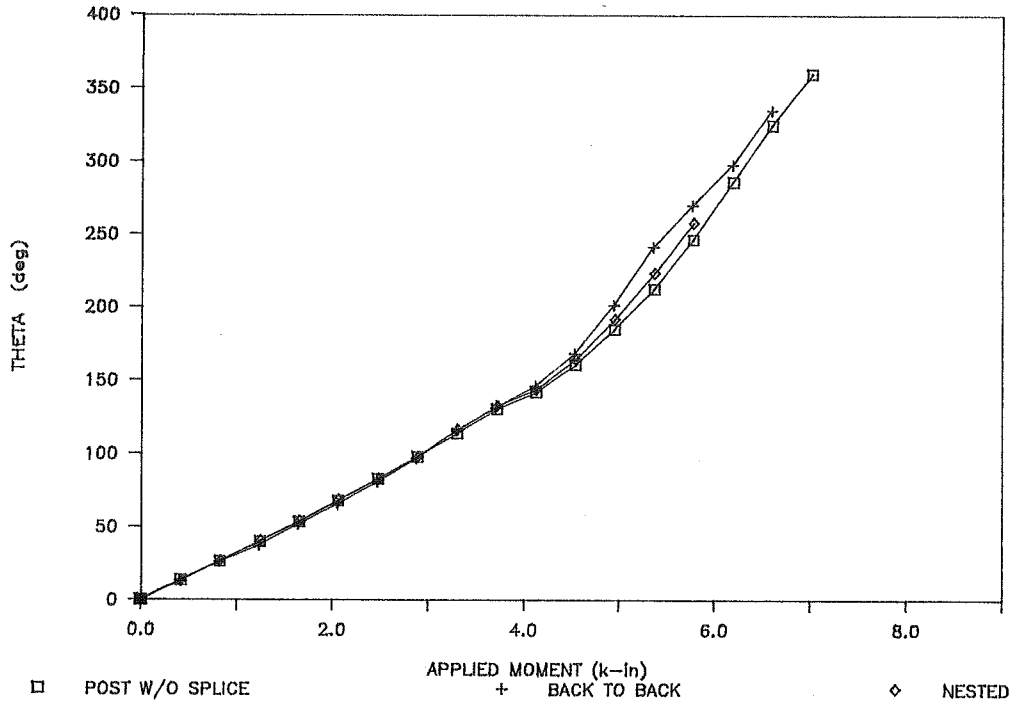

FIGURE 4.6. *APPLIED MOMENT VS POST ROTATION FOR FRANKLIN 4 LB/FT POST (NO SPLICE, BACK TO BACK AND NESTED SPLICES).*

Measured bolt tension for Marion back to back splices remained essentially constant for first 180 degrees of rotation. The same behavior was observed for 60 degrees for a Franklin back to back splice (Fig. 4.7). In addition, although not significant for wind loading, Marion nested splices demonstrated a longer bolt tension plateau than nested splices using Franklin posts. Once the bolt tension began to rise, the rate of change was similiar for all splices and manufacturers.

4.3 COMBINED BENDING AND TORSION TESTS (Appendices E,I,N,R)

Tables and graphs of combined bending and torsion test data presented in this and subsequent sections contain the following items:

Rotation: Rotation of post cross section at point of load (degrees).

Torque arm: Effective moment arm for applied load (in)

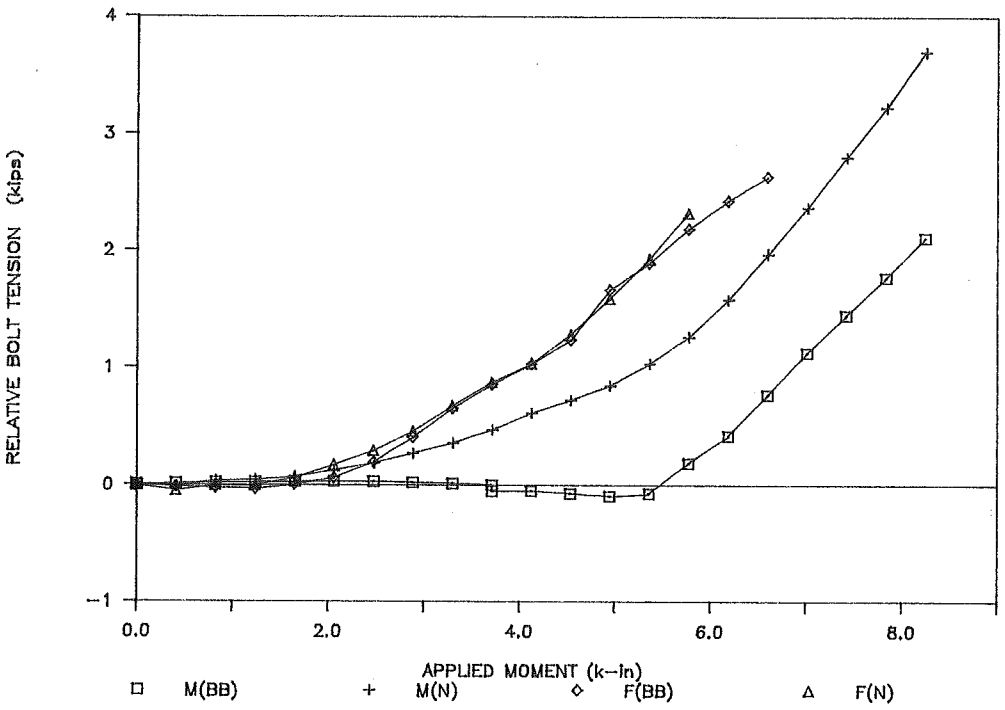

FIGURE 4.7. *APPLIED MOMENT VS RELATIVE BOLT TENSION IN CRITICAL BOLT FOR FRANKLIN AND MARION POSTS (BACK TO BACK AND NESTED SPLICES).*

The combined base stress for bending and torsion for all manufacturers and post weights exceeded the nominal yield stress of the posts (Table 4.3). This suggests that the proposed back to back and nested splices possess adequate strength for sign post installations.

Comparisons of critical bolt loads for bending and combined and torsion tests of 4 lb/ft posts in the critical orientation are plotted in Figs. 4.8-11. With the exception of the Franklin 4 lb/ft back to back test (Fig. 4.8), critical bolt loads for combined bending and torsion experienced a lower rate of change in tension than in the bending tests. This resulted in a lower measured bolt tension at a given calculated base stress. Combined bending and torsion tests were not run on face to face or box splices due to the results of the bending test results (Section 4.1).

Critical bolts in the combined bending and torsion tests with Marion back to back splices exhibited the load transfer delay discovered in the torsion tests (Fig. 4.10). Franklin back to back tests (Fig. 4.11) did not demonstrate this same bolt tension plateau.

TABLE 4.3. *SUMMARY OF RESULTS OF COMBINED BENDING AND TORSION TESTS FOR BACK TO BACK AND NESTED SPLICES.*

BENDING TEST RESULTS MINIMUM BASE STRESS AT BOLT FAILURE (ksi) Franklin and Marion Posts							
Mom Arm (in)	No Run	FRANKLIN - 60 ksi *			MARION - 80 ksi *		
		Gr Bolt	3 lb/ft Back Nest	4 lb/ft Back Nest	Gr Bolt	3 lb/ft Back Nest	4 lb/ft Back Nest
75	1	5	79.1 78.6	68.1 80.9	9	96.7 107.9	98.1 101.4

* Nominal yield stress

Bending (from Table 4.1)

Franklin 3 lb/ft: Grade 5 bolts spaced at three inches will develop the nominal yield stress (60 ksi) for back to back and nested splices.

Franklin 4 lb/ft: Grade 5 bolts spaced at four inches will develop the nominal yield stress (60 ksi) for nested splices only.

Marion 3 lb/ft: Grade 9 bolts spaced at three inches will develop the nominal yield stress (80 ksi) for back to back and nested splices.

Marion 4 lb/ft: Grade 9 bolts spaced at four inches will develop the nominal yield stress (80 ksi) for nested splices only.

Combined Bending and Torsion

Franklin 3 lb/ft: Grade 5 bolts spaced at three inches will develop the nominal yield stress (60 ksi) for back to back and nested splices.

Franklin 4 lb/ft: Grade 5 bolts spaced at four inches will develop the nominal yield stress (60 ksi) for back to back and nested splices.

Marion 3 lb/ft: Grade 9 bolts spaced at three inches will develop the nominal yield stress (80 ksi) for back to back and nested splices.

Marion 4 lb/ft: Grade 9 bolts spaced at four inches will develop the nominal yield stress (80ksi) for back to back and nested splices.

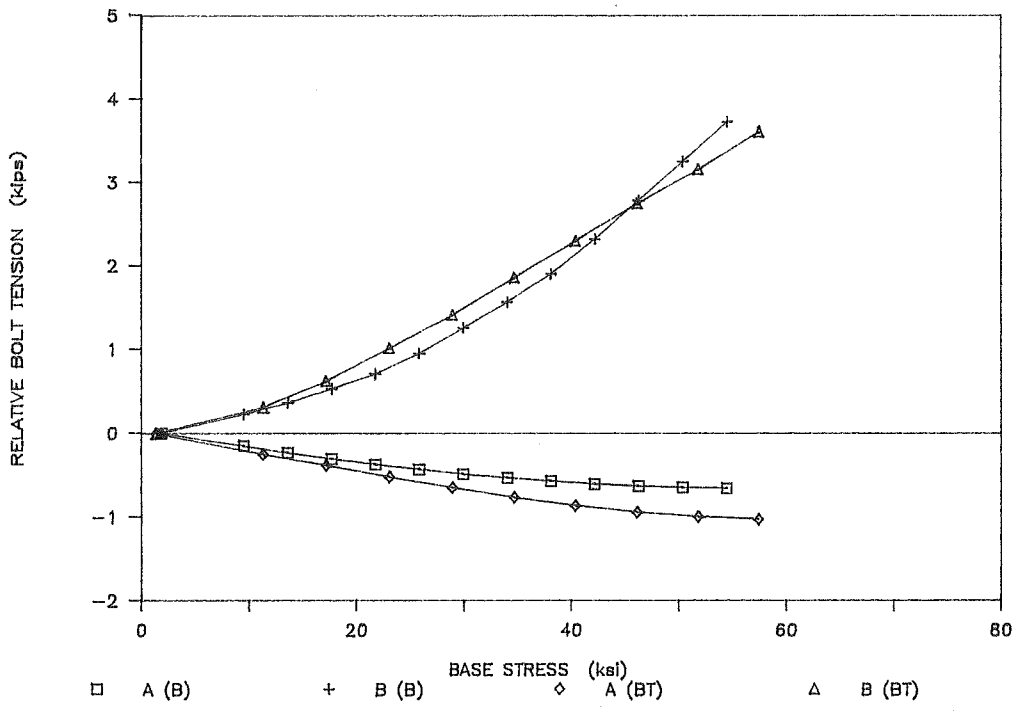

FIGURE 4.8. *BASE STRESS VS RELATIVE BOLT TENSION IN BENDING AND COMBINED BENDING AND TORSION (FRANKLIN 4 LB/FT - BACK TO BACK SPLICE).*

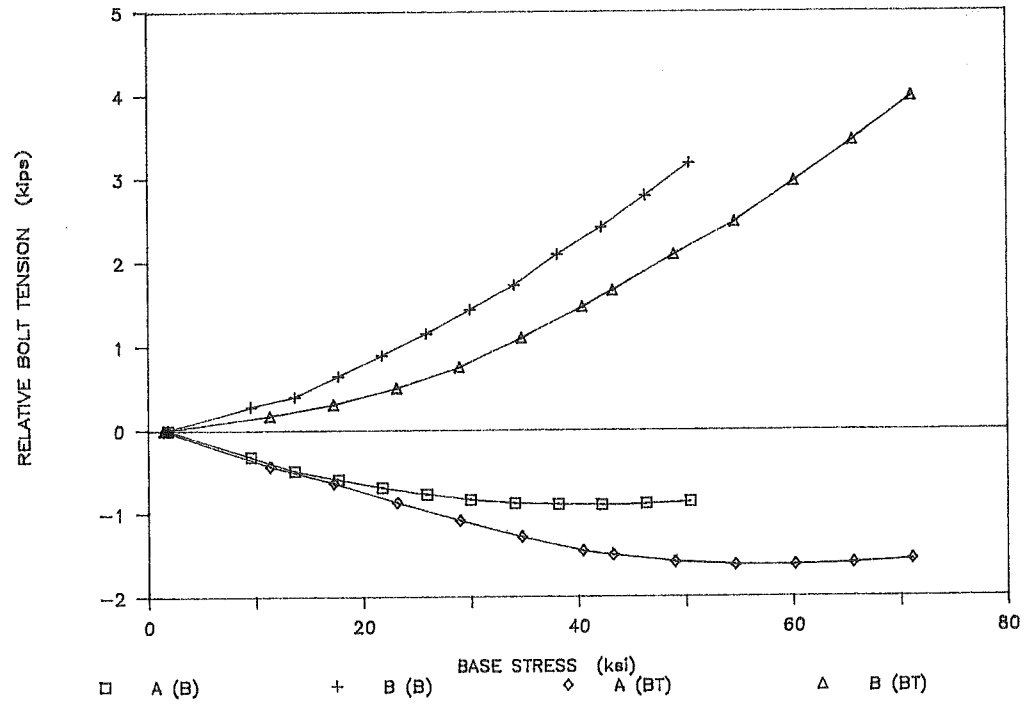

FIGURE 4.9. *BASE STRESS VS RELATIVE BOLT TENSION IN BENDING AND COMBINED BENDING AND TORSION (FRANKLIN 4 LB/FT - NESTED SPLICE).*

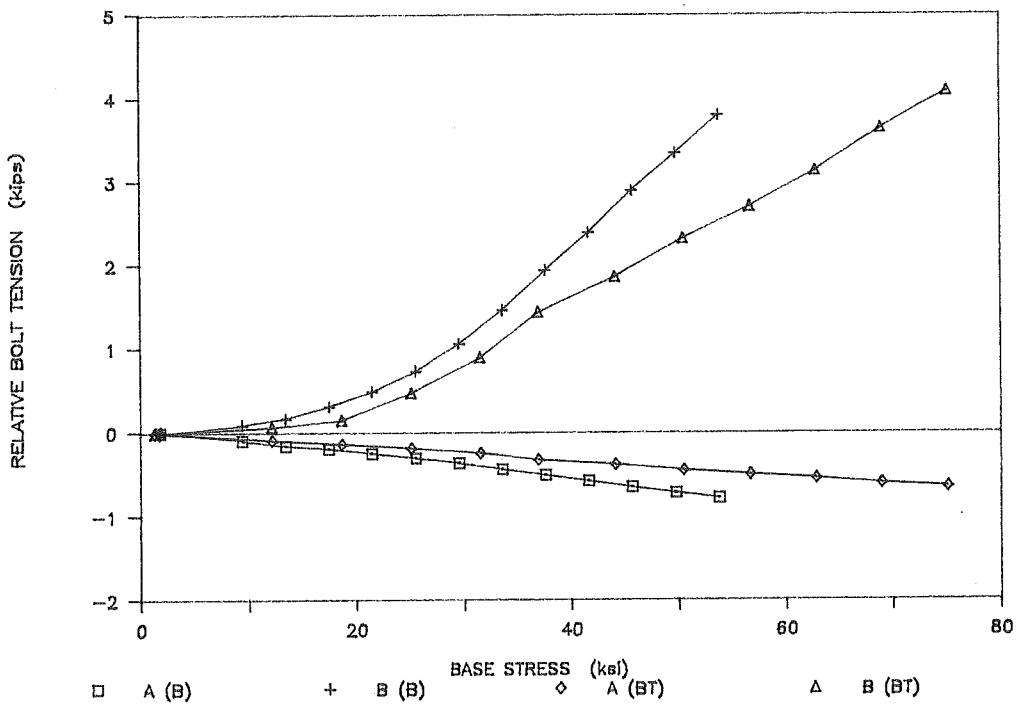

FIGURE 4.10. *BASE STRESS VS RELATIVE BOLT TENSION IN BENDING AND COMBINED BENDING AND TORSION (MARION 4 LB/FT - BACK TO BACK SPLICE).*

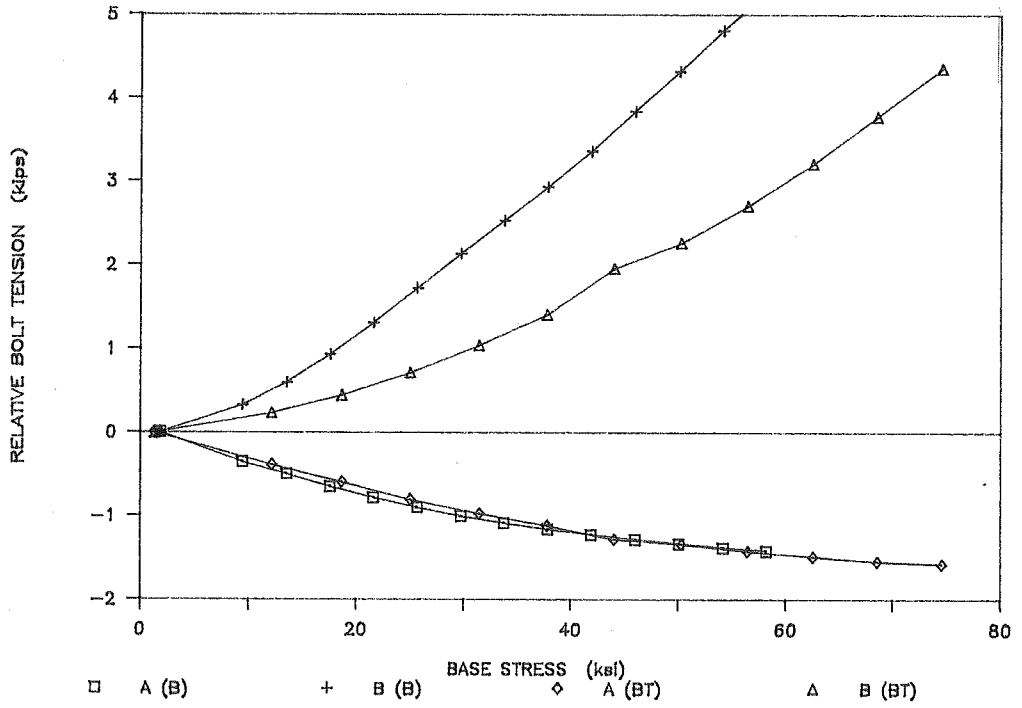

FIGURE 4.11. *BASE STRESS VS RELATIVE BOLT TENSION IN BENDING AND COMBINED BENDING AND TORSION (MARION 4 LB/FT - NESTED SPLICE).*

5 DISCUSSION

5.1 CRITICAL AND NON-CRITICAL SPLICE CONFIGURATIONS

The splices discussed in section 2 can be assembled and loaded in two configurations. Both configurations are illustrated for a back to back splice in Figs. 5.1,2 along with the designation for bolts A and B. because wind loads can be applied from any direction, the critical orientation is defined as that which requires the lowest wind load to fail one of the bolts. This splice configuration (Fig. 5.1) is critical because the load required to fail bolt B (critical bolt for the critical configuration) is lower than the failure load for bolt A in the non-critical orientation (Fig. 5.2). This load/orientation relationship is seen as higher bolt loads at a given base stress (Fig. 5.3) and lower base stresses at critical bolt failure for the critical orientation (Tables 5.1 and 5.2).

5.2 PREDICTED LOAD TRANSFER MECHANICS FOR BENDING

5.2.1 BOLTED SPLICES

Prior to loading the assembled splice, all of the bolt tension was distributed as compression at the backs (in a back to back splice), or spacers (in face to face and nested splices) of the u-post sections. As load was applied to the signpost, equilibrium was maintained in the splice as tension in the critical bolt increased. As long as the section backs or spacers remained in contact, some percentage of the measured tension was lost to compression in the section. However, when physical contact was lost between the backs or backs and spacers, (Fig. 5.4), all of the measured tension in the critical bolt was used to maintain equilibrium in the splice. Since the magnitude of bolt tension near critical bolt failure was important for material selection, bolt tension equations were derived with the assumption that all measured tension was restraining the splice (ie: post or spacers were not in contact with stub). As a result, the equations in this section do not apply until the predicted tension exceeds the initial value. For this reason the initial bolt tension was assumed to remain constant until the predicted tension equaled the initial bolt tension.

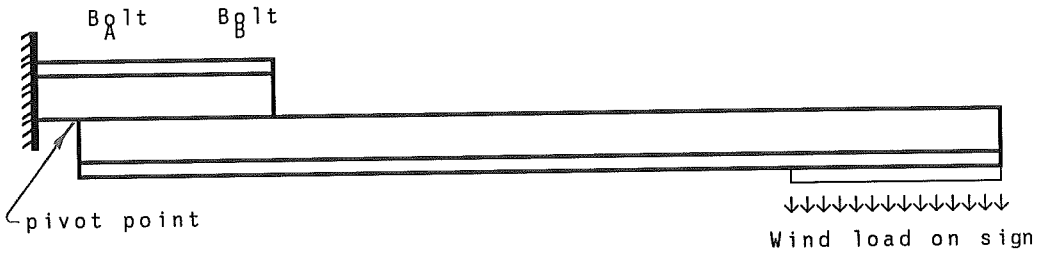

FIGURE 5.1. *ILLUSTRATION OF THE CRITICAL ORIENTATION FOR A BACK TO BACK SPLICE.*

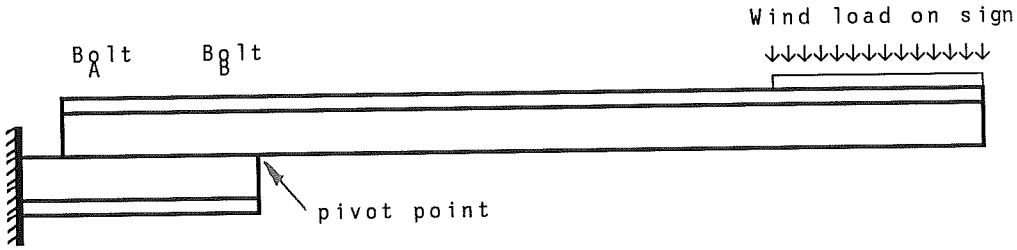

FIGURE 5.2. *ILLUSTRATION OF THE NON-CRITICAL ORIENTATION FOR A BACK TO BACK SPLICE.*

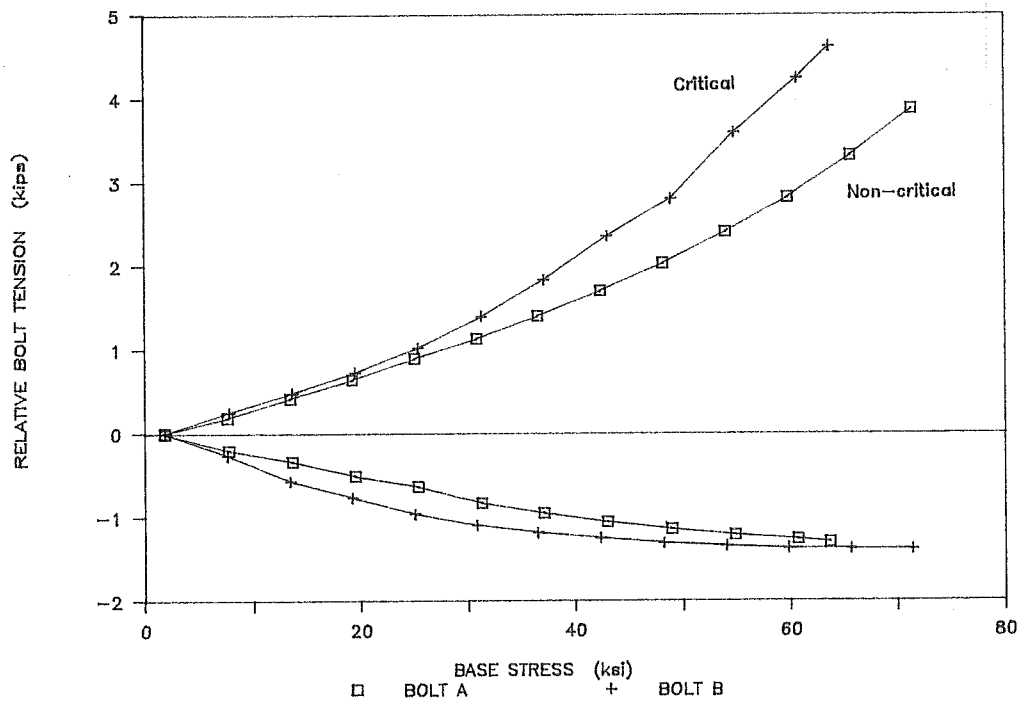

FIGURE 5.3. *BASE STRESS VS RELATIVE BOLT TENSION FOR A MARION 4 LB/FT NESTED SPLICE IN CRITICAL AND NON-CRITICAL CONFIGURATIONS.*

TABLE 5.1. *SUMMARY OF BASE STRESS CALCULATED AT FIELD BOLT FAILURE FOR FRANKLIN POSTS IN CRITICAL AND NON-CRITICAL BENDING TEST CONFIGURATIONS.*

BENDING TEST RESULTS BASE STRESS AT BOLT FAILURE (ksi) Franklin Posts - 60 ksi **									
Mom Arm (in)	Splice Length (in)	No of Tests	Gr Bolt	CRITICAL Back	CRITICAL Nest	CRITICAL Face	NON-CRITICAL Back	NON-CRITICAL Nest	NON-CRITICAL Face
				3 lb/ft					
17	3	1	5	65.9	78.7	#	85.3	85.4	72.3
71	3	1	5	77.3	69.1	--	--	--	--
				4 lb/ft					
17	4	1	5	56.6	61.3 (63.9)*	65.2	82.0	85.5 (87.2)*	81.4
51	4	5	5	54.1 (0.83)	59.8 (0.42)	--	--	--	--
71	4	1	5	56.0	60.2	--	--	--	--
145*	4	3	5	--	44.4 (1.50)	--	--	--	--
			8	--	57.3 (1.50)	--	--	--	--

** Nominal yield stress

-- Test not run

() Standard deviation from the mean

* Results from TTI Project RF4277[3]

()* Splice assembled backwards

\# Stub cracked and allowed excessive deflection - bolt did fail at stroke limit.

TABLE 5.2. *SUMMARY OF BASE STRESS CALCULATED AT FIELD BOLT FAILURE FOR MARION POSTS IN CRITICAL AND NON-CRITICAL BENDING TEST CONFIGURATIONS.*

BENDING TEST RESULTS BASE STRESS AT BOLT FAILURE (ksi) Marion Posts - 80 ksi *									
Mom Arm (in)	Splice Length (in)	No of Tests	Gr Bolt	CRITICAL Back	CRITICAL Nest	CRITICAL Face	NON-CRITICAL Back	NON-CRITICAL Nest	NON-CRITICAL Face
				3 lb/ft					
17	3	1	5	78.0	92.6	82.2	107.6	116.5	103.4
71	3	1	5	66.0	65.7	--	--	--	--
			9	87.4	87.4	--	--	--	--
72	3	1	5	63.1	68.5	60.6	66.0	66.0	65.8
	4	1	5	88.7	87.2	77.1	86.8	93.1	86.1
	5	1	5	101.2	105.4	103.3	109.6	122.7	105.4
				4 lb/ft					
17	4	1	5	63.3	--	--	86.1	89.6	--
			8	--	--	71.3	--	--	99.6
			9	84.9	87.0	--	110.9	115.5	--
51	4	5	5	75.3 (1.06)	78.2 (1.47)	--	--	--	--
71	4	1	5	57.8	64.6	--	--	--	--
			9	78.8	83.5	--	--	--	--

** Nominal yield stress

-- Test not run

() Standard deviation from the mean

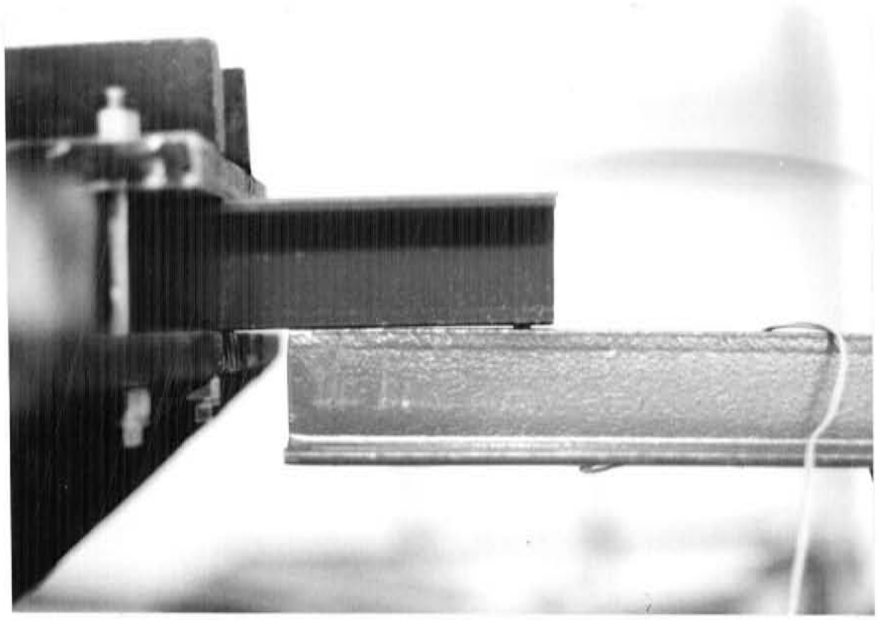

FIGURE 5.4. *PHOTOGRAPH ILLUSTRATING SEPARATION OF POST AND STUB IN BACK TO BACK SPLICE AS THE FAILURE LOAD IS APPROACHED.*

As the applied load increased and the resulting moment was transferred across the splice, part of the cross section begins to yield locally. As a result, the center of the compression force in the splice was not well defined. A bolt load envelope was therefore predicted and compared to the measured bolt tension (Appendix T).

BACK TO BACK SPLICES - CRITICAL CONFIGURATION

As a lower bound for the tension in bolt A (critical bolt for the critical configuration), consider the compressive force acting at the edge of the post (point O) in Fig. 5.5. All posts were punched with 0.375 inch diameter holes on one inch centers and all cuts were spaced equally between the holes, therefore λL can be set at 0.5 inches. Making this substitution and setting the moment at point O equal to zero results in the following equation

$$\sum M_o = 0; \qquad PL = (0.5)F_A + (S+0.5)F_B \qquad (5.1)$$

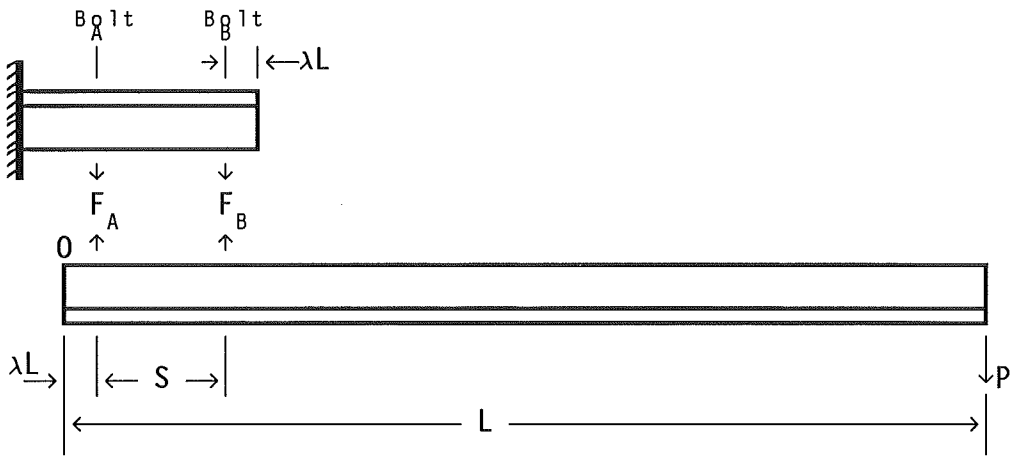

FIGURE 5.5. *FREE BODY DIAGRAM OF A BACK TO BACK SPLICE IN THE CRITICAL LOADING CONFIGURATION.*

where F_A and F_B corresponded to the tensile forces in bolts A and B. The strain in the post was assumed to be distributed linearly between point 0 and bolt B, and the following relationship for the strain in bolt A was derived

$$\epsilon_A = \frac{0.5\epsilon_B}{S+0.5} \tag{5.2}$$

Applying Hooke's Law, which states the deformation of an elastic body is directly proportional to the magnitude of the applied force, provided the elastic limit is not exceeded, and solving for F_{A1} results in

$$F_{Au} = \frac{0.5F_{B1}}{S+0.5} \tag{5.3}$$

Substituting equation 5-3 into 5-1 and solving for F_{B1} yields

$$F_{B1} = \frac{PL}{\frac{(0.5)^2}{(S+0.5)} + S + 0.5} \tag{5.4}$$

where F_{Au} and F_{B1} corresponded to the upper and lower limits of the force on bolts A and B, respectively.

The same free body diagram was used to develop the upper bound tension equation for bolt A since the center of the compressive load was assumed to coincide with bolt A. Setting the moment about bolt A equal

to zero, and solving for the force in bolt B gives the following relationship

$$\sum M_{Bolt_A} = 0; \qquad F_{Bu} = \frac{P(L-0.5)}{S} \tag{5.5}$$

Since the center of compression was assumed to act through bolt A, the tension in the bolt was constant and was therefore a lower bound.

BACK TO BACK SPLICES - NON-CRITICAL CONFIGURATION

Developing the bolt tension equations for the non-critical splice configuration required a different free body diagram (Fig. 5.6). As in the critical loading case, the lower bound equation for the tension in bolt A was derived by assuming the compressive force acted at the edge of the stub (point O). Summing moments about this point gave the following relationship

$$\sum M_o = 0; \qquad P(L-0.5-S-0.5) = (S+0.5)F_A + 0.5F_B \tag{5.6}$$

Making the same strain assumptions as the critical case, applying them to the non-critical free body diagram, and solving for F_B resulted in

$$F_{Bu} = \frac{0.5F_{A1}}{S+0.5} \tag{5.7}$$

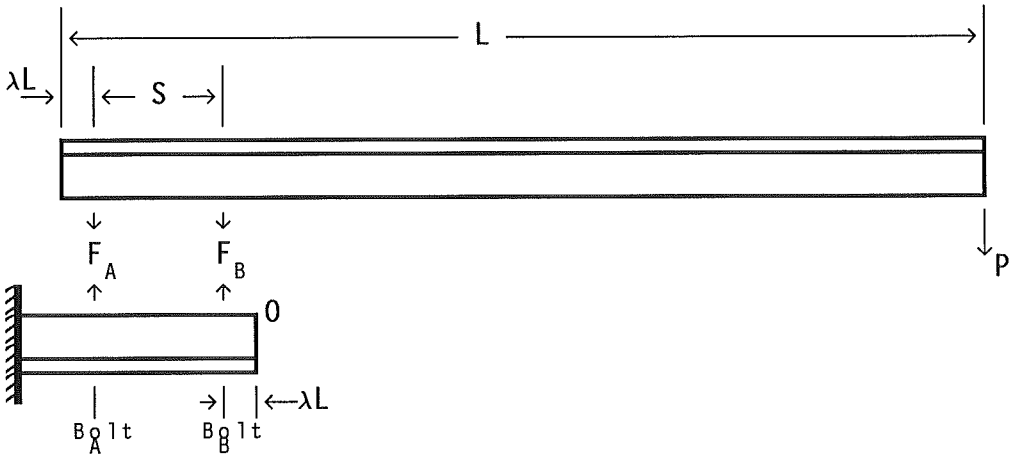

FIGURE 5.6. *FREE BODY DIAGRAM OF A BACK TO BACK SPLICE IN THE NON-CRITICAL LOADING CONFIGURATION.*

Substituting equation 5-7 into 5-6 and solving for F_{Al} yielded

$$F_{Al} = \frac{P(L-S-1.0)}{\frac{(0.5)^2}{(S+0.5)} + S + 0.5} \tag{5.8}$$

In this case, F_{Al} and F_{Bu} correspond to the upper and lower bounds for the bolt loads in a non-critical splice configuration.

The upper bound bolt tension equations were obtained by assuming that the center of the compression force was at bolt B. Setting the moments about this point equal to zero and solving for F_A resulted in

$$\sum M_{B_B lt} = 0; \qquad F_{Au} = \frac{P(L-S-0.5)}{S} \tag{5-9}$$

where F_{Au} was the predicted upper bound tension in bolt A. Since this derivation assumed the tension in bolt B remaind constant, it was the lower bound for a back to back splice in the non-critical configuration.

NESTED SPLICES - CRITICAL CONFIGURATION

Nested splices were assembled with a spacer placed between the post and stub at bolts A and B (Fig. 2.4) to prevent the stub from being drawn into the post and subsequently distorting the sections as the bolts were tightened. The location of the compressive load transfer was limited to these spacers, therefore a separate free body diagram was considered (Fig. 5.7). The lower bound for the predicted tension in bolt B (critical bolt for this configuration) was derived by assuming the compressive force was located at the edge of the spacer (point O). Equilibrating moments about this point resulted in the following relationship

$$\sum M_o = 0; \qquad P(L-\lambda L+0.4) = (0.4)F_A + (S+0.4)F_B \tag{5.10}$$

Where 0.4 is the radius of the spacer in inches. Linear strain and Hooke's law were assumed and the upper limit for the force in bolt A was found to be

$$F_{Au} = \frac{0.4F_{Bl}}{S+0.4} \tag{5.11}$$

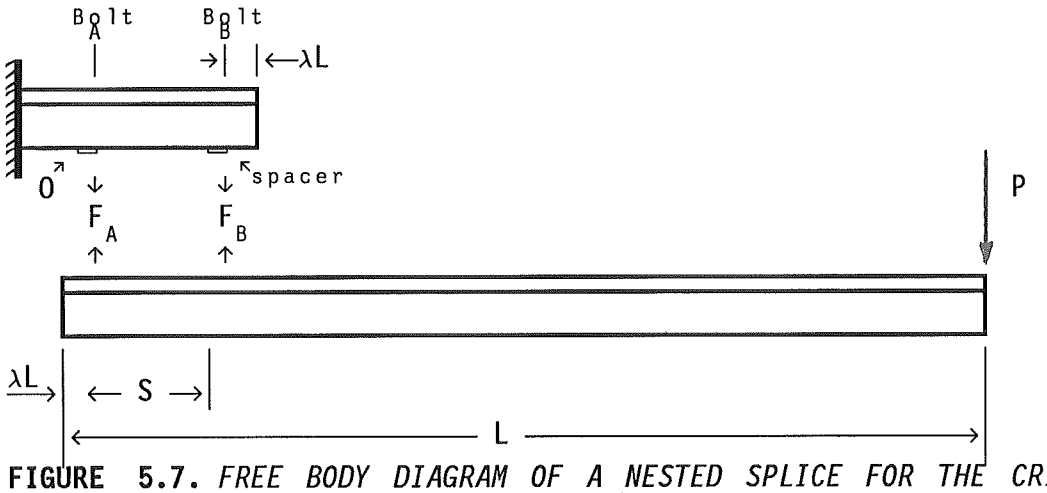

FIGURE 5.7. *FREE BODY DIAGRAM OF A NESTED SPLICE FOR THE CRITICAL LOADING CONFIGURATION/*

Note that the only difference between the nested and back to back equations for predicted bolt tension in critical loading was the distance between the center of the bolt and the edge of the spacer or post. Since the nested splice was assembled with 0.8 inch diameter spacers, the distance to the compressive load was 0.4 instead of 0.5 inches for the back to back case. The moment arm for a nested critical splice was therefore (L-0.1) instead of (L) as in a back to back splice. Substituting L-0.1 for L and 0.4 for 0.5 into equation 5.8 enabled the lower bound tension in bolt B to be written directly as

$$F_{B1} = \frac{P(L-0.1)}{\frac{(0.4)^2}{(S+0.4)} + S + 0.4} \tag{5.12}$$

with the upper bound expressed by

$$F_{Bu} = \frac{PL}{S} \tag{5.13}$$

Again, the center of compression was assumed to act at bolt A so bolt tension was predicted to remain constant.

NESTED SPLICES - NON-CRITICAL CONFIGURATION

Bolt tension equations for this load case were derived the same as the non-critical back to back splice, the exception being the distance from bolt B to the compressive load (point O). Referring to Fig. 5.8 and equations 5.6-9, the upper and lower bounds for the tension in bolts A and B could be written directly as

$$F_{Au} = \frac{P(L-S-0.4)}{S} \qquad F_{Al} = \frac{P(L-S-0.9)}{\frac{(0.4)^2}{(S+0.4)} + S + 0.4} \tag{5.14}$$

and

$$F_{Bl} = \text{constant} \qquad F_{Bu} = \frac{0.4F_{Al}}{S+0.4} \tag{5.15}$$

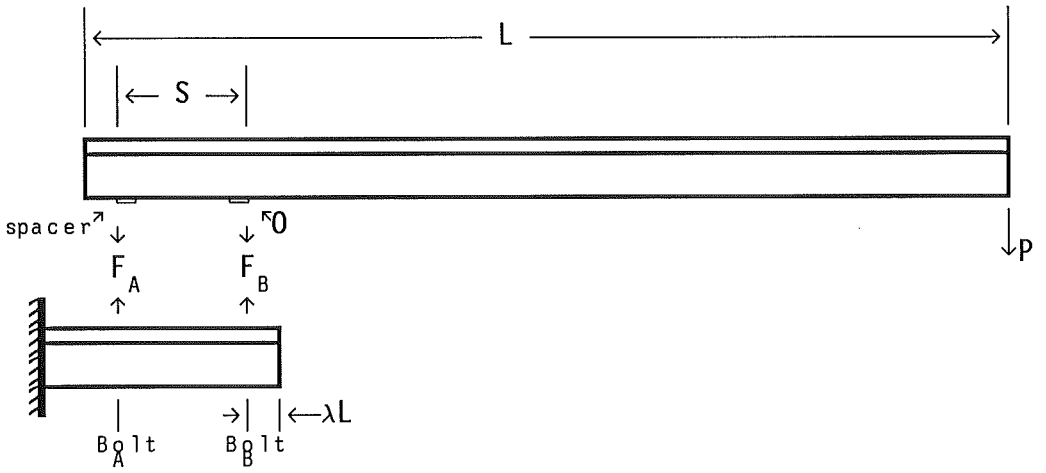

FIGURE 5.8. *FREE BODY DIAGRAM FOR A NESTED NON-CRITICAL LOADING CONFIGURATION.*

Note that in all four splice configurations the lower bound tension for the non-critical bolt was predicted to remain constant if no local yielding occurred in the u-post sections or the spacers.

FACE TO FACE SPLICES

Since the compressive loads were transferred through physical contact between the post and stub at the section faces, the geometry and load transfer mechanics for face to face and back to back splices are identical. As a result, the equations derived for back to back splices apply.

5.2.2 BOX SPLICES

Load is transferred from the post to the stub through bearing between the box and post sections, so the bolt is a non-structural element. The load distribution along the box was assumed linear and independent of the splice configuration (back to back or face to face). Box loads for both back to back and face to face splices in the critical configuration were derived by looking at a free body diagram of the box section (Fig. 5.9). The strains were assumed to remain elastic and distributed linearly from the front to the rear of the channel, and the following equation was obtained

$$\sum M_o = 0; \qquad F(x) = \frac{3(17P)}{x^2} \qquad \text{for } 0 < X < 4" \qquad (5.16)$$

where F(x) has units of pounds inch. If the post is installed on the other side of the stub (Fig. 5.10), a non-critical load configuration

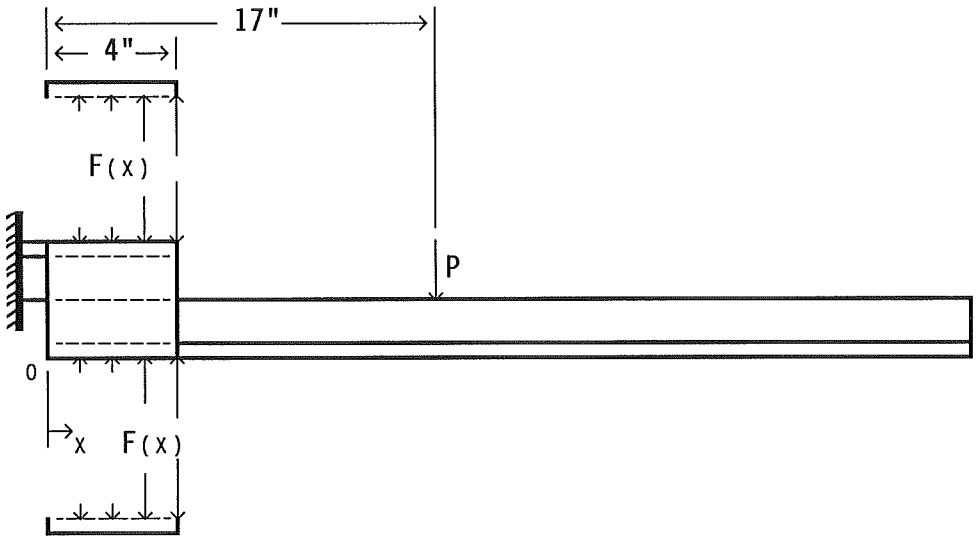

FIGURE 5.9. *FREE BODY DIAGRAM OF A BACK TO BACK BOX SPLICE IN THE CRITICAL CONFIGURATION ILLUSTRATING LOADS ON BOX SECTION.*

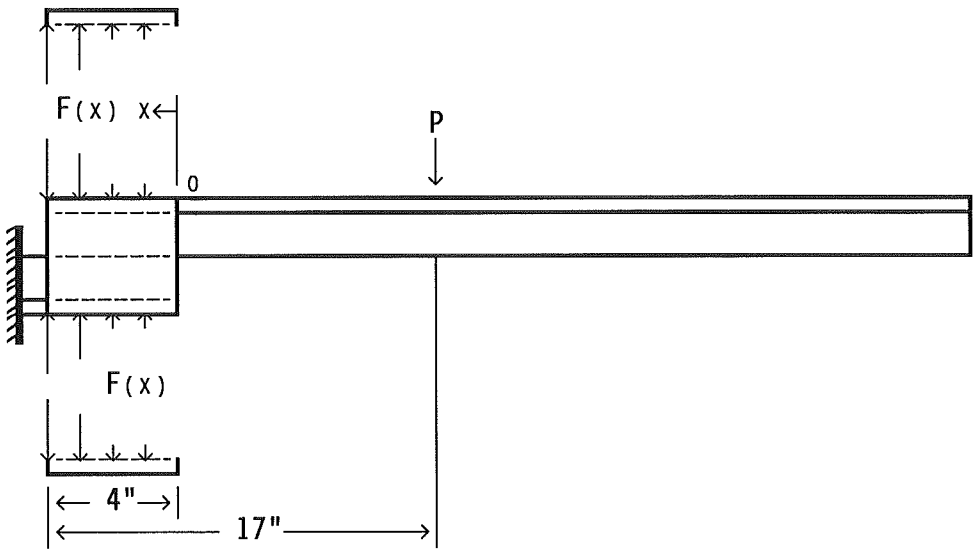

FIGURE 5.10. *FREE BODY DIAGRAM OF A BACK TO BACK BOX SPLICE IN THE NON-CRITICAL ORIENTATION.*

results. Setting the moments about point 0 equal to zero gives the following box section load

$$\sum M_o = 0; \qquad F(x) = \frac{3P(17-S)}{x^2} \qquad \text{for } 0 < X < 4" \qquad (5.17)$$

where S is the length of the box section (4 inches).

5.3 SPLICE PERFORMANCE IN BENDING

5.3.1 BACK TO BACK AND NESTED SPLICES

Marion posts (80 ksi) were found to have less deflection than Franklin (60 ksi) posts at a given base stress. Deflection is a function of M/EI, (Equation 1.2) so the only variable at a given base stress is the sections moment of inertia. Since the *actual* yield stress of the signposts was never reached and the measured deflection correlated to the sections inertia, the increased deflection for Franklin posts is attributed to the lower inertia of the section rather than the lower nominal yield stress of the steel.

Base stress calculated at bolt failure for back to back splices was found to be 5% lower than nested splices when loaded in the non-critical configuration. This is most likely due to the restraint imposed on the bolts in the back to back configuration rather than the load transfer

mechanics (Section 5.3). Nested splices (Fig. 2.4) were assembled with washers for spacers (Table 2.1). The holes punched in the washers are larger in diameter than the bolts, so the washers are capable of sliding over one another and undergoing small lateral and longitudinal displacements. This displacement relieves strain in the bolt by allowing the bolt to rotate relative the stub. A back to back splice (Fig. 2.3) has no spacer so the same longitudinal or lateral loads result in bending and shear strains in the bolt. These strain effects may be cause of critical field bolt failures at 75-85% of the proof load of the bolts (7.5 kips for grade 5, and 11.2 kips for grade 9).

Relative bolt tension measured in the critical bolt at a given base stress was higher for Marion than Franklin posts (Fig. 4.3). This was a result of the higher stiffness (moment if inertia) of the section as discussed above. The relative critical bolt tension in nested splices was 20% higher than back to back splices. This was probably the result of the area of compressive load transfer and the resulting stiffness of the splice. The area of compressive load transfer in a back to back splice is distributed along the length of the splice. Compression transfer in a nested splice however, is limited to the spacer around the non-critical bolt. Less restraint is therefore imposed in bending on the cross section between the bolts in a nested splice and the post was able to rotate around the spacer surrounding the non-critical bolt (Fig. 5.7). Back to back splices have the post and stub in contact through the length of the splice (Fig. 5.5) so bending stresses in cross section aided in resisting the bending loads and reducing the tension in the critical bolt. As a result, the critical bolt tension increases faster for a nested splice.

5.3.2 FACE TO FACE SPLICES

Stability problems in the face to face splices (Fig. 2.5) centered around the geometry of the splice and the spacer lengths required between the post and stub (Table 2.1). The function of the spacers in a face to face splice was to keep the cross sections from being drawn together during assembly. As the bolts were tightened, the compressive forces were distributed at the face of the cross section only until the spacer bears against the back of the post and stub. This initial deflection (1/32 inch) induced negligible bending stresses in the cross section. Once the spacers contacted the post and stub backs any additional increase in bolt tension was tramsmitted to the spacer. As a result, the

spacers limited the stresses in the signpost and eliminate the chance of yielding the post or stub during assembly.

The rotation of the splice in its non-critical orientation (Fig. 5.11) was attributed to local yielding of the spacer surrounding bolt B where it bears against the post and stub (Fig. 5.12). As load was applied to the post, the zone of compression in the faces shifted toward the end of the stub and the tension in bolt A increased, this in turn induced higher compressive stresses at the front of the spacer surrounding bolt B. Since the spacer material was common 1/2 inch diameter 36 ksi pipe, it began to yield at a stress where the post (60 - 80 ksi) was elastic (Fig. 5.13). As the compression force at the face of the post and stub increased, the cross section distorted and the spacer yielded, resulting in 2.7 kips of tension loss in bolt B (Fig. 5.14). Also, as the tension in bolt A increased, the compression in the spacer surrounding Bolt A decreased.

The compression in the spacer surrounding bolt A decreased as the tension in bolt A increased due to load transfer and the tension in bolt B decreased due to the yielding of the spacer surrounding it. Because the compression in both spacers decreased, the lateral stability of the splice was reduced. Since the lateral stability of a face to face splice depends on compression in the spacers induced by bolt tension, the splice offered little resistance against lateral forces or an eccentricity in the applied load. A similiar situation existed in a non-critical loading of a nested splice (Fig. 2.4). Nested splices remained stable because the maximum spacer length was 1/2 instead of 3-1/16 inches for the face to face splice. As a result, the bolts were loaded in shear instead of the spacers being loaded in bending.

The stability problem was observed only in the 17 inch bending tests because the load source (MTS 20 kip actuator) was mounted to a beam through a universal joint to insure only axial compression is applied through the load cell. This joint provided a hinge at the beam (ie: no lateral restraint capicity), and the translation of the post occurred when the lateral load due to eccentricity (F_e) exceeded the lateral capacity of the splice (Fig. 5.15).

FIGURE 5.11. *PHOTOGRAPH OF 18 INCH LATERAL TIP DEFLECTION MEASURED DURING A FACE TO FACE TEST IN THE NON-CRITICAL CONFIGURATION.*

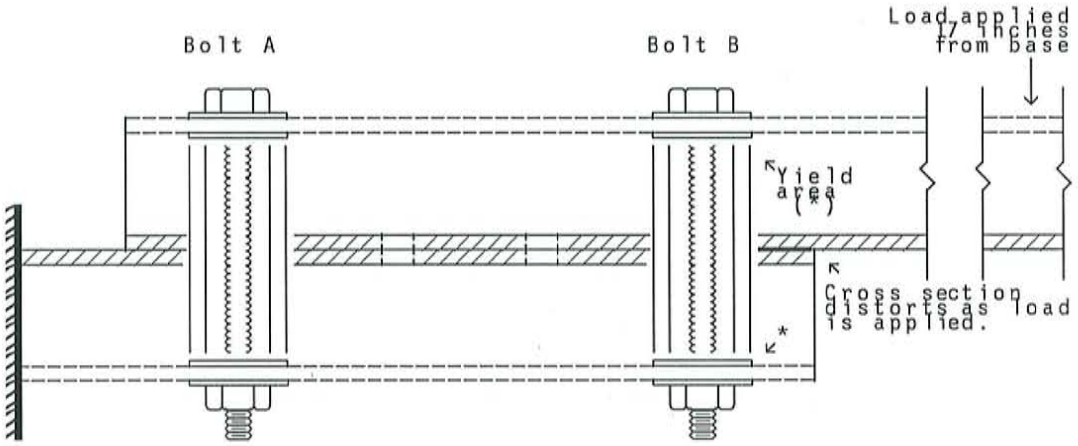

FIGURE 5.12. *CROSS SECTION OF FRANKLIN FACE TO FACE SPLICE (NON-CRITICAL ORIENTATION) SHOWING LOCATION OF LOCAL YIELDING IN FRONT SPACER.*

FIGURE 5.13. *PHOTOGRAPH ILLUSTRATING LOCAL YIELDING AT THE ENDS OF THE SPACER SURROUNDING BOLT B.*

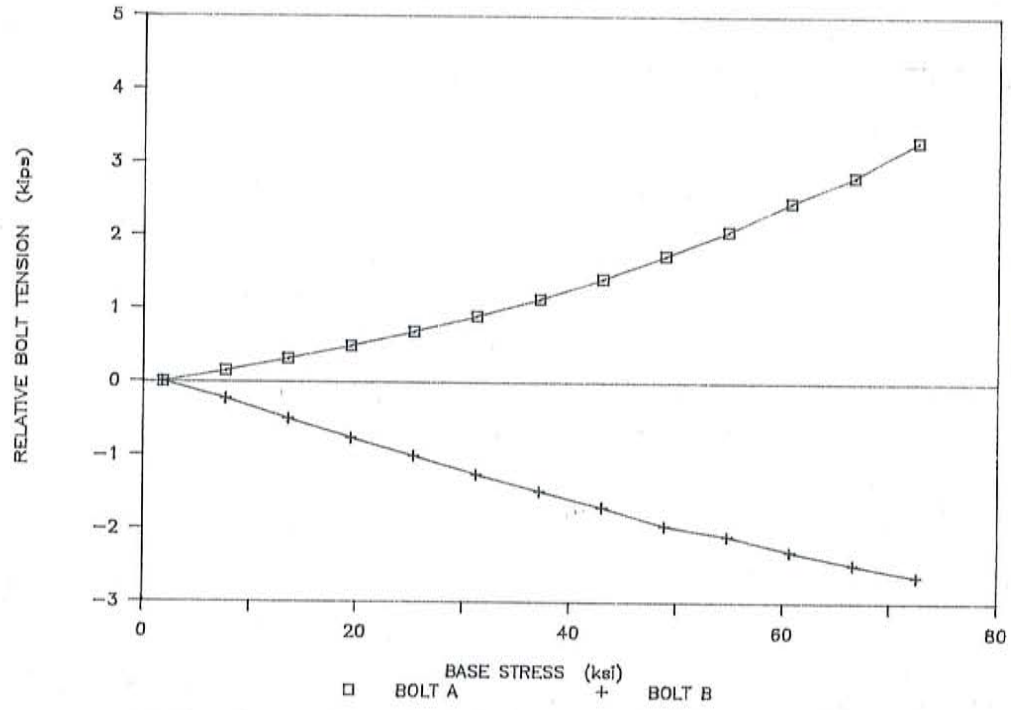

FIGURE 5.14. *BASE STRESS VS RELATIVE BOLT LOAD FOR A MARION 4 LB/FT FACE TO FACE SPLICE (NON-CRITICAL ORIENTATION)*

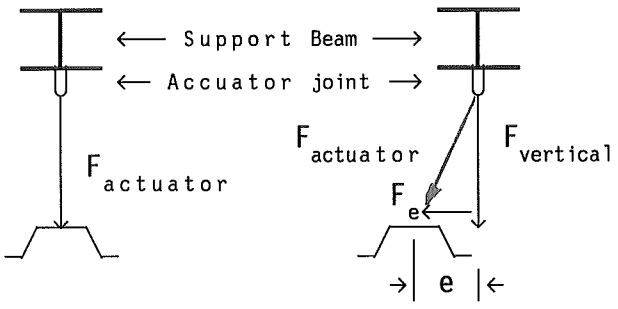

FIGURE 5.15. *ILLUSTRATION OF LATERAL LOAD APPLIED TO U-POST DUE TO LOAD ECCENTRICITY.*

Lateral instability was not observed in the 71 inch bending tests because the load was applied to the post by hanging weights from the post tip (Fig. 3.2). Because a gravity load was applied, the splice was not subject to lateral forces due to eccentricity. As a result, the lateral load on the splice was reduced and the failure mechanism for the 17 inch tests was not seen. The stability in the splice may have been corrected by a more sophisticated spacer design, however since simplicity of the splice was essential, the face to face design was not pursued.

5.3.3 BOX SPLICES

Splices made up of box sections (Fig. 2.6) were eliminated due excessive post deflection resulting from yielding in the box section. Since the nominal yield stress of the Franklin posts was 60 ksi, the box section (36 ksi) began to deform before the yield stress of the post was reached. This resulted in yielding in areas of load transfer concentration. In addition to large post deflections, the splice, which was tight at the onset of a test, became loose due to 1/4 inch distortion at the front of the box section and 1/8 inch distortion on the sides (Fig. 5.16).

The load transfer path across the front rather than along the length of the box was found to control yielding in the section. Load was transferred through a back to back box splice (Fig. 5.17A), in bearing at the corners of the box section. However in a face to face box splice (Fig. 5.17B) the resulting stresses are transferred through the center of the box section. The corners of the box section are stiffer than the center, therefore the box section distorts more in face to face configuration. Increasing the box length would have increased the

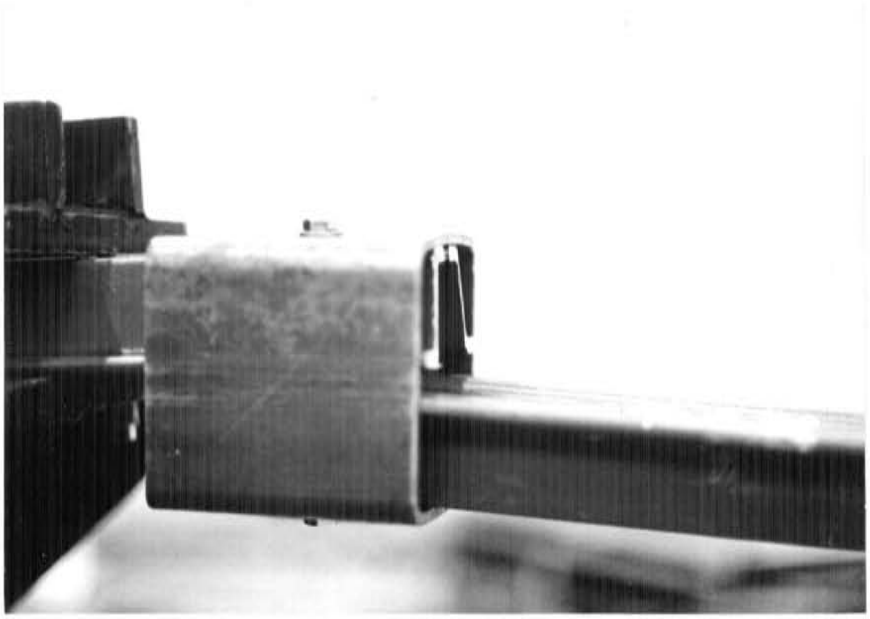

FIGURE 5.16. *PHOTOGRAPH OF BOX SECTION DEFORMATION RESULTING FROM LOAD TRANSFER.*

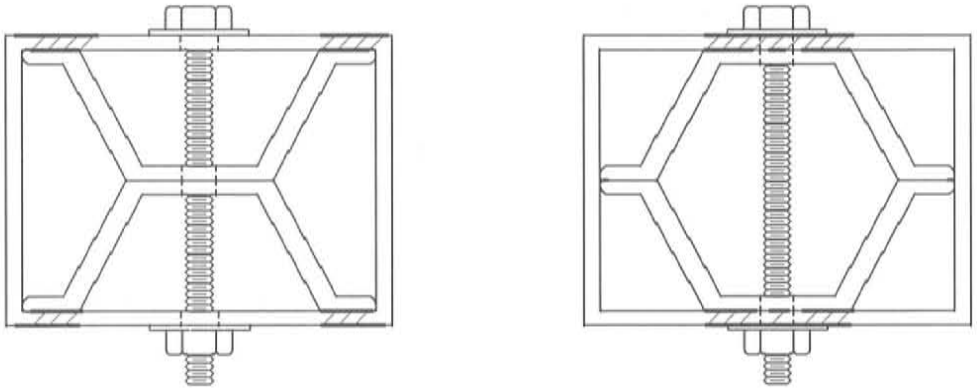

FIGURE 5.17. *END VIEW OF (A) BACK TO BACK AND (B) FACE TO FACE BOX SECTION SPLICES ILLUSTRATING CHANNEL LOADS.*

capacity of the box splice, but the main purpose of a box section was to reduce the total splice length to 4 1/2 inches (bolted splice heights are 5 1/2 inches for 4 lb/ft posts), therefore increasing the box length was not considered. In addition, commonly available materials were a criteria for all splice designs, the use of a higher strength steel was not considered. Finally, aligning and inserting the bolt through holes in the post, stub and box was a tedious operation in the lab and

therefore undesireable for field assembly. As a result, box section splices were rejected.

5.4 SPLICE PERFORMANCE IN TORSION

5.4.1 BACK TO BACK SPLICES

The bolt load plateau observed with the Marion posts was due to the cross sectional shape. When a Marion post and stub were assembled in a back to back configuration, the resulting compression on the section was concentrated at the raised ribs on either side of the section (Fig. 5.18). As torque was applied, load was transferred through the splice as an increase in the compressive forces on one rib and a reduction on the other. The bolts in the splice did not resist the applied torsion until the compression on the rib of one side of the section approached zero. Once this plateau torque was reached, additional torsion was resisted by the bolts in the splice and the measured tension.

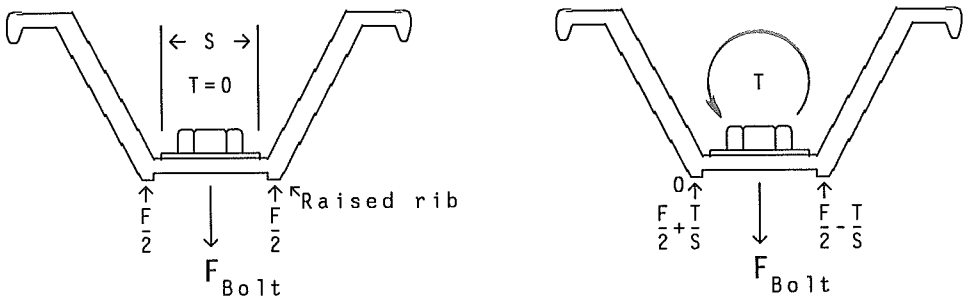

FIGURE 5.18. *ILLUSTRATION OF TORSIONAL LOAD TRANSFER AT THE RIBS DURING BOLT LOAD PLATEAU PHASE (T < F/2s) FOR MARION POST WITH A BACK TO BACK SPLICE.*

Franklin posts were not rolled with the raised ribs, and as a result, the measured bolt loads had a lower plateau torque. Bolt loads were found to increase after 66 degrees of rotation for a 4 lb/ft post. Since there was no area to concentrate the initial compression, the compression zone was distributed across the backs of the post and stub and less torque was required to shift the compression zone to one side (Fig. 5.19). Once the compressive bearing forces were shifted to one side, the post and stub sections began to rotate relative to each other around the the edge of contact (point 0 in Fig. 5.19) and equlilibrium was maintained with an increase in bolt tension.

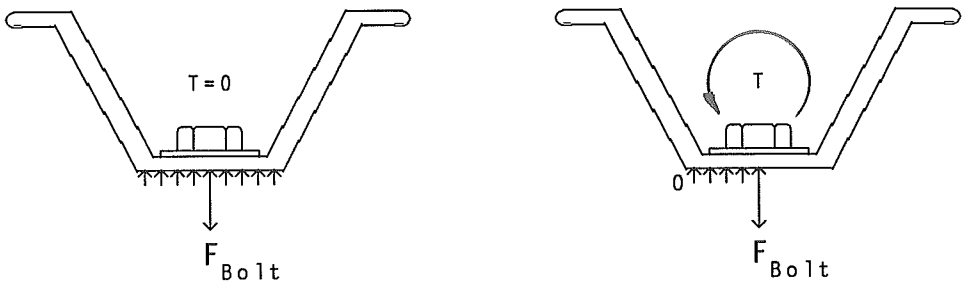

FIGURE 5.19. *ILLUSTRATION SHOWING TORSIONAL LOAD TRANSFER FOR FRANKLIN POSTS WITH A BACK TO BACK SPLICE RESULTING IN SHORT PLATEAU PHASE.*

5.4.2 NESTED SPLICES

Nested splices were found to experience a bolt load plateau in the initial section of the torsion tests. Splices using Franklin posts were rotated 105 and 65 degrees before the bolt tension began to increase for 3 and 4 lb/ft posts respectively. Marion posts demonstrated the same plateau through 80 and 25 degrees for the same post weights.

Franklin posts were able to undergo more rotation than Marion posts before transferring the torsional loads to the bolts because the cross section has greater torsional stiffness. Since Franklin posts are smaller in dimension (height and width) than Marion posts, the legs of the section are thicker and the torsion constants for Franklin 3 and 4 lb/ft posts are 70% and 37% greater than Marion 3 and 4 lb/ft posts.

Section stiffness is related to measured bolt tension through the torsional load transfer in the splice. In the absence of applied torque, the spacers surrounding the bolts were placed in uniform compression and the both legs of the section were in contact (Fig. 5.20). As torque was applied, the post and stub distort and rotate relative to one another about the spacers edge. The legs begin to bear in compression on one side and the rotation within the splice was restrained by the sections torsional stiffness. As the applied torque increases, the stiffness of the section becomes insufficent to resist the loads without excessive rotation. As a result, the back of the section begins to rotate about the spacers edge in Fig. 5.20, and equilbirium was maintained as the tension in the bolts increased.

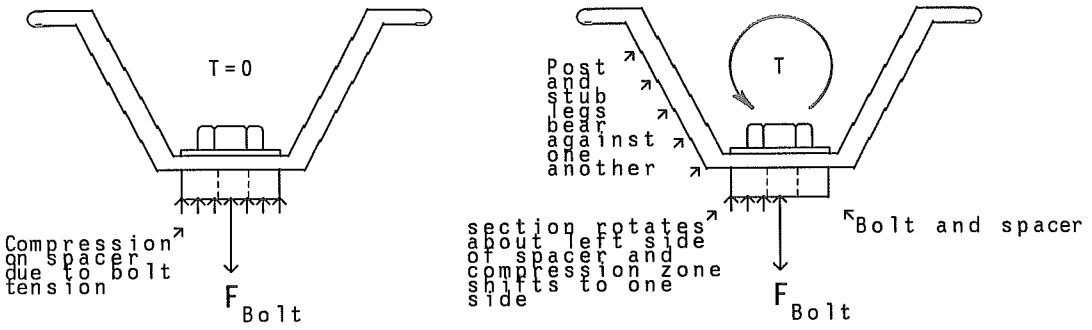

FIGURE 5.20. *ILLUSTRATION SHOWING TORSIONAL LOAD TRANSFER THROUGH A NESTED SPLICE.*

5.4.3 COMPARISON OF BACK TO BACK AND NESTED SPLICES

Once the bolt tension began to increase, the rate of change was slower for nested than back to back splices. However, the increase in bolt tension was the same for Franklin and Marion posts using the same splice (Fig. 4.7) since the dimensions across the backs of both posts (S in Fig. 5.18) were within 1/8 inch. In a back to back splice, once the bolt tension plateau is exceeded, the bolt tension change is

$$T_{Bolt} = \frac{Torque}{(S/2)} \qquad (5.18)$$

Since S was similiar for both manufacturers, the measured tension increase was also similiar. Relative bolt tension for nested splices, although lower than back to back splices due to the torsional resistance of the post and stub in bearing (discussed above), were similiar for the same geometric reasons.

5.5 SPLICE PERFORMANCE IN COMBINED BENDING AND TORSION

Combined bending and torsion tests were run on back to back and nested splices in the critical configuration and base stress was calculated as a principal combination of bending stresses as well as shear and partial warping stresses due to torsion (Section 1.2). The change in eccentricity for the applied load was calculated as a function of the measured tip rotation (Section 3.3). Field bolt failure occurred after 40 to 50 and 35 to 40 degrees of rotation for 3 and 4 lb/ft posts respectively. Base stress calculated at bolt failure indicated that both back to back and nested splice designs were capable of developing the nominal yield strength of the post in combined bending and torsion.

Furthermore, the base stress developed at field bolt failure exceeded that for bending alone. This apparent strength increase in combined bending and torsion is due to the splices ability to transfer torsion through the plateau phase without a corresponding increase in bolt tension as discussed in Section 5.4.

The magnitude of applied load at field bolt failure for combined bending and torsion decreased relative to bending alone. This behavior was due to the shear load imposed on the critical bolt (bolt B) in the combined tests. The eccentricity of the applied load induced torsion in the cross section and as the splice rotated, shear as well as tension was transmitted to bolt B.

Back to back splices failed in combined bending and torsion at 9% to 26% lower loads than in bending alone. Nested splices were found to fail at 1% to 18% lower loads for the same criteria (Table 5.3). This behavior futher demonstrates the relation of section stiffness to load transfer for nested splices as described in Section 5.3.

Marion back to back tests exhibited a bolt tension plateau similiar to the torsion tests (Section 5.5). Measured tension in the non-critical bolt (bolt A) was found to decrease as described in Section 5.2. The variance in the rate of change in measured bolt tension between a back to back and nested splice for 3 lb/ft posts was 9% and 17% higher for Franklin and Marion posts respectively. The opposite behavior was observed in the 4 lb/ft posts. Slope change was found to be 11% and 23% less for nested than back to back splices with Franklin and Marion posts. Since only one test was run, and the trends for increasing bolt tension were contradictory, no correlation was made between splice configuration and post manufacturer.

TABLE 5.3. *SUMMARY OF BASE MOMENTS AT FIELD BOLT FAILURE FOR BENDING AND COMBINED BENDING AND TORSION TESTS (CRITICAL CONFIGURATION).*

BENDING AND COMBINED BENDING AND TORSION
TEST RESULTS (Critical Configuration)

BASE MOMENT AT FIELD BOLT FAILURE (k-in)

Franklin Posts - 60 ksi ***
Marion Posts - 80 ksi ***

Post Manu * (lb/ft)	Splice Length (in)	Gr Bolt	BENDING ** Back to Back	BENDING ** Nested	BENDING & TORSION (Incl Warping)** Back to Back	BENDING & TORSION (Incl Warping)** Nested
F (3)	3	5	30.6	27.2	23.7	23.7
F (4)	4	5	30.6	32.9	28.4	34.4
M (3)	3	9	35.1	35.1	29.5	33.3
M (4)	4	9	41.9	44.5	40.5	42.3

* F: Franklin
M: Marion

** Moment arm for bending test was 71 in.
Moment arm for combined bending & torsion test was 75 in.

*** Nominal yield stress

5.6 *EFFECTIVE SPLICE LENGTH*

The effective splice length (ESL) is an empirical parameter that is used to evaluate the efficiency of a bolted splice. ESL is defined as the distance from the center of compression (COC) to the critical bolt (bolt A for the critical and bolt B for the non-critical configuration). The assumption of the effective splice length calculation is that the ideal splice design is achieved when the ESL equals the actual splice length (S) when the signpost is loaded in bending.

The ESL was calculated by ignoring the non-critical bolt (ie: assuming $F_A = 0$) and forcing the moment inside the splice to equal the moment at the front of the splice. For example, equilibrating moments to the right and left of the non-critical bolt (bolt A) in Fig. 5.21 gives

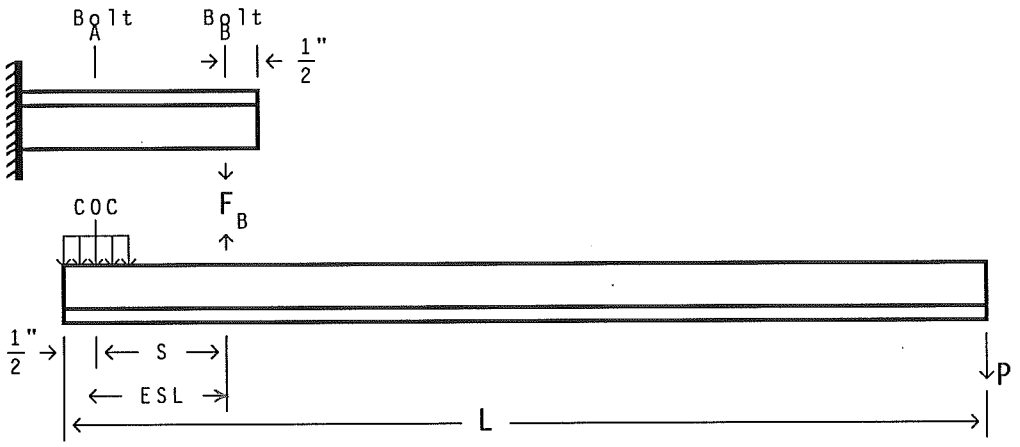

FIGURE 5.21. *FREE BODY DIAGRAM OF BACK TO BACK SPLICE FOR THE CRITICAL ORIENTATION.*

$$\sum M_{Bolt_A} = 0 \qquad \Delta F_B(ESL) = P(L-S-0.5) \qquad (5.19)$$

where ΔF_B was the tension change in bolt B. Solving this equation for ESL results in

$$ESL = \frac{P(L-S-0.5)}{\Delta F_B} \qquad (5.20)$$

If the ESL from the above equation exceeded the actual splice length (S), the center of compresson would lie outside the splice and the subsequent tension increase for bolt A must be included. Linear strain was assumed and the moments to the right and left of bolt B equal were equilibrated resulting in

$$ESL = \frac{P(L-S-0.5)+\Delta F_A(S)}{\Delta F_A+\Delta F_B} \qquad (5.21)$$

The ESL for back to back and nested splices in the non-critical orientation were derived in a similiar manner (Table 5.4).

ESL equations for face to face splices were not included in Table 5.4 because the splice was rejected. However, calculations would proceed the same as the back to back splices because the relative bolt, stub and post geometry of the two splices were identical.

ESL values (Table 5.5) were calculated with the formulae that apply for ESL $\leq$ S. ESL values in parentheses were calculated using the equations that apply when ESL > S. Asterisks indicate that the non-critical bolt measured no increase in tension for any part of the test so equation 5.21 cannot be applied.

Values were also omitted where splice failure resulted from bolt fatigue. The calibrated bolts were found to last 20 to 25 tests before failing. All failures originated at the cone tip formed when the bolts were bored for strain gauge insertion (Fig. 5.22). Omitted values were the result of non-linear strains measured as the fatigue crack grew to critical length.

TABLE 5.4. *SUMMARY OF EFFECTIVE SPLICE LENGTH FORMULAE OF THE CRITICAL ORIENTATION FOR BACK TO BACK AND NESTED SPLICES, AND NON-CRITICAL ORIENTATION FOR NESTED SPLICES.*

Case	Back to Back (crit)	Nested (crit)	Nested (non-crit)
ESL $\leq$ S	$\frac{P(L-0.5)}{\Delta F_A}$	$\frac{P(L-S-0.4)}{\Delta F_B}$	$\frac{P(L-0.4)}{\Delta F_A}$
ESL > S	$\frac{P(L-0.5)+\Delta F_A(S}{\Delta F_A+\Delta F_B}$	$\frac{P(L-S-0.4)+\Delta F_B(S)}{\Delta F_A+\Delta F_B}$	$\frac{P(L-0.4)+\Delta F_A(S)}{\Delta F_A+\Delta F_B}$

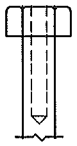

FIGURE 5.22. *ILLUSTRATION OF CONE FORMED IN BOLT SHANK.*

The loss of tension in the non-critical bolts (bolt A for critical and bolt B for non-critical orientations) resulted from a combination of local yielding and bearing. Local yielding in the region of the non-critical bolt reduced the load transfer to that bolt. Cracking and crushing of the paint in the region of the non-critical bolt may account for the typical observed tension loss of up to 1 kip (.0003 inches of deformation corresponds to a 1 kip tension loss) as seen in Fig. 5.23.

No measured tension loss was attributed to slip in the strain gauge epoxy. The bolts assembled with the Micro Measurements AE-10 epoxy had no significant hysteresis through their calibrated load cycle (Fig. 5.24). The TML epoxy, did not perform as well and was only used in the first series of bolts. These bolts were used in the initial 71 inch tests of the Marion 3 lb/ft posts and as a result, the confidence in the bolt readings for these tests results was limited.

Since the ESL is a empirical representation of the performance of a splice, a correlation between the calculated and actual splice lengths had a 20% higher calculated ESL than the non-critical tests (Table 5.5,6). Although this illustrated that the critical loading case was more efficient and therefore critical, the calculated splice lengths exceed the actual splice lengths by 0.8 inches to 2.9 inches. Since the stub or spacer extended 0.4 to 0.5 inches from the non critical bolt, there was no material to transfer the compressive forces at the calculated splice length, and the ESL was meaningless for this case.

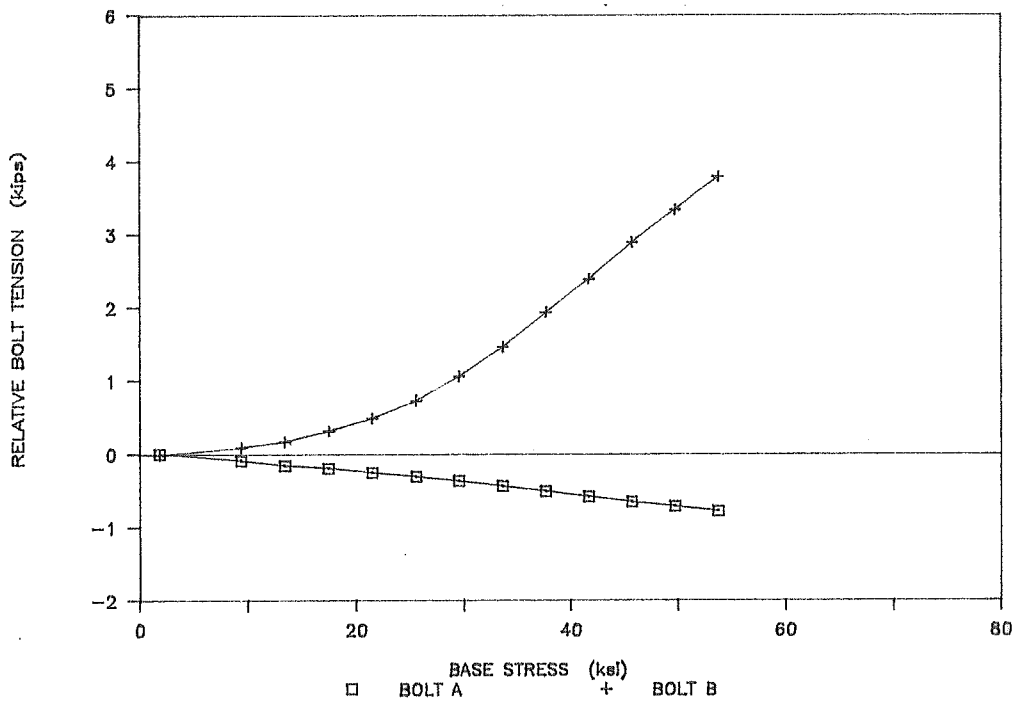

FIGURE 5.23. *BASE STRESS VS RELATIVE BOLT LOAD FOR MARION 4 LB/FT BACK TO BACK SPLICE (NON-CRITICAL ORIENTATION).*

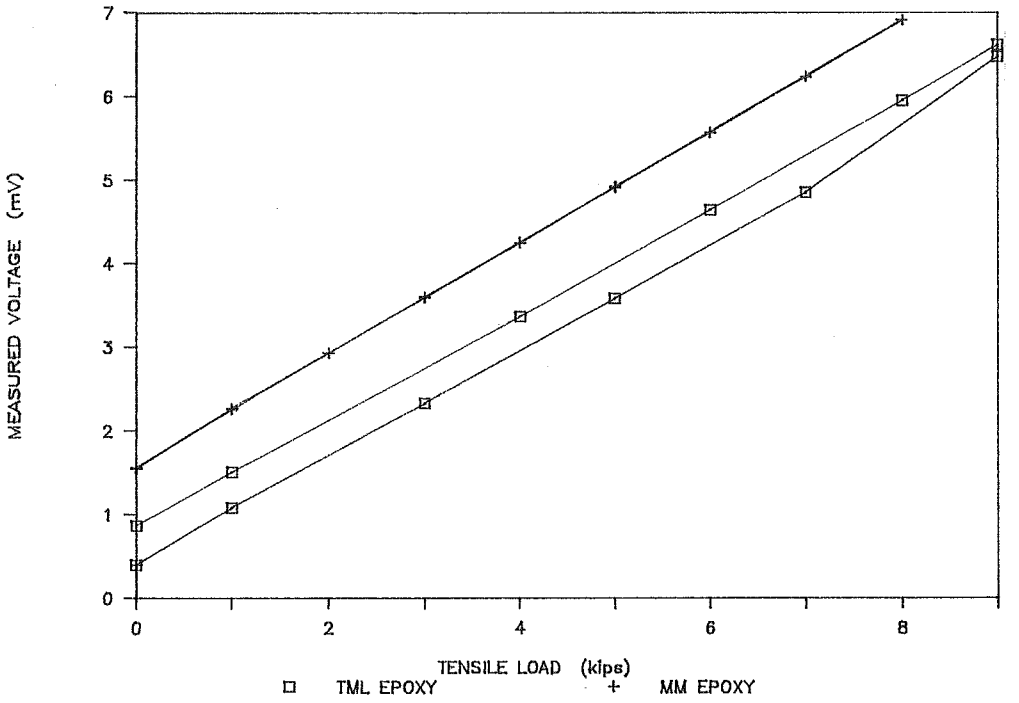

FIGURE 5.24. *CALIBRATION CURVE FOR A STRAIN GAUGED BOLT ASSEMBLED WITH TML AND MICRO MEASUREMENTS AE-10 EPOXY LOADING AND UNLOADING PHASE.*

TABLE 5.5. *SUMMARY OF EFFECTIVE SPLICE LENGTHS FOR FRANKLIN POSTS IN BENDING TESTS.*

BENDING TEST RESULTS EFFECTIVE SPLICE LENGTH (in) Franklin Posts - 60 ksi *								
Moment Arm (in)	Splice Length (in)	CRITICAL Back	CRITICAL Nest	CRITICAL Face	NON-CRITICAL Back	NON-CRITICAL Nest	NON-CRITICAL Face
		3 lb/ft					
17	3	3.3 (3.3)	3.5 (3.4)	3.4 **	4.0 (4.0)	4.5 (4.4)	3.8 **
71	3	3.8 (3.8)	3.4 (3.2)	-- --	-- --	-- --	-- --
		4 lb/ft					
17	4	4.4 **	4.7 **	4.4 **	5.6 (5.6)	6.1 (6.1)	6.3 **
71	4	4.0 **	3.8 (3.8)	-- --	-- --	-- --	-- --

* Nominal yield stress

-- Test not run

** Effective splice length calculation not valid

() Effective splice length based on both bolts

TABLE 5.6. *SUMMARY OF EFFECTIVE SPLICE LENGTHS FOR MARION POSTS IN BENDING TESTS.*

BENDING TEST RESULTS EFFECTIVE SPLICE LENGTH (in) Marion Posts - 80 ksi *							
Moment Arm (in)	Splice Length (in)	CRITICAL Back	CRITICAL Nest	CRITICAL Face	NON-CRITICAL Back	NON-CRITICAL Nest	NON-CRITICAL Face
		3 lb/ft					
17	3	6.2 **	5.2 (5.1)	4.1 **	*** ***	4.9 **	5.1 **
71	3	3.4 **	3.1 **	-- --	-- --	-- --	-- --
72	3	5.0 **	3.8 (3.8)	3.1 **	5.0 **	4.9 (4.6)	4.0 **
	4	4.3 **	3.8 **	4.2 **	4.4 **	*** ***	4.1 **
	5	## ##	## ##	5.1 **	## ##	## ##	5.4 (5.4)
		4 lb/ft					
17	4	4.9 **	4.7 **	4.6 **	6.9 **	6.2 **	5.7 **
71	4	4.0 **	4.0 **	-- --	-- --	-- --	-- --

* Nominal yield stress
-- Test not run
** Effective splice length calculation not valid
() Effective splice length based on both bolts
*** Bolt gauge malfunction - data omitted
Bolt nearing end of life - data omitted

Tests of 4 lb/ft posts run in the critical orientation (Table 5.5,6) had effective splice lengths that correspond to the actual geometry. The 4 lb/ft posts developed splice lengths between 3.8 inches and 4.0 inches in the 71 inch bending tests. This ESL compared well with the actual splice length of 4 inches. The 3 lb/ft post, which used a 3 inch bolt spacing, developed effective splice lengths which varied from 3.3 to 5.0 inches. This indicated that local yielding affected the ESL calculation. The back of the 4 lb/ft posts was 1.4 to 1.7 times the thickness the 3 lb/ft posts, therefore the 4 lb/ft posts were less affected by local yielding. Nested splices were typically found to have a lower ESL than the back to back splices. The results confirm the bolt load equations in Section 5.3 which predicted that the nested case was critical from a bolt load standpoint.

The ESL for the critical configuration of the 17 inch tests were found to exceed the 71 inch tests by 15%. Since shear deflection was ignored (Section 1.3), this behavior was attributed to the difference in the deflection at bolt B due to bending. When Castigliano's theorem for deflection due to moment (Section 1.2) was applied to a 4 lb/ft post (Fig. 5.25), the deflection at bolt B (δ_B) for a 17 inch critical test exceeded a 71 inch test by 27% (Eq 1.2).

The applied load at 17 inches had to be 4.2 times that at 71 inches to develop the same normal base stress in bending. As a result, the shear at the base was also 4.2 times higher so the combined stress was 10% higher for a 17 inch test. Since the combined base stress and the deflection due to strain energy was higher for a 17 inch test, higher bolt loads and shorter effective splice lengths were expected.

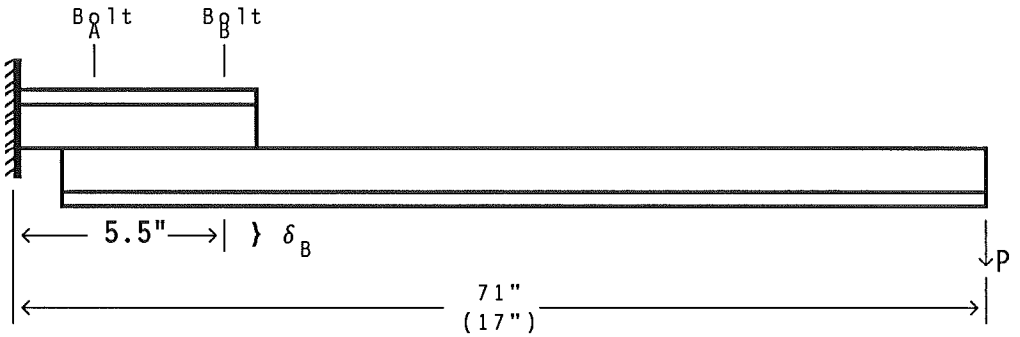

FIGURE 5.25. *ILLUSTRATION OF 17 AND 71 TESTS FOR THE CRITICAL LOADING CONFIGURATION (δ_B CORRESPONDS TO THE DEFLECTION AT BOLT B DUE TO THE APPLIED LOAD P).*

5.7 NESTED SPLICE CONFIGURATIONS

Of all the bolted splices tested (back to back, face to face and nested), only the nested splice could be assembled in the critical or non-critical configuration with the sign facing in the same direction (Fig. 5.26). The two different nested splice orientations can be achieved by bolting the signpost to either side of the stub after it is driven into the ground. Since there is no default assembly technique (ie: if stub is driven backwards, the sign faces the wrong direction as in a back to back splice), care must be taken in informing the maintenance crews of the particulars for nested splice assembly.

Current federal specifications (2,5) set limits on the maximum velocity change an 1800 pound vehicle can undergo during collision with a breakaway/yielding support sign at 15 feet/second. Crash tests are run (in compliance with the federal requirements) with the splice orientation that was most likely to be struck by a vehicle. Since a signpost has the highest probability of being struck by vehicles traveling on the right side of the roadway, crash tests are run with the splice in this configuration. For example, a back to back splice will be tested dynamically with an non-critical splice configuration (Fig. 5.26A). Nested splices, which can be assembled in either splice configuration, will be tested in the critical configuration (Fig. 5.26B) since this is the most common installation; however, the behavior will be different.

Seventeen inch bending tests (bumper height of the test vehicle) of nested splices in the non-critical orientation required 30% more load to fail the critical bolt than in the critical orientation (Table 4.1). Since the failure load for the splice was less in the critical orientation (Fig. 5.26B), dynamic testing will proceed with this configuration and splice will be accepted based on its performance in the crash tests. If a nested splice in the critical configuration passes the dynamic tests and is implemented in the field, it is essential that field crews assemble the splice correctly so that, in the event of impact, the splice assembly fails with the least force.

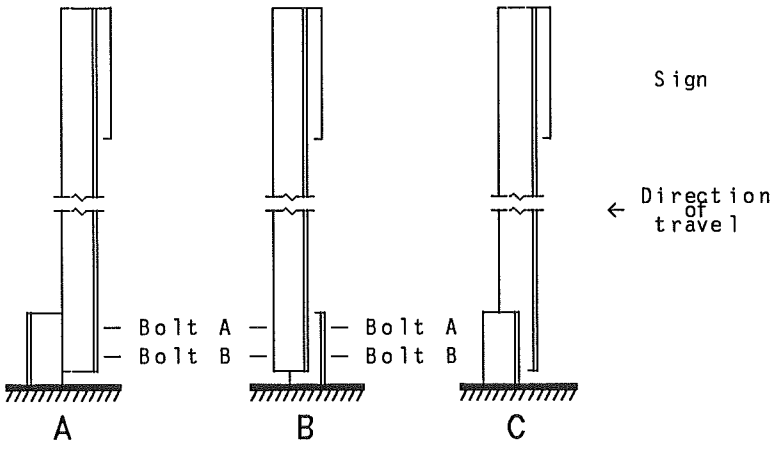

FIGURE 5.26. *EXAMPLES OF SPLICE CONFIGURATIONS A) BACK TO BACK - NON-CRITICAL, B) NESTED - CRITICAL C) NESTED - NON-CRITICAL.*

5.8 SUPERPOSITION AND PRINCIPAL BASE STRESS CALCULATIONS

The principal base stress for the combined bending and torsion tests is a three dimensional combination of normal and shear stresses. Since a u-post is a non-circular cross section, it is subject to warping as well as shear stresses due to torsional loads. As a result, a three dimensional state of bending and warping stresses exists. There is no doubt that normal and shear stresses due to bending as well as torsional shear stresses combine at the base of the cross section. However, since the base of the section is not absolutely confined (i.e. end of section is not welded to base), the degree of end restraint and therefore the magnitude of warping stress in the section was not known.

In order to ascertain the degree of end restraint, strain gauge data was compiled and compared between the 71 inch bending and combined bending and torsion tests. The calculated strain for the bending tests (My/IE) was an average 4.6 percent less than the measured gauge strains and is attributed to the systematic errors in the test procedures. It was assumed that the magnitude of warping strains could be determined from the known solutions for a hat section. The calculated strains corresponding to full and no end restraint were the upper and lower bounds, and the 4.6 percent error in the bending strain gauge results provided the bounds for calibration of the model.

To determine the magnitude of warping stress present, a hat section (Fig. 5.27) with dimensions and area similiar to a Franklin 4 lb/ft post was analyzed. Solutions to the torsional warping strains[3] of this section were compared to the measured strains in the actual section to determine the warping stresses present. When warping strains were neglected, the calculated strains were found to underpredict the measured strains by 5.8 percent.

Figure 5.28 illustrates the warping stress distribution along the face of the cross section. At the tip of the face, there is a 4.97 psi stress increase due to warping, and at the inside corner, there is a 4.01 psi stress decrease. If the location of the center of the strain gauge is assumed to lie at the center of the face (0.275 inches from the tip), a 2.5 psi stress increase is expected. The corresponding strain increase results in 0.4 percent strain underprediction through superposition of warping and normal stresses. Therefore, in order to match the 4.6 percent strain underprediction in the bending tests, 22 percent of full warping restraint must exist in the combined bending and torsion tests.

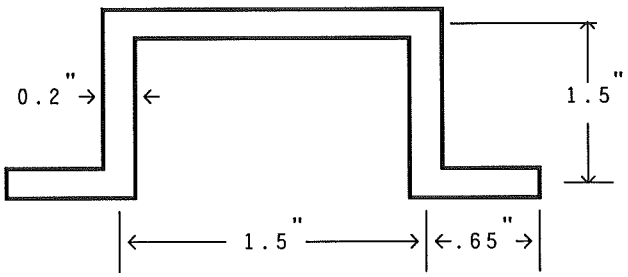

FIGURE 5.27. *ILLUSTRATION OF HAT SECTION WITH DIMENSIONS SIMILAR TO A FRANKLIN 4 LB/FT POST.*

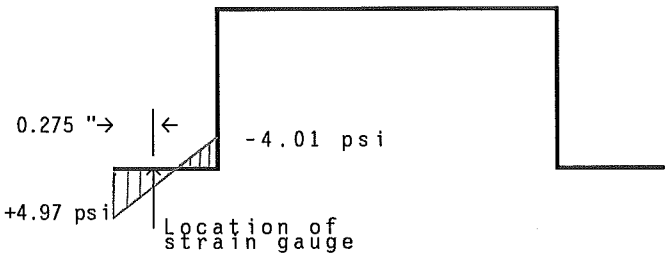

FIGURE 5.28. *ILLUSTRATION OF WARPING STRESS DISTRIBUTION (KSI) AT FACE OF CROSS SECTION*

This degree of restraint is reasonable since full restraint is developed by welding the cross section to the base, and the restraint for the tests was developed through friction between the back and face of the cross section and the base and plate which secured the section to the fixed base.

5.9 STATIC TEST CONCLUSIONS

Results of the static tests indicate that either a back to back or nested splice (Section 3) can develop at least 95% of the yield stress of a steel u-post. Both splice designs are therefore candidates for dynamic testing.

The NCHRP report 230 (2) limits the velocity change of an 1800 pound vehicle to 15 feet/second during an impact with a highway sign. This report specifies that the orientation of the splice for a dynamic test is that which has the greatest probability of impact. Therefore, a nested splice will be tested in its critical configuration while the back to back splice will be tested in the non-critical configuration (Section 5.7). Since the load required to fail a bolt in the critical configuration is less than the non-critical (Section 5.3), the nested splice is probably the better choice for the full scale crash tests. Results of the pendulum tests, which are an intermediate test between static and full scale crash tests, are presented in Chapter 6 for signposts using back to back and nested splices. Full scale crash tests, which were run using only nested splices are presented in Chapter 7.

6 PENDULUM TEST RESULTS

6.1 PURPOSE

The purpose of the pendulum tests was to determine the failure characteristics of a single leg installation when impacted by a 1800 pound vehicle. Tests were run with back to back and nested splices using Franklin (60 ksi) and Marion (60 & 80 ksi) u-post channels.

6.2 APPURTENANCE DESCRIPTION

The sign installation used in this test consisted of a small regulatory aluminum sign panel mounted on either a Marion or Franklin u-post support. The support was mounted on a 42 in stub which had been driven 36 in into a standard NCHRP strong soil. The supports were attached to the stub using a back to back or nested (sign supports behind the stub) using the specified hardware. A typical installation is shown in Figure 6.1. The post and splice type as well as the bolt grade used for each pendulum test is summarized in Table 6.1.

6.3 PENDULUM FACILITY

The sign installations were tested at the TTI outdoor pendulum testing facility. This facility is pictured in Figure 6.2 with the completly assembled sign support in place for testing. Figure 6.3 illustrates the five module crushable nose installed on the 2250 pound pendulum. The facility has a pit which was filled with the standard NCHRP soil.

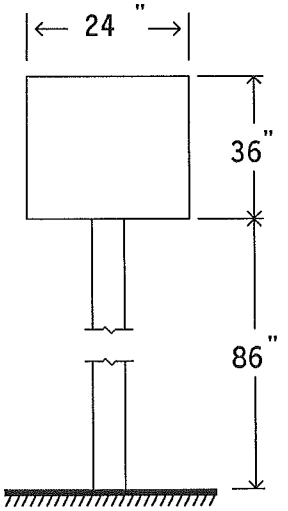

FIGURE 6.1. *ILLUSTRATION OF SIGN INSTALLATION USED FOR PENDULUM TESTS.*

TABLE 6.1. *SUMMARY OF POST TYPE AND CONFIGURATION USED IN PENDULUM TESTS*

Test No.	Manufacturer	Post Wt. (lbs/ft)	Bolt Grade	Configuration
RF7024-P1	Marion	3	9	Nested
RF7024-P2	Marion	4	9	Nested
RF7024-P3	Marion	3	9	Back to Back
RF7024-P4	Marion	4	9	Back to Back
RF7024-P5	Franklin	4	5	Back to Back
RF7024-P6	Franklin	4	5	Nested
RF7024-P7	Marion	4	9	Back to Back
RF7024-P8	Marion	4	9	Nested
RF7024-P9	Marion	4	9	Back to Back
RF7024-P10	Marion	4	9	Nested

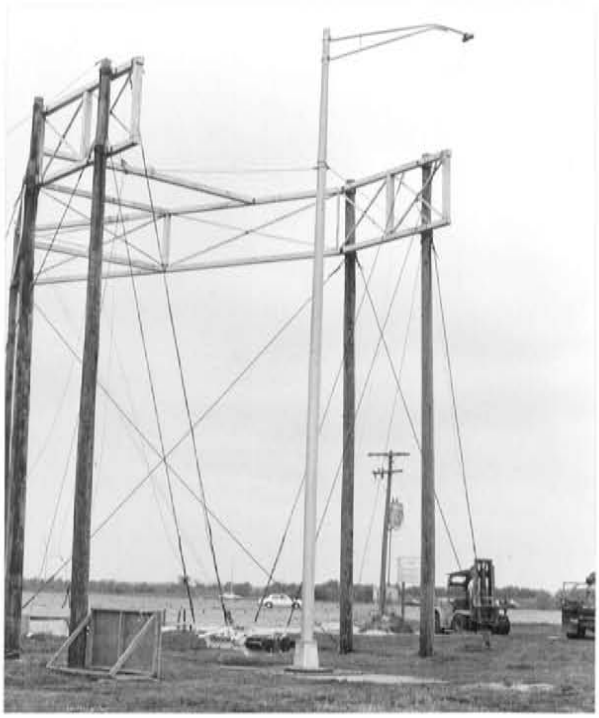

FIGURE 6.2. *TEXAS TRANSPORTATION INSTITUTE OUTDOOR PENDULUM TEST FACILITY.*

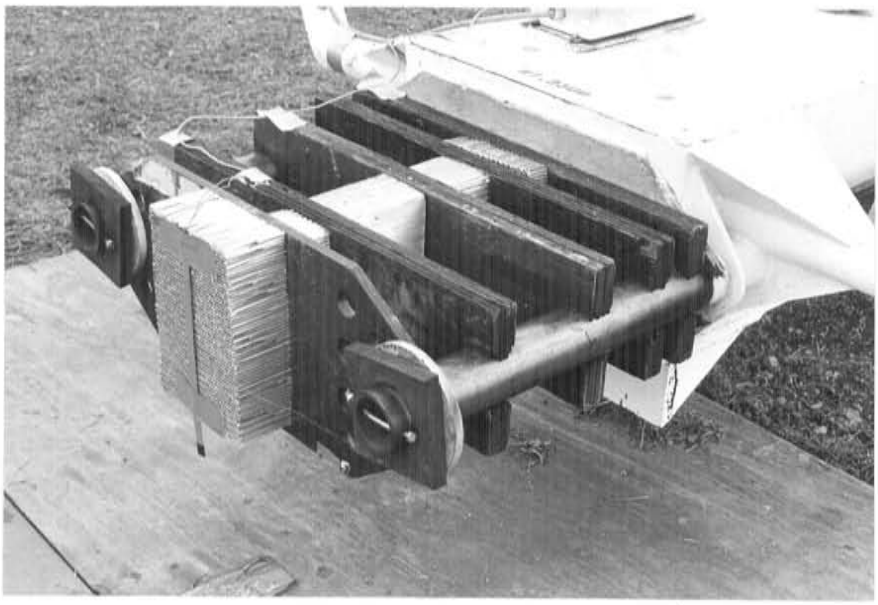

FIGURE 6.3. *BOGI VEHICLE WITH CRUSHABLE NOSE BEFORE TEST.*

6.4 ELECTRONIC INSTRUMENTATION

A low impedance, pizoelectric accelerometer was mounted on the rear surface of the pendulum to measure acceleration in the longitudinal direction. An impact actuated contact switch was mounted such that pendulum struck it at the same time it contacted the transformer base. The signals from the accelerometer and the contact switch were telemetered to a base reciever station and recorded on magnetic tape for a permanent record. The filtered analog data were digitized and processed on a digital computer for analysis and presentation.

6.5 PHOTOGRAPHIC INSTRUMENTATION

A standard motion picture camera was used to document the pendulum facility, the crushable pendulum nose, and before and after conditions of the stub and posts tested. A high speed camera was used to record the impact behavior and aid in data reduction.

6.6 TEST RESULTS

Results of the tests performed on the Franklin and Marion steel u-posts are summarized in table 6.2. Accelerometers were used to measure the change in velocity (ΔV) and the change in momentum (ΔMV) for an

impact velocity of 20 mph. A copy of the accelerometer traces are found in Appendix W.

Predicted velocity changes for multiple supports for the 2250 lb pendulum tests are based on the energy absorbed during an impact with a single post installation. This change of energy is

$$\frac{1}{2} MV_i^2 = \frac{1}{2} M(V_i - V_f)^2 + \Delta KE \qquad (6.1)$$

For each test, the pendulum mass (M = 2250 lb/32.2 ft/s^2), the initial (V_i) and final (V_f) velocities are known so ΔKE, the change in kinetic energy during impact for a single post installation is easily calculated. Velocity change predictions for two and three post installations were calculated by multiplying ΔKE by the number of posts and solving for V_f in equation 6.1. Predicted velocity changes for an 1800 lb. vehicle proceed the same way with the exception that the mass in this case is 1800 lb/32.2 ft/s^2.

6.7 SUMMARY

According to the performance limits set forth in NCHRP 230 (2), the change in velocity should be less than 15 fps for 1800 lb. pendulum tests at 20 mph. Both Franklin and Marion posts using back to back and nested splices would pass the test for a single sign support. For signs using two supports; Marion 80 ksi posts with a nested splice, Marion 80 ksi - 4 lb/ft posts with a back to back splice, and Franklin 60 ksi post with a nested splice passed the test. For signs requiring three supports, only Marion 80 ksi (3 and 4 lbs/ft) posts using nested splices were predicted to meet the 15 fps criterion.

As a result of the pendulum tests, it was recommended that a three support sign using Marion 80 ksi posts and a nested splice be used for the full scale crash tests. Although this system was predicted to pass based on the pendulum tests, velocity change corrections for the inertia of the sign were neglected. This increase was assumed to be small (less than 1%), and would not alter the three support veloctiy change results enough to predict failure.

TABLE 6.2. *SUMMARY OF PENDULUM TEST RESULTS.*

SINGLE POST PENDULUM TEST RESULTS Pendulum Weight: 2250 lbs Impact Velocity: 20 mph (29.3 fps) Splice Length: 4 in					PREDICTED VELOCITY CHANGE				
					2250 lbs		1800 lbs		
Test No	Manu[A] (lb/ft)	Nominal Strength (ksi)	Splice Type	Change in Vel (fps)	Two Posts (fps)	Three Posts (fps)	One Post (fps)	Two Posts (fps)	Three Posts (fps)
P1	M (3)*	80	Nested	2.09**	4.35	6.84	2.63	5.56	8.91
P2	M (4)	80	Nested	2.99	6.37	10.33	3.79	8.26	13.95
P3	M (3)*	80	Back to Back	6.22	14.93	***	8.06	22.78	***
P4	M (4)	80	Back to Back	3.84	8.40	14.43	4.90	11.11	21.45
P5	F (4)	60	Back to Back	7.91	21.73	***	10.39	***	***
P6	F (4)	60	Nested	3.58	7.76	13.03	4.56	10.21	18.68
P7	M (4)	60	Back to Back	5.93	14.03	***	7.66	20.63	***
P8	M (4)	60	Nested	8.33	25.38	***	11.01	***	***
P9	M (4)	60	Back to Back	8.93	***	***	11.86	***	***
P10	M (4)	60	Nested	6.07	14.44	***	7.86	21.46	***

[A] F: Franklin
M: Marion

* Marion 3 lb/ft posts were tested with a 3 in splice.
(Static testing developed a 3 lb/ft, 80 ksi nominal yield strength post with a 3 in splice)

** Velocity change estimated from highest 50 msec acceleration.

*** Velocity change during impact exceeds initial velocity in ft/sec.

7 Full Scale Crash Tests

7.1 INTRODUCTION

The purpose of the full scale crash tests was to determine the impact characteristics of multi-leg installations when impacted at 20 mph and 60 mph as established through NCHRP 230 (2) and AASHTO standards (5).

7.2 INSTRUMENTATION AND DATA ANALYSIS

The vehicles were equipped with triaxial accelerometers mounted near the center of gravity. In addition, yaw, pitch and roll rates were measured by on-board instruments. The electronic signals were telemetered to a base station for recording on magnetic tape and for display on a real- time strip chart. Provision was made for transmisson of calibration signals before and after the test, and an accurate time reference signal was simultaneously recorded with the data.

Contact switches on the bumper were actuated just prior to impact by wooden dowels. This system indicated the elapsed time over a known distance and provided a measurement of impact velocity. The initial contact also produced an "event" mark on the data record to establish the instant of impact. Data from the electrinic tranducers was digitized using a microcomputer for analyses and evaluation of performance.

In accordance with NCHRP 230 (2) an unrestrained, uninstrumented special purpose 50th percentile anthropomorphic test dummy was positioned in the front seat of the vehicle. This dummy was used to evaluate typical unsymmetrical vehicle mass distribution and its effect on vehicle stability during impact.

Still and motion photography were used to document the test, to obtain time-displacement data, and to observe phenoma occurring during the impact. Still photography was used to record conditions of the test vehicle and sign installation before and after the test. Motion photography was used to record the colision event.

7.3 U-POST TEST INSTALLATIONS

The sign installation used in the crash tests consisted of a 8 ft wide by 7 ft high 5/8 inch plywood sign panel mounted on three 10-ft Marion 80 ksi, 3 lb/ft and 4 lb/ft steel supports. These supports were three 42 in stubs which had been driven 36 inches into crushed limestone base material (NCHRP Report 230 Strong Soil) at 3 ft-7 in on center

spacing. The supports were attached to the stubs using a 4 in nested splice (sign supports behind the stubs) with 1/2 inch spacers and grade 9 bolts, nuts, and washers. The bottom of sign mounting height was 5 ft.

7.4 TEST RESULTS

7.4.1 TEST 7024-24

TEST DESCRIPTION

The 1979 Honda shown in Figure 7.1 was directed into the sign installation (Fig. 7.2) using 3 - Marion 80 ksi 4 lb/ft u-posts with a cable reverse tow and guidance system. The test inertia mass of the vehicle was 1800 lbs (817 kg) and its gross static mass was 1970 lbs (894 kg). Impact point was such that the vehicle bumper contacted all three legs of the sign installation. The height from the ground to the lower edge of the bumper was 14.25 in (36.20 cm) and 18.75 (47.63 cm) to the top of the bumper. The vehicle was free-wheeling and unrestrained at impact.

The speed of the vehicle at impact was 20.6 mi/h (33.1 km/h). Approximately 0.062 seconds after impact, the right support fractured at bumper height and at 0.079 seconds, the center support broke away at the stub. The left support caused the left side of the vehicle to rise slightly before the support broke away from the stub at about 0.198 s. The vehicle lost contact with the sign installation at 0.313 seconds. Shortly thereafter, the sign pannel fell to the ground and the vehicle rolled forward coming to rest over the stubs (Fig 7.3).

The right support was fractured 22.5 (57.2 cm) above the ground and the center support was bent. The stub on the left side was pushed back as shown in Figure 7.4. The vehicle sustained minor damage to the bumper and hood, and the windshield was cracked (Fig 7.5). Maximum crush to the left front of the vehicle at bumper height was 5.0 in (12.7 cm).

TEST RESULTS AND EVALUATION

The test results are summarized in Figure 7.6. Change in velocity was 19.1 mi/h (30.7 km/h) and change in momentum was 1566 lb-s. Occupant impact velocity was 21.9 ft/s (6.7 m/s) and the maximum 0.010-second average occupant ridedown acceleration was -2.7 g.

The sign installation yielded to the vehicle by fracturing at bumper height and at the stubs. The sign pannel fell to the ground and did not penetrate the occupant compartment or present undue hazard to other traffic. The vehicle recieved minor damage with a maximum crush of 5.0 in (12.7 cm). The occupant impact velocity was high (NCHRP Report 230 limit is 20 ft/s) and the change in momentum was over the limit of 1100 lb-s. *This sign installation was not acceptable* according to the evaluation criteria recommended in NCHRP Report 230 (2) and the AASHTO standards (5).

FIGURE 7.1. *VEHICLE USED IN TESTS 7024-24,5.*

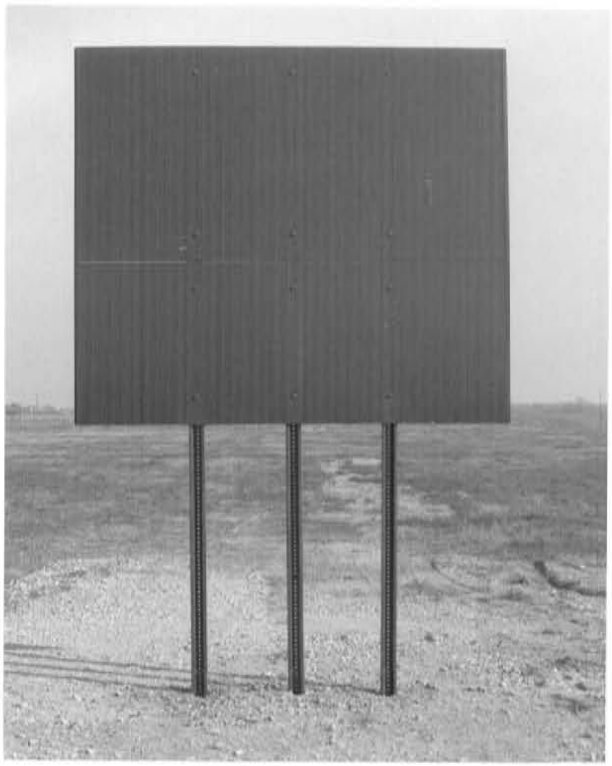

FIGURE 7.2. *SIGN INSTALLATION USED IN TEST 7024-24.*

FIGURE 7.3. *VEHICLE RESTING POSITION FOLLOWING TEST 7024-24.*

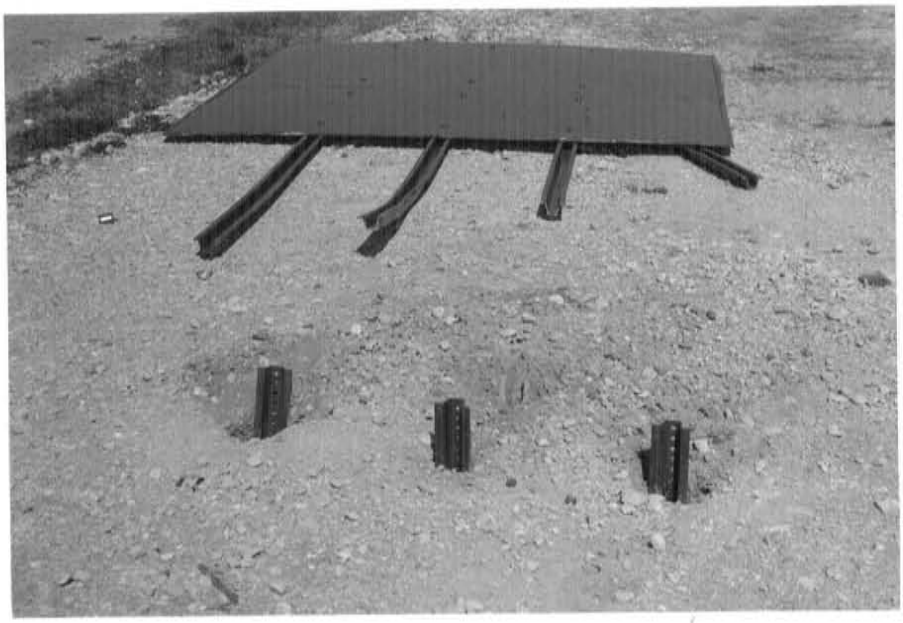

FIGURE 7.4. *SIGN SUPPORTS FOLLOWING TEST 7024-24.*

FIGURE 7.5. *VEHICLE DAMAGE FOLLOWING TEST 7024-24.*

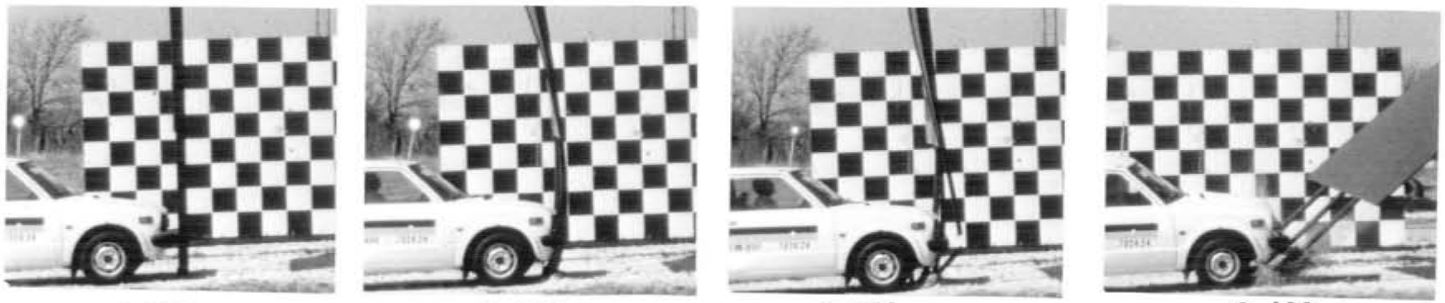

0.000 s | 0.049 s | 0.074 s | 0.409 s

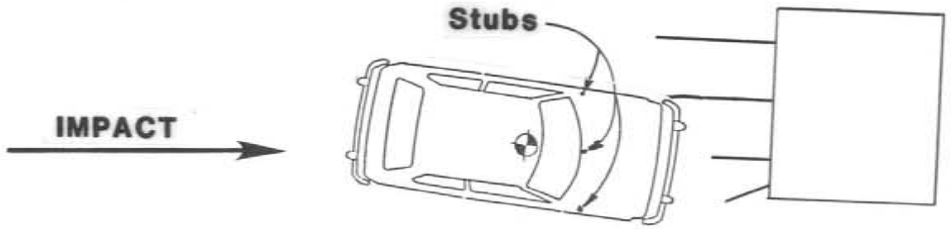

Test No. 7024-24
Date 3/02/87
Test Article . . . . . Sign Installation
Support. . . . . Three Marion 80 ksi, 4 lb-ft Supports
Vehicle. . . . . 1979 Honda
Vehicle Weight
  Test Inertia . . . . . 1800 lb (817 kg)
  Gross Static . . . . . 1970 lb (894 kg)
Vehicle Damage Classification
  TAD. 12FD1
  SAE. 12FDEW1

Impact Speed. . . . . 20.6 mi/h (33.1 km/h)
Change in Velocity. . . . . 19.1 mi/h (30.7 km/h)
Change in Momentum . . . . 1566 lb-s
Occupant Impact Velocity
  Longitudinal. . . . . 21.9 ft/s (6.7 m/s)
  Lateral . . . . . None
Occupant Ridedown Accelerations
  Longitudinal. . . . . -2.7 g
  Lateral . . . . . N/A
Maximum Vehicle Crush
  Bumper Height . . . . . 5.0 in (12.7 cm)

FIGURE 7.6. *SUMMARY OF RESULTS FOR TEST 7024-24.*

7.4.2 TEST 7024-25

TEST DESCRIPTION

The 1979 Honda shown in Figure 7.1 was directed into the sign installation (Fig.7.7) using 3 - Marion 80 ksi 4 lb/ft u-posts with a cable reverse tow and guidance system. This vehicle had been used in test 7024-24. The bumper was replaced, the dents pulled out and the crack in the windshield was marked. The test inertia mass of the vehicle was 1800 lbs (817 kg) and its gross static mass was 1970 lbs (894 kg). Impact point was such that the vehicle bumper contacted all three legs of the sign installation. The height from the ground to the lower edge of the bumper was 14.25 in (36.20 cm) and 18.75 (47.63 cm) to the top of the bumper. The vehicle was free-wheeling and unrestrained at impact.

The speed of the vehicle at impact was 62.6 mi/h (100.7 km/h). Shortly after impact, the center support fractured at bumper height and broke away from the stub. By 0.015 s after impact, the other supports had broken away from their stubbs. The vehicle lost contact with the supports at approximately 0.065 seconds. As the vehicle continued forward, the sign installation went up and over the vehicle. The brakes were applied and the vehicle came to rest 230 ft (70 m) beyond impact point (Fig. 7.8).

The right support came loose from the sign pannel, the center support broke 14.0 (35.6 cm) above the ground, and the left support was bent. The sign pannel also came apart as shown in Figure 7.9. A piece of rubber section of the left corner of the bumper was jammed into the left stub.

The front of the vehicle was deformed as shown in Figure 7.10. The left front corner recieved 6.0 in (15.2 cm) crush at bumper height. The center and right sides were crushed 3.0 in (7.6 cm) at bumper height. There was also a slight scrape on the rear of the roof where the sign pannel grazed the vehicle as it went over the vehicle.

TEST RESULTS AND EVALUATION

A summary of data is provided in Figure 7.11. Change in vehicle velocity at 0.200 seconds (end of significant vehicle response) was 9.0 mi/hr (14.5 km/h) and change in momentum was 738 lb-sec. Longitudinal occupant impact was 13.2 ft/s (4.0 m/s) and the maximum 0.010-second

average ridedown acceleration was -0.6 g.

The sign installation yielded to the vehicle by fracturing and breaking away from the stubs. The supports and sign pannel went up and over the vehicle but did not penetrate the occupant compartment. The debris remained in the vehicle path and therefore did not present undue hazard to other traffic. Maximum crush to the vehicle was 6.0 in (15.2 cm). The occupant impact velocity and change in momentum were within the specified limits. According to these results, *this sign installation met the evaluation criteria* recommended in NCHRP Report 230 (2) and the AASHTO Standards (5).

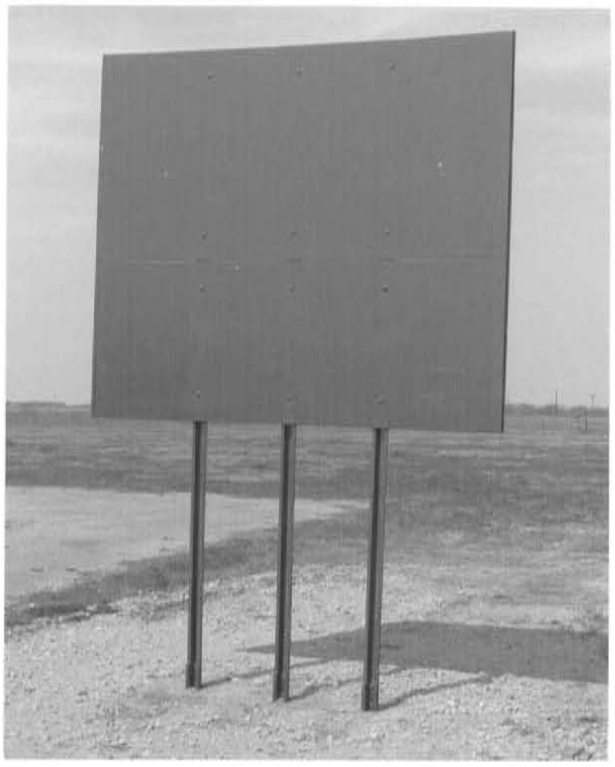

FIGURE 7.7. *SIGN INSTALLATION USED IN TEST 7024-25.*

FIGURE 7.8. *VEHICLE PRIOR TO TEST 7024-25.*

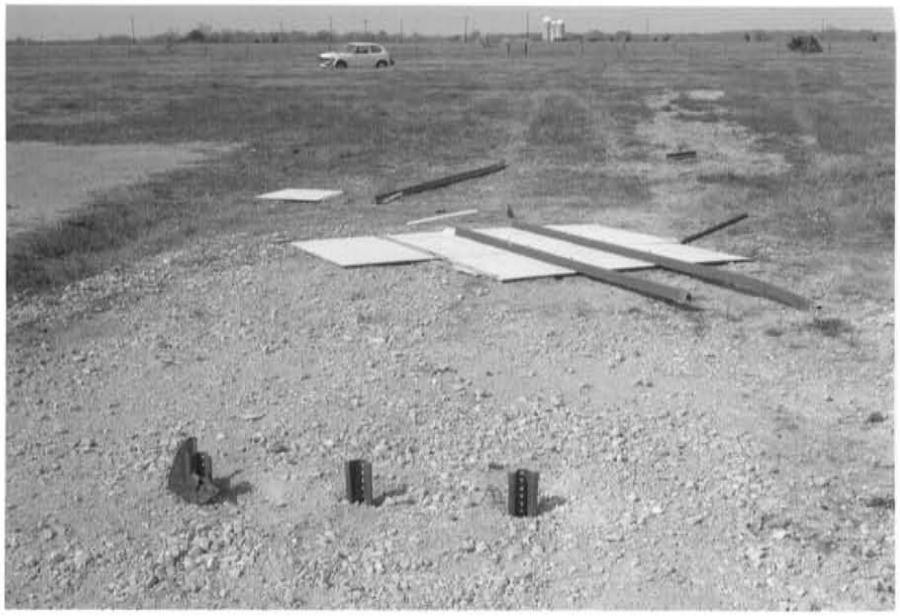

FIGURE 7.9. *SIGN INSTALLATION FOLLOWING TEST 7024-25.*

FIGURE 7.10. *VEHICLE DAMAGE FOLLOWING TEST 7024-25.*

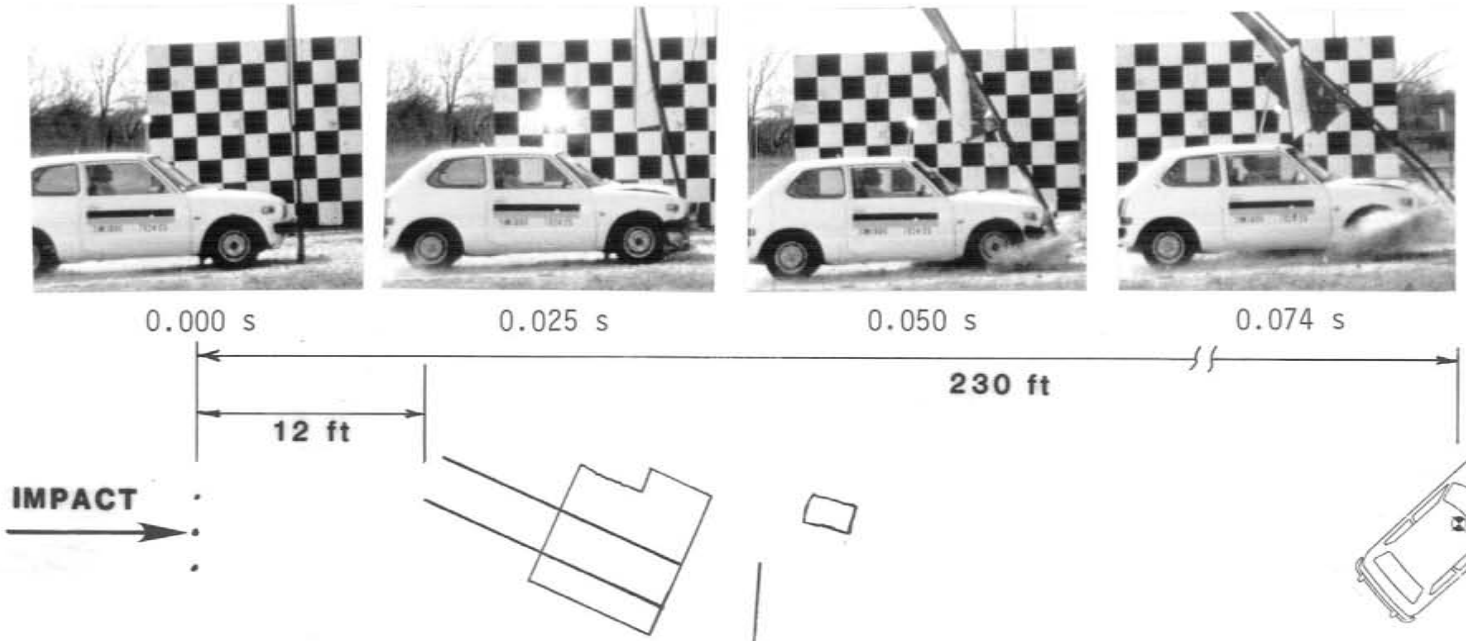

Test No.	7024-25
Date	3/02/87
Test Article	Sign Installation
Support	Three Marion 80 ksi, 4 lb-ft Supports
Vehicle	1979 Honda Civic
Vehicle Weight	
Test Inertia	1800 lb (817 kg)
Gross Static	1970 lb (894 kg)
Vehicle Damage Classification	
TAD	12FD1
SAE	12FDEW1
Impact Speed	62.6 mi/h (100.7 km/h)
Change in Velocity	9.0 mi/h (14.5 km/h)
Change in Momentum	738 lb-s
Occupant Impact Velocity	
Longitudinal	13.2 ft/s (4.0 m/s)
Lateral	No Contact
Occupant Ridedown Accelerations	
Longitudinal	-0.6 g
Lateral	N/A
Maximum Vehicle Crush	
Bumper Height	6.0 in (15.2 cm)

FIGURE 7.11. *SUMMARY OF RESULTS FOR TEST 7024-25.*

7.4.3 TEST 7024-26

TEST DESCRIPTION

The 1979 Honda shown in Figure 7.12 was directed into the sign installation (Fig. 7.13) using 3 - Marion 80 ksi 3 lb/ft u-posts with a cable reverse tow and guidance system. The test inertia mass of the vehicle was 1800 lbs (817 kg) and its gross static mass was 1973 lbs (896 kg). Impact point was such that the vehicle bumper contacted all three legs of the sign installation. The height from the ground to the lower edge of the bumper was 15.25 in (38.74 cm) and 20.00 in (50.80 cm) to the top of the bumper. The vehicle was free-wheeling and unrestrained at impact.

The speed of the vehicle at impact was 21.7 mi/h (34.9 km/h). Approximately 0.054 seconds after impact, the left support fractured at bumper height and shortly thereafter, the others broke away from the stub. The vehicle lost contact with the sign supports at 0.310 seconds. As the vehicle continued forward, it again contacted the supports and eventually came to rest on the sign pannel (Fig.7.14).

The left support was fractured 20.0 in (50.8 cm) above the ground and the other supports were bent. The top of the left stub was torn (Fig. 7.15). As shown in Figure 7.16, the vehicle sustained minor damage to the bumper. Maximum crush to the right side of the vehicle at bumper height was 2.0 in (5.1 cm).

TEST RESULTS AND EVALUATION

The test results are summarized in Figure 7.17. Change in velocity was 8.6 mi/h (13.8 km/h) and change in momentum was 705 lb-s. Occupant impact velocity was 12.5 ft/s (3.8 m/s) and the maximum 0.010-second average occupant ridedown acceleration was -0.5 g.

The sign installation readily yielded to the vehicle by fracturing at bumper height and breaking away at the stubs. The sign installation did not penetrate the occupant compartment or present undue hazard to other traffic. The vehicle received minor damage with a maximum crush of 2.0 in (5.1 cm). The occupant impact velocity and change in momentum were within the recommended limits. *This sign installation met the evaluation criteria* recommended in NCHRP Report 230 (2) and the AASHTO Standards (5).

FIGURE 7.12. *VEHICLE USED IN TESTS 7024-26,7.*

FIGURE 7.13. *SIGN INSTALLATION USED IN TEST 7024-26.*

FIGURE 7.14. *VEHICLE RESTING POSITION FOLLOWING TEST 7024-24.*

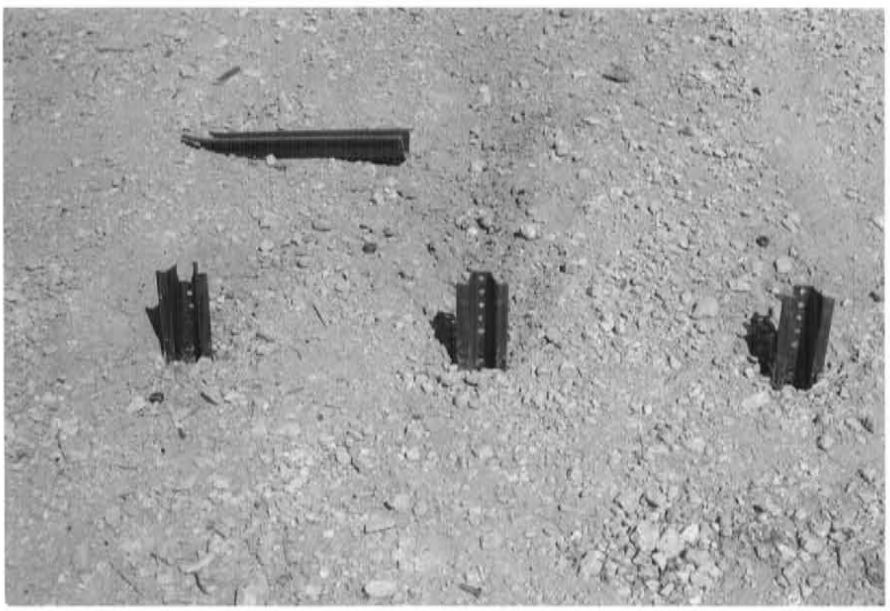

FIGURE 7.15. *SIGN SUPPORTS FOLLOWING TEST 7024-24.*

FIGURE 7.16. *VEHICLE DAMAGE FOLLOWING TEST 7024-26.*

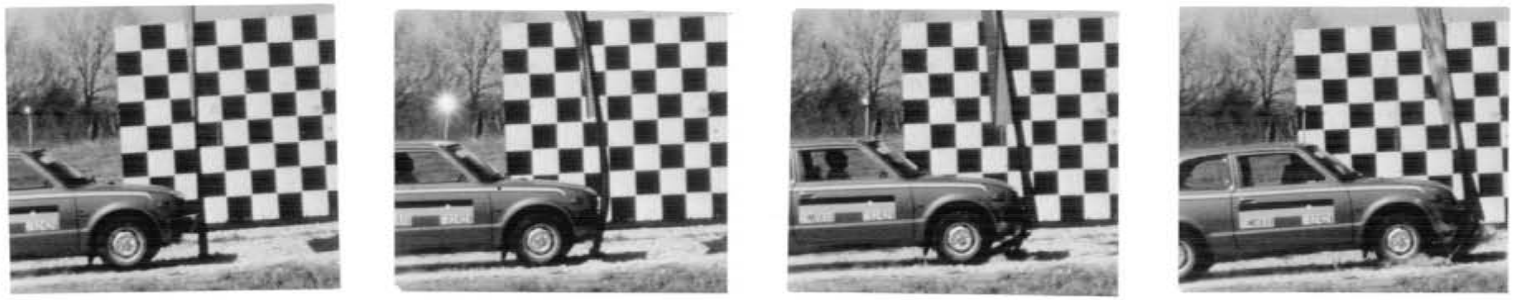

0.000 s 0.037 s 0.062 s 0.148 s

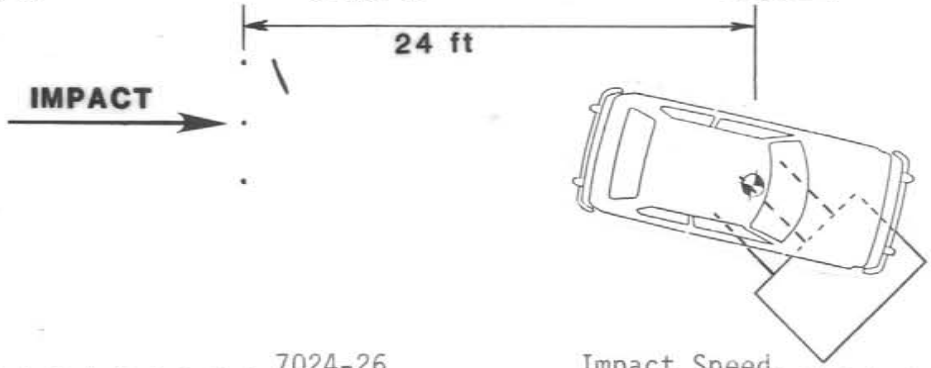

Test No.	7024-26
Date	3/05/87
Test Article	Sign Installation
Support.	Three Marion 80 ksi, 3 lb-ft Supports
Vehicle.	1979 Honda Civic
Vehicle Weight	
Test Inertia	1800 lb (817 kg)
Gross Static	1973 lb (896 kg)
Vehicle Damage Classification	
TAD.	12FD1
SAE.	12FDEW1

Impact Speed.	21.7 mi/h (34.9 km/h)
Change in Velocity. . . .	8.6 mi/h (13.8 km/h)
Change in Momentum . . .	705 lb-s
Occupant Impact Velocity	
Longitudinal.	12.5 ft/s (3.8 m/s)
Lateral	None
Occupant Ridedown Accelerations	
Longitudinal.	-0.5 g
Lateral	N/A
Maximum Vehicle Crush	
Bumper Height	2.0 in (5.1 cm)

FIGURE 7.17. *SUMMARY OF RESULTS FOR TEST 7024-26.*

7.4.4 TEST 7024-27

TEST DESCRIPTION

The 1979 Honda shown in Figure 7.12 was directed into the sign installation (Fig.7.18) using 3 - Marion 80 ksi 3 lb/ft u-posts with a cable reverse tow and guidance system. This vehicle had been used in test 7024-26. The bumper was repaired before this test. The test inertia mass of the vehicle was 1800 lbs (817 kg) and its gross static mass was 1973 lbs (896 kg). Impact point was such that the vehicle bumper contacted all three legs of the sign installation. The height from the ground to the lower edge of the bumper was 15.25 in (38.70 cm) and 20.00 (50.80 cm) to the top of the bumper. The vehicle was free-wheeling and unrestrained at impact.

The speed of the vehicle at impact was 61.6 mi/h (99.1 km/h). Shortly after impact, the right support broke away from the stub and by 0.012 s, the others had separated from the stubs. The vehicle lost contact with the supports at 0.047 s. As the vehicle continued forward, the sign installation went up and over the vehicle. The sign pannel contacted the telemetry antenna at about 0.087 s and the hit the top rear of the vehicle at 0.124 s. The vehicle was braked to a stop at 325 ft (990 m) beyond impact point (Fig.7.19).

All supports were bent about 18 in (46 cm) above the ground. The left stubs were pulled back and there were also tire marks on the right stub (Fig. 7.20). The front of the vehicle was deformed as shown in Figure 7.21. The left front corner recieved 8.0 in (20.3 cm) crush at bumper height. The center and right sides were dented. The top rear of the roof was scraped.

TEST RESULTS AND EVALUATION

A summary of data is provided in Figure 7.22. Change in vehicle velocity at 0.200 seconds (end of significant vehicle response) was 6.2 mi/hr (10.0 km/h) and change in momentum was 508 lb-sec. There was no occupant impact during the test period. The sign installation yielded to the vehicle by breaking away at the stubs. The detached elements went up and over the vehicle (as the vehicle proceeded forward) but did not penetrate the occupant compartment. The debris remained in the vehicle path therefore presenting no undue hazard to other traffic. The vehicle remained stable and upright with a maximum crush of 8.0 in (20.3 cm).

The occupant impact velocity and change in momentum were within the specified limits. *This sign installation met the evaluation criteria* recommended in NCHRP Report 230 (2) and the AASHTO Standards (5).

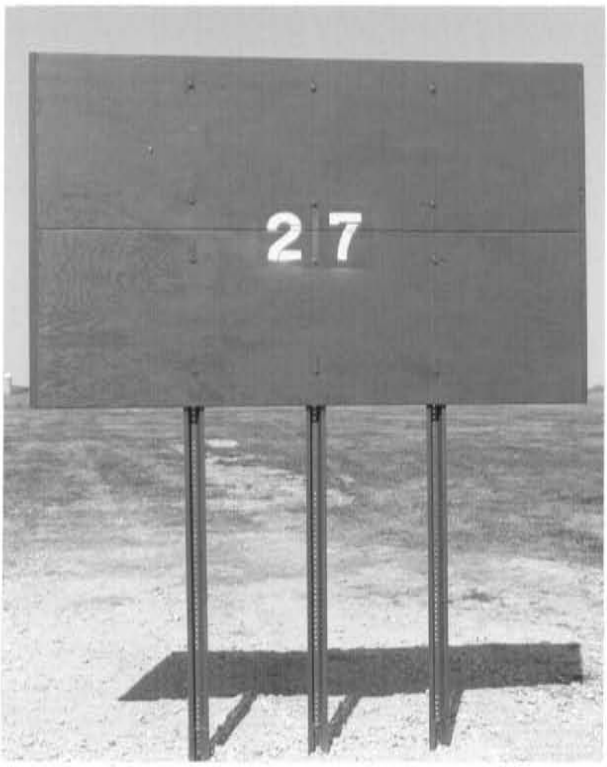

FIGURE 7.18. *SIGN INSTALLATION USED IN TEST 7024-27.*

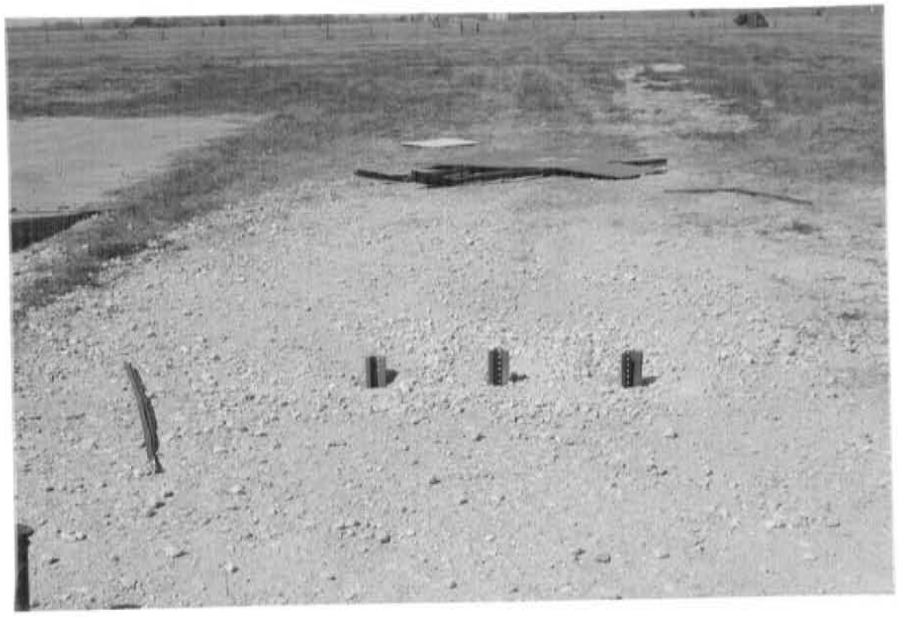

FIGURE 7.19. *SIGN INSTALLATION FOLLOWING TEST 7024-27.*

FIGURE 7.20. *SIGN INSTALLATION FOLLOWING TEST 7024-27.*

FIGURE 7.21. *VEHICLE DAMAGE FOLLOWING TEST 7024-27.*

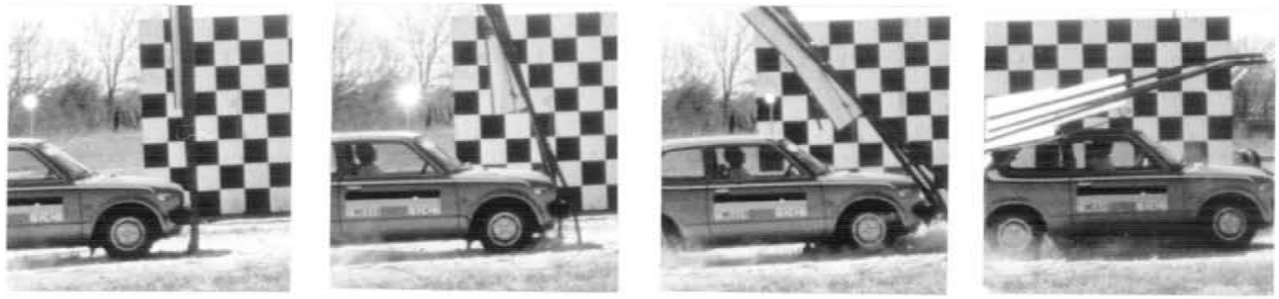

0.000 s 0.025 s 0.049 s 0.124 s

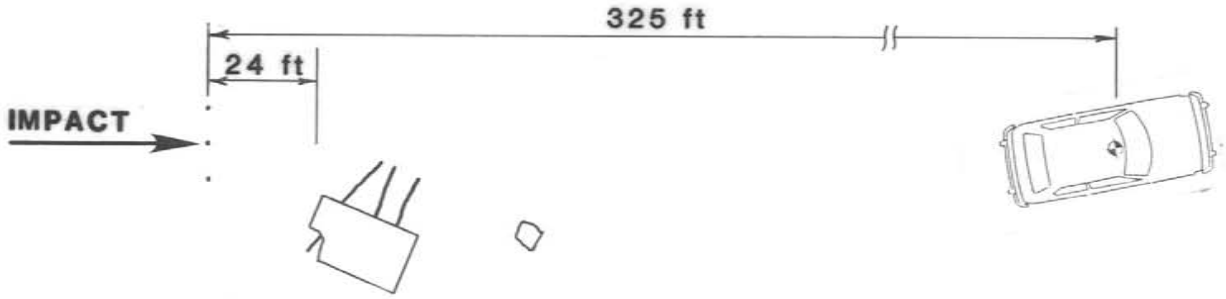

Test No.	7024-27
Date	3/05/87
Test Article	Sign Installation
Support	Three Marion 80 ksi, 3 lb-ft Supports
Vehicle	1979 Honda
Vehicle Weight	
Test Inertia	1800 lb (817 kg)
Gross Static	1973 lb (896 kg)
Vehicle Damage Classification	
TAD	12FD1
SAE	12FDEW2
Impact Speed	61.6 mi/h (99.1 km/h)
Change in Velocity	6.2 mi/h (10.0 km/h)
Change in Momentum	508 lb-s
Occupant Impact Velocity	
Longitudinal	No Contact
Lateral	No Contact
Occupant Ridedown Accelerations	
Longitudinal	N/A
Lateral	N/A
Maximum Vehicle Crush	
Bumper Height	8.0 in (20.3 cm)

FIGURE 7.22. *SUMMARY OF RESULTS FOR TEST 7024-27.*

7.5 SLIP-BASE TEST INSTALLATIONS

The sign installation used in these tests consisted of a 6 ft wide x 5 ft high plywood sign panel mounted on three P2 Uni-Strut supports. These supports were attached to three triangular retrofit slip bases with 3/8 in grade 2 bolts, nuts, and flat washers. The lower slip base attachments were anchored in concrete footings at 21 in on center spacing. Teflon gaskets were used between the slip bases attached to the sign supports and the anchored slip bases. The support slip bases were attached to the anchored slip bases with 1/2 in grade 5 bolts, nuts, and flat washers. The bottom of the sign was mounted at 5 ft. Details of the installation assembly are shown in Figure 7.23 and the completed installation is shown in Figure 7.24.

7.6 SLIP-BASE TEST RESULTS

7.6.1 TEST 7024-29

TEST DESCRIPTION

A 1979 Honda Civic (shown in Figure 7.25) impacted the sign installation (shown in Figure 7.26) at 18.7 miles per hour (30.1 km/h) using a cable reverse tow and guidance system. Test inertia mass of the vehicle was 1,800 lb (817 kg) and its gross static mass was 1,967 lb (892 kg). The height to the lower edge of the vehicle bumper was 14.5 inches (36.8 cm) and 19.5 inches (49.5 cm) to the top edge of the bumper.

The vehicle was free wheeling and unrestrained just prior to impact. The point of impact was the center line of the sign with the center of the vehicle. Upon impact, the sign installation supports began to slip from the stub base mounts. At approximately 0.020 seconds, the left and center leg were completely detatched from their slip base and at 0.043 seconds the right leg was activated by the vehicles right front fender. The sign installation yielded by smoothly passing over the roof of the test vehicle. As the vehicle lost contact with the sign installation at approximately 0.873 seconds, the brakes were applied and the vehicle came to rest approximately 87.0 ft (26.5 m) from point of impact.

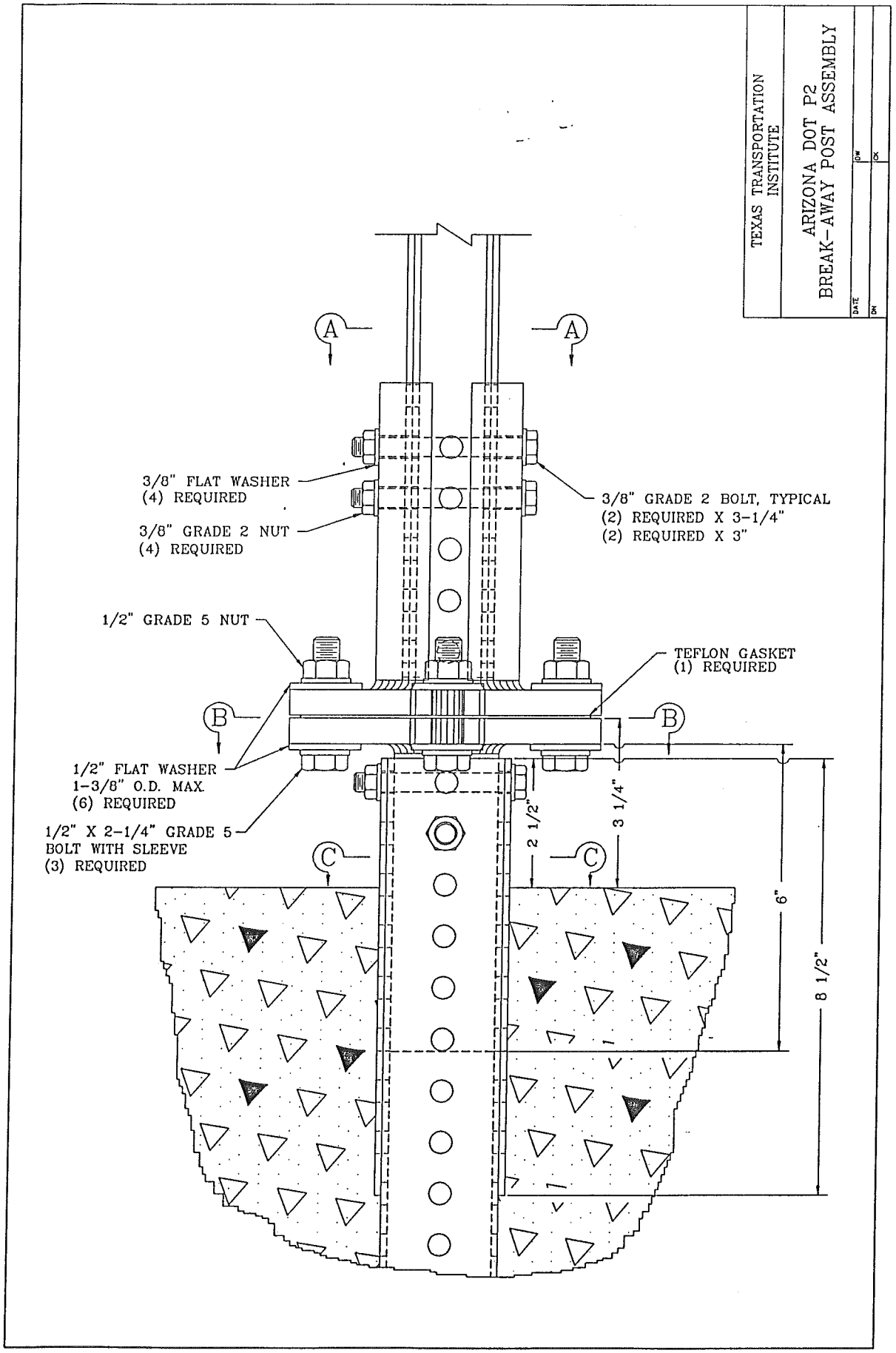

FIGURE 7.23A. *DETAILS OF SIGN INSTALLATION FOR TEST 7024-29 AND 7024-30*

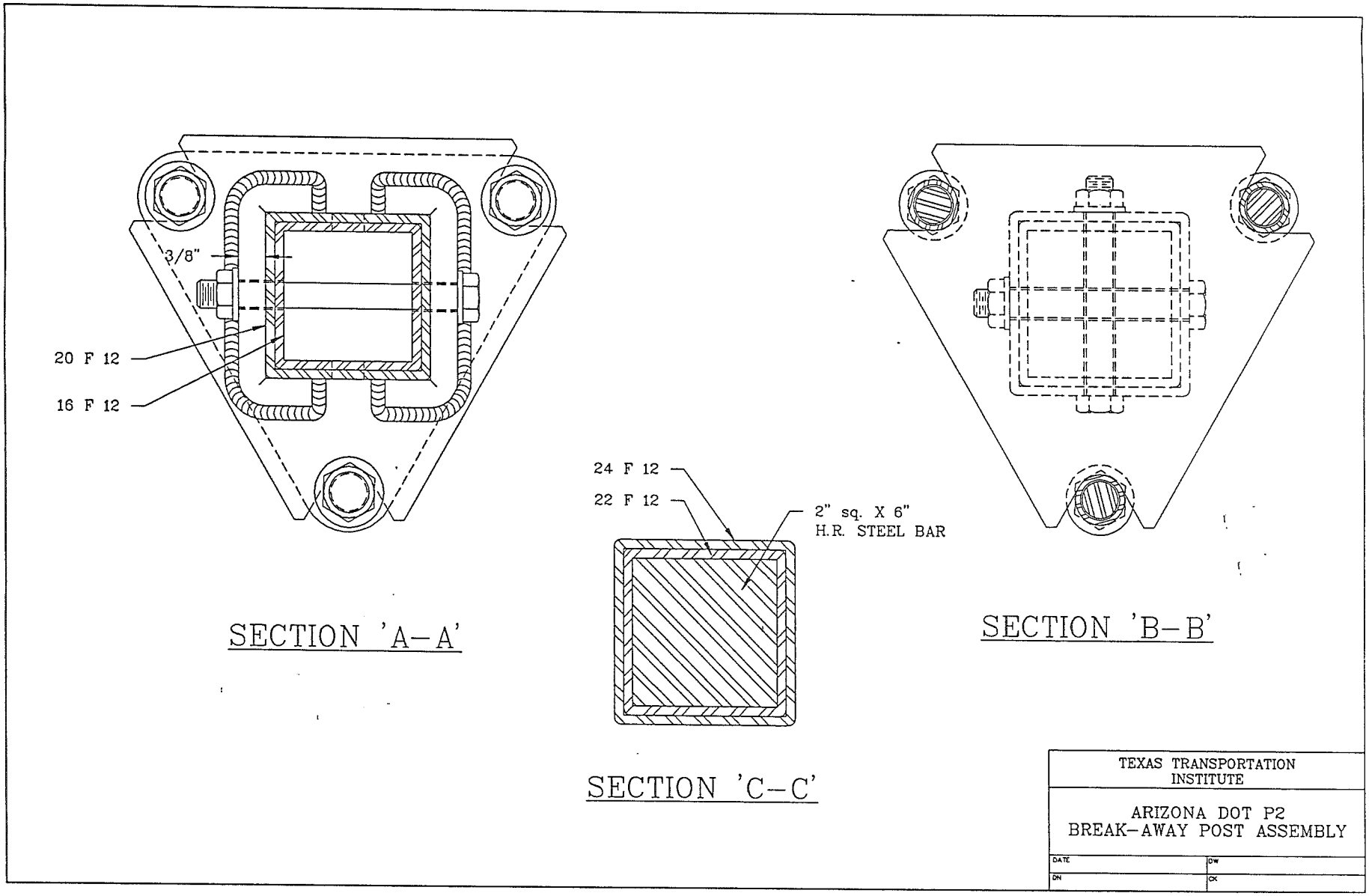

FIGURE 7.23B. *DETAILS OF SIGN INSTALLATION FOR TEST 7024-29 AND 7024-30*

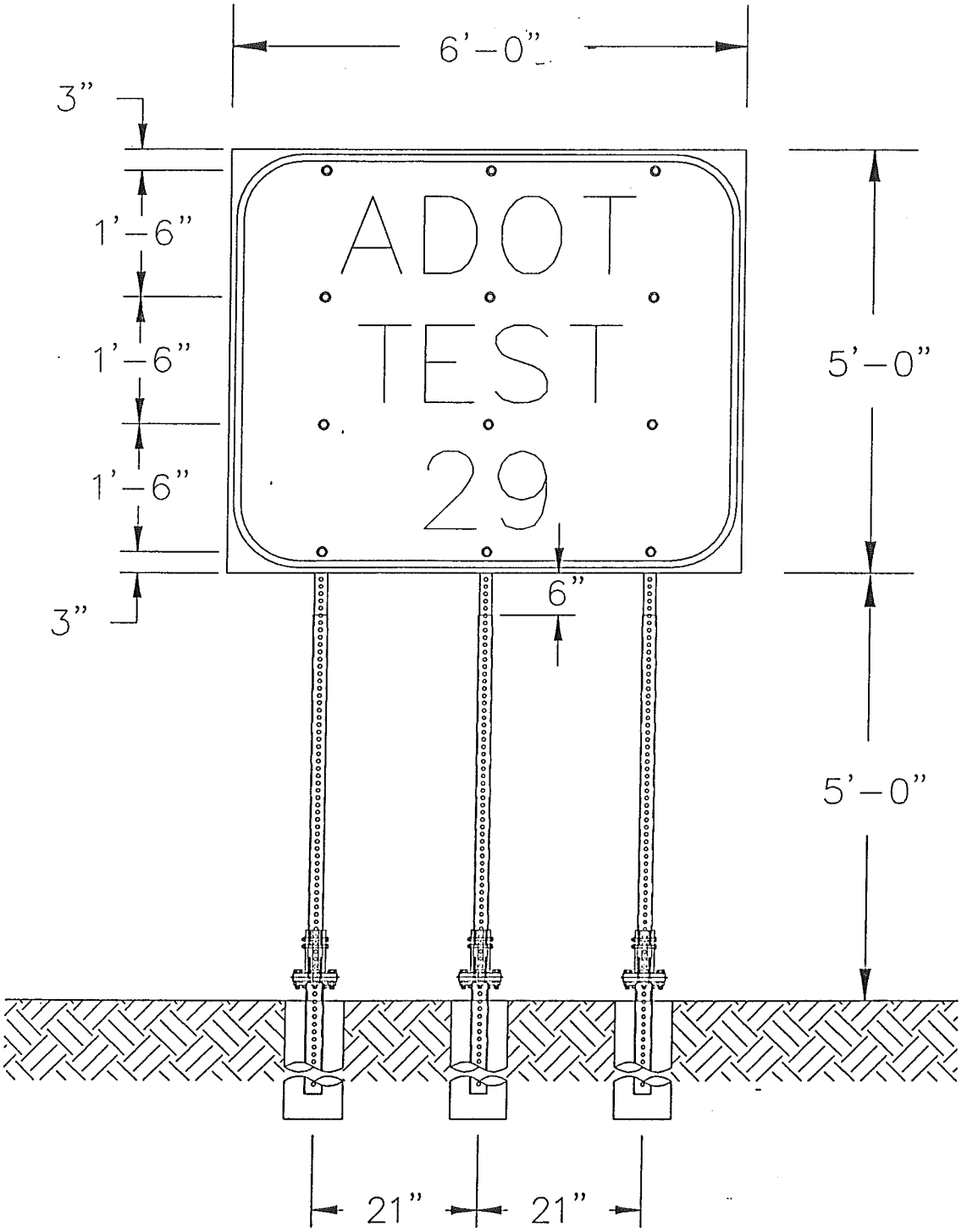

NOTE: SIGN FASTENER HARDWARE TO BE 5/16" ø GRADE 5 BOLT WITH 1-3/8" O.D. WASHER (1/8" THICK)

FIGURE 7.24. *SIGN INSTALLATION FOR TEST 7024-29*

FIGURE 7.25. *VEHICLE PRIOR TO TEST 7024-29*

FIGURE 7.26. *SIGN INSTALLATION USED IN TEST 7024-29.*

TEST RESULTS AND EVALUATION

The sign installation sustained minimal damage and came to rest approximately 16.0 ft (4.88 m) from point of impact (Fig. 7.27). In addition, the vehicle sustained minor damage to the bumper and right front fender as shown in Figure 7.28.

A summary of the test results and other information pertinent to this test are given in Figure 7.29. The maximum 0.050 second average acceleration experienced by this vehicle was -1.19 g in the longitudinal direction and -0.92 g in the lateral direction. Occupant impact velocity in the longitudinal direction was 8.86 feet per second (2.7 m/s) and 6.16 feet per second (1.88 m/s) in the lateral direction. The highest 0.10 second occupant ridedown accelerations were -0.84 g in the longitudinal direction and -0.81 g in the lateral direction. Change in velocity was 7.07 mi/h (11.38 km/h) and change in momentum was 582 lb-s.

In summary, the sign installation yielded to the vehicle by slipping at stub base mounts. The vehicle sustained very minor damage and did not present undue hazard to other traffic. The occupant impact velocity was acceptable (NCHRP Report 230 limit is 15 ft/s) and the change in momentum was under the recommended limit of 1100 lb-s. This sign installation conformed to the evaluation criteria recommended in NCHRP Report 230 and the AASHTO Standards.

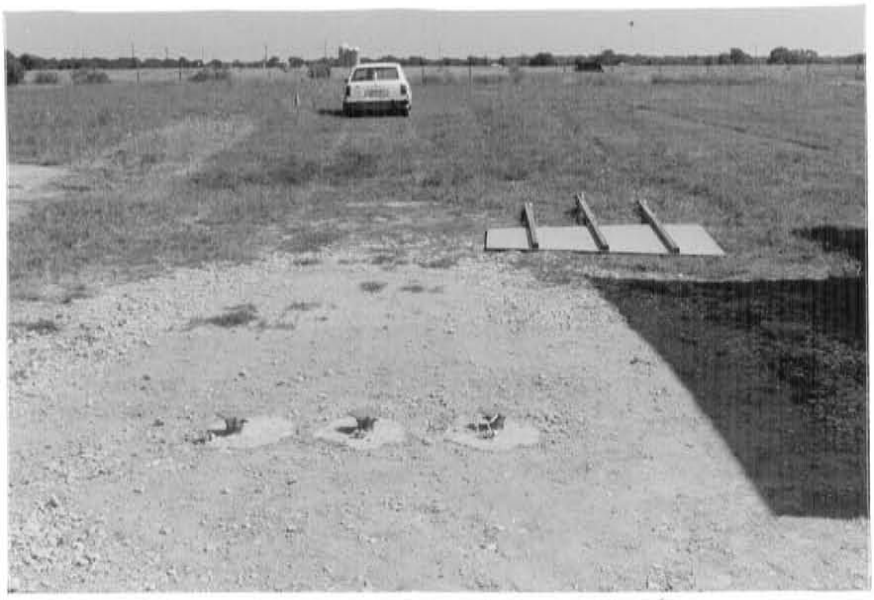

FIGURE 7.27. *SIGN INSTALLATION FOLLOWING TEST 7024-29.*

FIGURE 7.28. *VEHICLE DAMAGE FOLLOWING TEST 7024-29.*

0.000 s 0.249 s 0.499 s 0.748 s

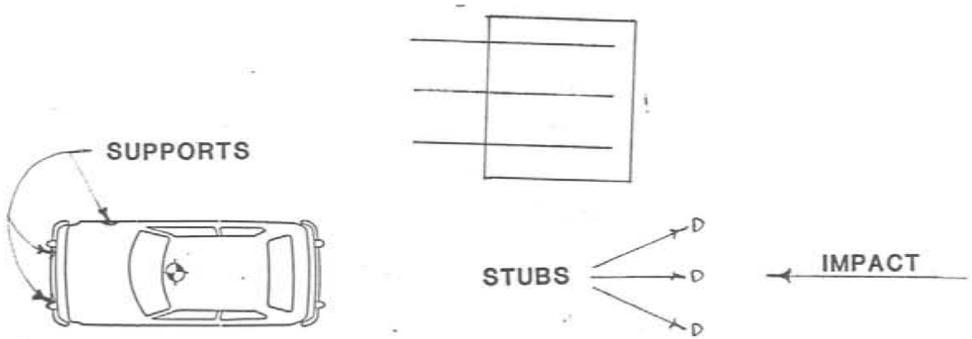

Test No	7024-29
Date	05/17/88
Test Article	Sign Installation
Support	Three Uni-Strut Triangular Retrofit Slipbases with P2 Post Assemblies
Vehicle	1979 Honda
Vehicle Weight	
Test Inertia	1,800 lb (817 kg)
Gross Static	1,967 lb (892 kg)
Vehicle Damage Classification	
TAD	12FD1
SAE	12FDLW1

Impact Speed	18.7 mi/h (30.1 km/h)
Change in Velocity	7.1 mi/h (11.4 km/h)
Change in Momentum	582 lb-s
Vehicle Accelerations (Max. 0.050-sec Avg)	
Longitudinal	-1.19 g
Lateral	-0.92 g
Occupant Impact Velocity	
Longitudinal	8.86 ft/s (2.70 m/s)
Lateral	6.16 ft/s (1.88 m/s)
Occupant Ridedown Accelerations	
Longitudinal	-0.84 g
Lateral	-0.81 g

FIGURE 7.29. *SUMMARY OF RESULTS FOR TEST 7024-29.*

7.6.2 TEST 7024-30

TEST DESCRIPTION

A 1979 Honda Civic (shown in Figure 7.30) impacted the sign installation at 61.5 miles per hour (98.9 km/h) using a cable reverse tow and guidance system. Test inertia mass of the vehicle was 1,800 lb (817 kg) and its gross static mass was 1,967 lb (892 kg). The height to the lower edge of the vehicle bumper was 14.5 inches (36.8 cm) and 19.5 inches (49.5 cm) to the top edge of the bumper.

The vehicle was free wheeling and unrestrained just prior to impact. The point of impact was the center line of the sign with the center of the vehicle. Upon impact, the sign installation supports began to slip from the stub base mounts. At approximately 0.010 seconds, the sign supports had completely detached from the slip bases. Shortly thereafter as the sign installation yielded, the face of the sign slapped the roof of the test vehicle. The vehicle lost contact with the sign installation at approximately 0.173 seconds, the brakes were applied and the vehicle came to rest approximately 306.0 ft (93.3 m) from point of impact.

TEST RESULTS AND EVALUATION

The sign installation sustained minimal damage (Figure 7.31) and came to rest approximately 84.0 ft (25.6 m) from point of impact. The vehicle sustained minor damage to the bumper, hood, and roof as shown in Figure 7.32. Maximum crush to the left front of the vehicle at bumper height was 2.5 in (6.35 cm). In addition, the left front tire aired out upon exiting the crash site.

A summary of the test results and other information pertinent to this test are given in Figure 7.33. The maximum 0.050 second average acceleration experienced by this vehicle was -3.57 g in the longitudinal direction and -0.87 g in the lateral direction. Occupant impact velocity was 9.01 ft/s (2.75 m/s) in the longitudinal direction and was 5.30 feet per second (1.62 m/s) in the lateral direction. The highest 0.10 second occupant ridedown accelerations were -0.70 g in the longitudinal direction and -0.62 g in the lateral direction. Change in velocity was 7.3 mi/h (11.8 km/h) and change in momentum was 599 lb-s.

In summary, the sign installation yielded to the vehicle by slipping at stub base mounts. The vehicle sustained very minor damage and did not present undue hazard to other traffic. The occupant impact velocity was acceptable (NCHRP Report 230 limit is 15 ft/s) and the change in momentum was under the recommended limit of 1100 lb-s. This sign installation conformed to the evaluation criteria recommended in NCHRP Report 230 and AASHTO Standards.

FIGURE 7.30. *VEHICLE PRIOR TO TEST 7024-30.*

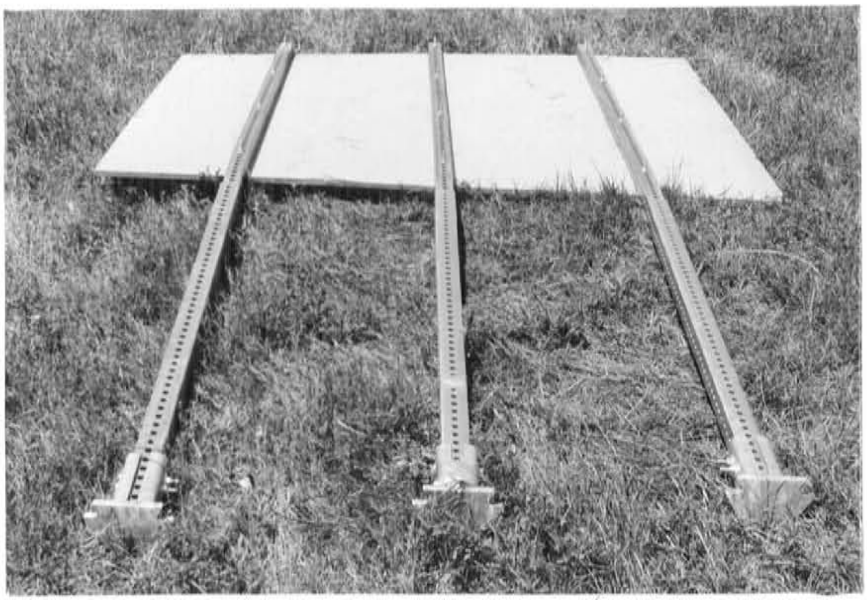

FIGURE 7.31. *SIGN INSTALLATION FOLLOWING TEST 7024-30.*

FIGURE 7.32. *VEHICLE DAMAGE FOLLOWING TEST 7024-30.*

0.000 s 0.070 s 0.140 s 0.215 s

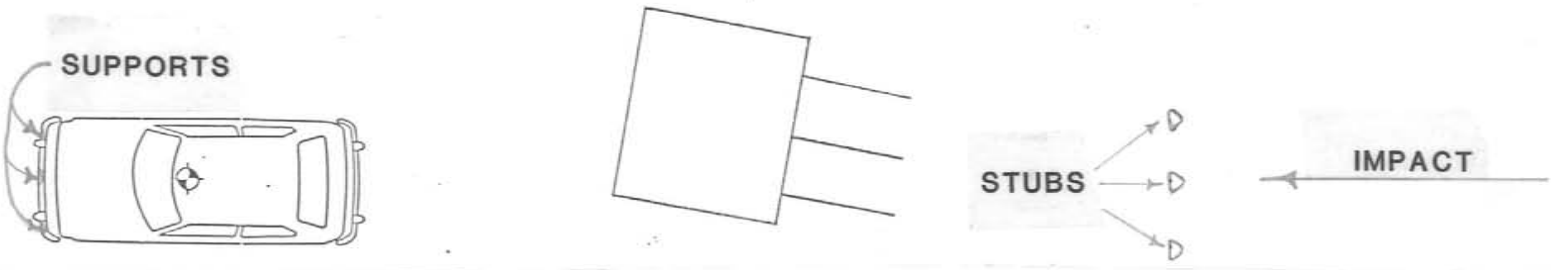

Test No.	7024-30	Impact Speed.	61.5 mi/h (98.9 km/h)
Date	05/17/88	Change in Velocity	7.3 mi/h (11.8 km/h)
Test article	Sign Installation	Change in Momentum	559 lb-s
Support	Three Uni-Strut Triangular Retrofit Slipbases with P2 Post Assemblies	Vehicle Accelerations (Max. 0.050-sec Avg)	
		Longitudinal.	-3.57 g
		Lateral	-0.87 g
Vehicle	1979 Honda	Occupant Impact Velocity	
Vehicle Weight		Longitudinal.	9.01 ft/s (2.75 m/s)
Test Inertia	1,800 lb (817 kg)	Lateral	5.30 ft/s (1.62 m/s)
Gross Static	1,967 lb (892 kg)	Occupant Ridedown Accelerations	
Vehicle Damage Classification		Longitudinal	-0.70 g
TAD	12FD1	Lateral	-0.62 g
SAE	12FDEW1 & 12TBDW9	Maximum Vehicle Crush	
		Bumper Height	2.5 in. (6.35 cm)

FIGURE 7.33 *SUMMARY OF RESULTS FOR TEST 7024-30.*

8 Conclusions

Results of this research indicate that three-3 lb/ft or (based on energy based analysis) two-4 lb/ft 80 ksi Marion steel u-post supports and stubs assembled using a 4 in nested splice (support assembled behind the stub) with 1/2 in spacers and grade 9 bolts, nuts and washers will meet the evaluation criteria recommended in NCHRP 230 (2) and the AASHTO standards (5) on change in velocity[1]. This same configuration was found to develop the nominal material yield stress (80 ksi) under static bending loads. In a single post installation, subjected to combined bending and torsion, this ground mounted u-post lap splice system still will develop at least 95% of the nominal yield stress under static loads. As a result of the tests run for this project, the forementioned splice (also described in Chapters 2 and 3) is recommended for use along highway right of ways.

It also is apparent from the results of this study that a slip-base retrofit for a sign support system with up to three P2 Uni-Strut posts will meet the evaluation criteria recommended in NCHRP 230 (2) and the AASHTO standards (5).

In all cases, tests were conducted in NCHRP Report 230 (2) Classification S1 (STRONG) soil. In cases where installation in a "weak" soil is anticipated, further evaluation is required.

---

[1]It should be noted that AASHTO recommends a maximum stub height less than that used in these test; however, there was no snagging in any of the tests herein reported and none is anticipated.

References

(1) Boresi, A., Sidebottom O., Seely, F. and Smith, J., Advanced Mechanics of Materials, Third Edition, John Wiley and Sons, 1978.

(2) "Recommended Procedures for the Safety Performance Evaluation of Highway Appurtenances," National Cooperative Highway Research Program Report 230 (1981).

(3) Roark, R.J. and Young, W.C., Formulas for Stress and Strain, Fifth Edition, McGraw-Hill, 1975.

(4) Ross, H.E. Jr., Robertson, R.G. and Sicking, D.L., "Static Load Tests of Franklin Steel Signposts," Texas Transportation Institute Report 4277-1, December, 1981.

(5) "Standard Specifications for Structural Supports for Highway Signs, Luminaries and Traffic Signals," AASHTO Subcommittee on Bridges and Structures.